Petroleum Source Rocks in the Brushy Canyon Formation (Permian), Delaware Basin, Southeastern New Mexico

by

Heidi Anne Justman

Submitted in partial fulfillment of the requirements
to the degree of Masters of Science in Geology

New Mexico Institute of Mining and Technology
Department of Earth and Environmental Science

Socorro, New Mexico

May, 2001

ABSTRACT

The lower unit of the Brushy Canyon Formation consists dominantly of reservoir quality sandstones and interbedded organic-rich siltstones. Sandstones are generally massive or faintly laminated and are composed of very fine to medium grained quartz and feldspar. The organic-rich siltstones, composed of silt-sized grains of quartz and feldspar, exhibit horizontal lamination and soft-sediment deformation features. Organic matter consists dominantly of amorphous-sapropellic and herbaceous material (type I and II kerogen) with minor woody and intertinitic components. The quantity of organic carbon is sufficient to generate significant quantities of hydrocarbons with thermal maturation. Total organic carbon levels range from 0.56 to 2.41 wt. % for the lower Brushy Canyon, and 0.54 to 1.92 wt. % in the upper Brushy Canyon member. Maturity levels of the kerogen are within the oil generation window. T_{max} values range from 439 to 448 ° C with highest levels of maturity along the western and shallowest portion of the study area. Productivity index values range between 0.1 and 0.25, with an average value of 0.19. TAI values are all between 2.4 and 2.8. Kerogen within the lower Brushy Canyon organic-rich siltstones is present in sufficient quantity and is of the right type and maturation to make the units very likely sources for the oil and gas found within the interbedded channel sands. Trends of the source rock within the lower Brushy Canyon may have some influence on the location of oil fields within the Brushy Canyon Formation. Production trends match fairly well with areas high in net thickness of

organic-rich siltstones. The Brushy Canyon siltstones appear to act as both source rocks for hydrocarbon accumulations and as seals for the interbedded reservoirs.

ACKNOWLEDGMENTS

This study is part of a much larger project that is funded by the Department of Energy: Risk Reduction with a Fuzzy Expert Tool (DE-AC-26-99BC15218). My thank you to the New Mexico Bureau of Mines and Mineral Resources for its resources, Geochem Laboratories for performing the kerogen assessments and Rock-Eval pyrolysis procedures, and Caprock Laboratories for the thin-section preparation. I also want to thank Strata Production Company for use of the Nash Draw Unit No. 23 core.

A very big thank you to my committee, Ron Broadhead, Dr. Peter Mozley, and Dr. Dave Johnson, for their constructive criticism and guidance. In addition, I must give a heartfelt thank you to my family and friends who have helped me through this work, mostly in the form of emotional support. Karla J. Kirst and Amanda S. Price have been the best friends anyone could have. I also want to thank my father, the late Curtis O. Justman. Even though he hasn't been around on Earth this last decade, I am in debt to him for the many things he taught me early on, such as patience, dedication, and willpower.

TABLE OF CONTENTS

Page

LIST OF TABLES

Page

LIST OF FIGURES

LIST OF ABBREVIATIONS

$\%R_o$ = percent reflectance (of vitrinite).

FID = flame ionization detector

FNL = from north line

FWL = from west line

g = grams

HC = hydrocarbons

H I = hydrogen index

inc. = incorporated

KB = kelly bushing

OI = oxygen index

PI = productivity index

pph = parts per hundred

ppt = parts per thousand

pub. = publication

sed. = sediment

TAI = thermal alteration index

T_{max} = thermal maximum

TOC = total organic carbon

INTRODUCTION

The Brushy Canyon Formation of the Delaware Mountain Group (Permian: Guadalupian) was deposited within the Delaware Basin (Figure 1) of southeastern New Mexico and western Texas. This basin covers an area of over 13,000 mi^2 (Hills, 1984). Exploration efforts within the last 15 years have led to numerous commercial discoveries of oil and gas within the Brushy Canyon.

Several essential features define petroleum systems (Magoon and Dow, 1994). They must contain sufficient source rocks to generate significant quantities of hydrocarbons (HC). The petroleum system must have reservoir rocks with adequate porosity and volume to hold the hydrocarbons generated from the source rock. The system must also have seals and traps. It has already been established, based on production from the Brushy Canyon Formation, that reservoirs, seals, and traps exist. However, there is a lack of information available on the source rocks. Source rocks are very important to petroleum systems, but are an often-overlooked component. Source rocks should be analyzed in order to determine what types of hydrocarbons have been generated, the volume that has been generated, and also where the hydrocarbons have been generated.

Three main factors should be assessed to determine the potential of a source rock for generating hydrocarbons. The source rock must contain adequate levels of organic carbon, it must have generative types of kerogen, and the source rock must have been

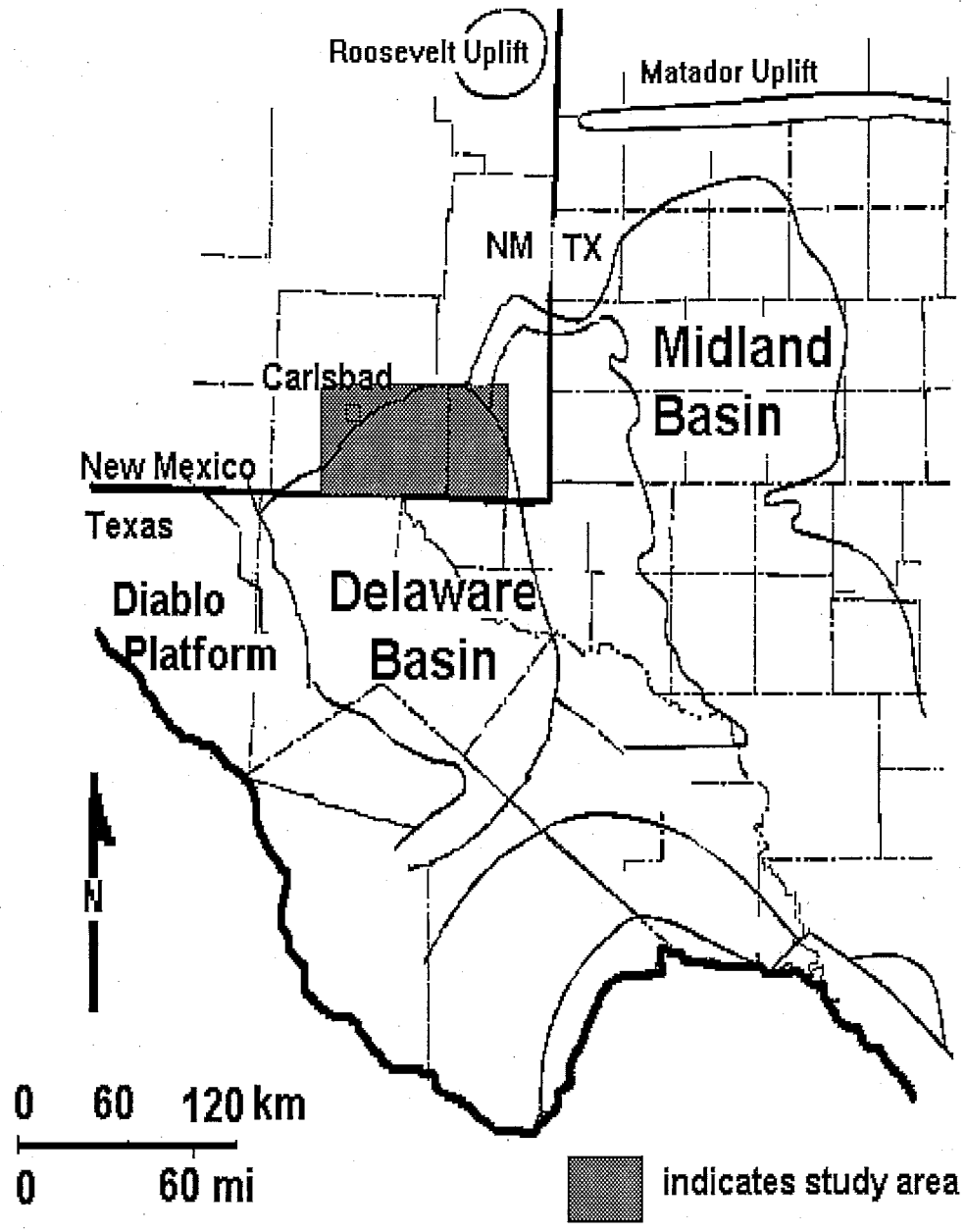

Figure 1—Map of Delaware Basin. Study area highlighted (modified from Hills, 1984).

thermally matured (Peters and Cassa, 1994). These factors have been utilized in this study to assess the source rocks within the Brushy Canyon Formation.

Previous work by Hays and Tieh (1992) indicates that the Delaware Mountain Group is, at least in part, self-sourced. They looked at TOC levels, kerogen types, and maturity of organic-rich siltstones using both visual analyses and Rock-Eval pyrolysis. A positive correlation of oil and gas accumulations to source rocks was established. This was done through analysis of carbon and sulfur stable isotopes, biomarker comparisons and a trace element study. Hays and Tieh assessed all three members of the Delaware Mountain Group (descending): the Bell Canyon Formation, the Cherry Canyon Formation, and the Brushy Canyon Formation. Their sampling was mostly done from cored intervals from eight wells in the Waha Field area in Reeves County, Texas, and four wells from the Big Eddy Unit in Eddy County, New Mexico. Oils and formation waters from five of the cored wells were sampled. Petrographic studies were performed on 124 sandstone and siltstone samples. Scanning electron microscopy, electron microprobe analysis, neutron activation analysis and stable isotope mass spectrometry were all used to study these samples. In addition, organic matter was subject to Rock-Eval pyrolysis, coupled gas chromatography/mass spectrometry, and total organic carbon analysis.

In their study, Hays and Tieh determined source rocks with type II and type III kerogen (dominantly type II) to be the source for gas and oil accumulations within the Brushy Canyon Formation. The only non-correlation between source rock and hydrocarbons was for oil located within the Brushy Canyon Formation in Loving County, Texas. That oil was determined to be from a different oil family. With the exception of

this one location, Hays and Tieh determined the organic-rich siltstones of the Delaware Mountain Group to be of the right type, of sufficient abundance, and of an advanced state of thermal maturity to release carboxylic acids and CO_2 during burial. These siltstones yielded the oil for the fields in their study area. In my study, focus is on the Brushy Canyon Formation, with greatest emphasis on the lower member of the Brushy Canyon Formation. Within the Brushy Canyon, the majority of production comes from the lower unit. This lower unit also contains the greatest percentage of organic-rich siltstones within the Brushy Canyon Formation. My study area covers the region between 32 and 33 degrees north latitude, and –103.3 and –104.5 degrees west longitude (Figure 1), Eddy and Lea Counties.

TECTONIC HISTORY OF THE DELAWARE BASIN

The Delaware Basin (Figure 1) is a broad, asymmetrical structure located in northeastern New Mexico and western Texas (Hills, 1984). Much of the shape resulted from block faulting in the Pennsylvanian (Figure 2). The basin covers an area of approximately 80 miles (120 kilometers) by 120 miles (180 kilometers). A series of tectonic events formed the current-day basin by first creating the Tobosa Basin (Hills, 1972). The Tobosa Basin began to form in the late Precambrian and continued to take shape into the middle Paleozoic. This basin was the precursor to the Permian Basin (Hills, 1972). In the Early Pennsylvanian, block faulting and successive movement along Proterozoic lines of weakness caused uplift of the Central Basin Platform (Figure 2), which currently divides the Permian Basin into two separate basins, the eastern Midland Basin and the western Delaware Basin (Hills, 1984). This block faulting gave the Delaware Basin much of its present shape (Payne, 1976). During the Tertiary, further tectonism and faulting caused uplift of the western side of the basin, giving it a slight eastern tilt (Hills, 1984). The Delaware Basin is now bordered to the west by the Diablo Platform, to the east by the Central Basin Platform, to the south by the Marathon Ouachita Fold Belt, and to the north by the Northwest Shelf (Figure 1).

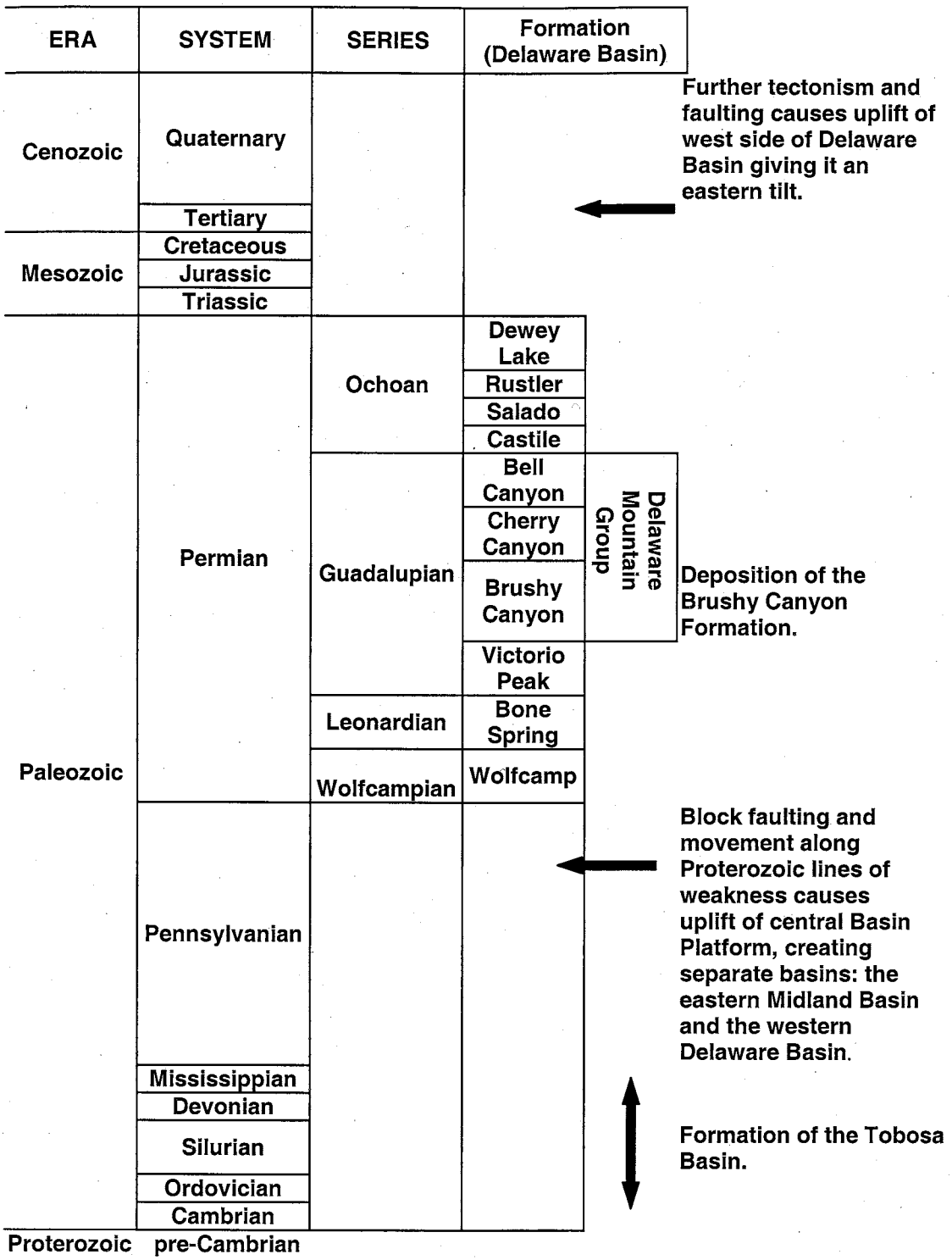

Figure 2—Tectonic history chart for Delaware Basin (after Hills, 1984; Payne, 1976).

METHODS AND PROCEDURES

DATA COLLECTION AND MAPPING

Over 700 resistivity/gamma ray logs were collected. A number of these logs also have bulk density and neutron porosity curves. The 700 well logs cover an area of approximately 180 townships (Figure 3) with well log density (well control) decreasing where drilling was prohibited. Correlations for the tops of the upper Brushy Canyon, lower Brushy Canyon, and Bone Spring were made on the well logs (Figure 4). Cross-sections were loop-tied for quality control. Structure maps (Figure 5) were created for all three tops using the Surfer 7.0 mapping program. Overlays of source rock characteristics over structure were constructed in order to evaluate possible correlations between the two. Production maps were also studied in order to determine any positive connection between the lower Brushy Canyon source rocks and productive lower Brushy Canyon reservoirs.

A majority of the data for this study is from the lower Brushy Canyon Formation because it contains the majority of the Brushy Canyon producing intervals as well as the greatest percentage of source rock. Net thickness and percentage source rock for the lower Brushy Canyon were calculated from well logs based on high gamma ray intensity and high resistivity. Net thickness indicates the sum thickness of all organic-rich units within the lower Brushy Canyon. Percentage source rock is the ratio of net thickness source rock to the total thickness of the lower Brushy Canyon multiplied by 100 percent.

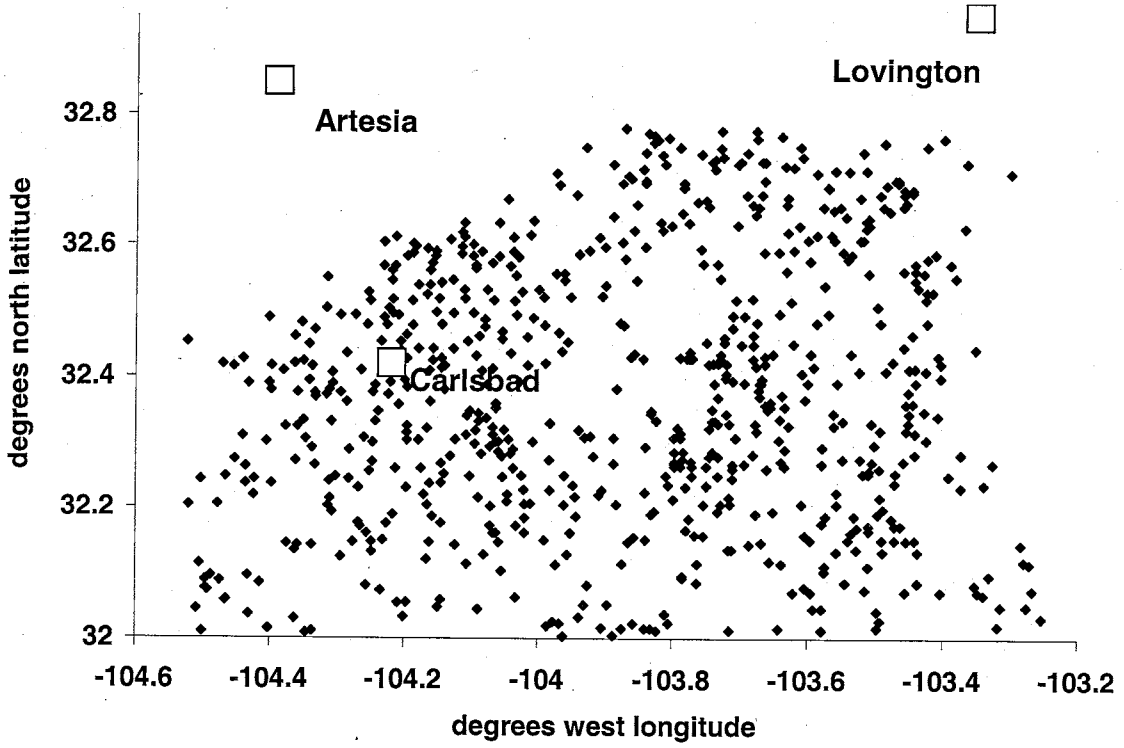

Figure 3—Map showing density and location for well logs used for correlation, cross-sections, and structure maps.

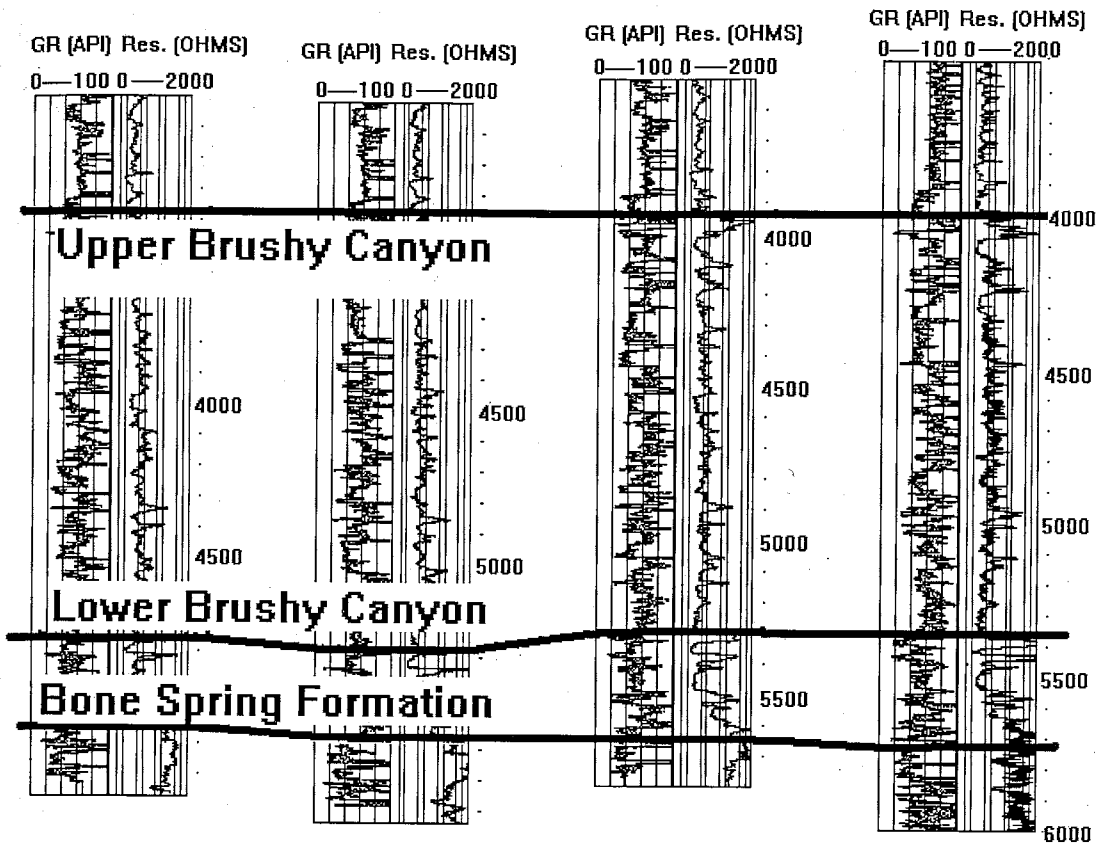

Figure 4—Sample logs and cross-section showing tops chosen for Bone Spring, lower Brushy Canyon, and upper Brushy Canyon Formations using gamma ray and resistivity logs. Depth is in feet. Organic-rich siltstones are commonly marked by highly resistive and highly radioactive units. Organic-poor sandstones are marked by lower resistivity and radioactivity.

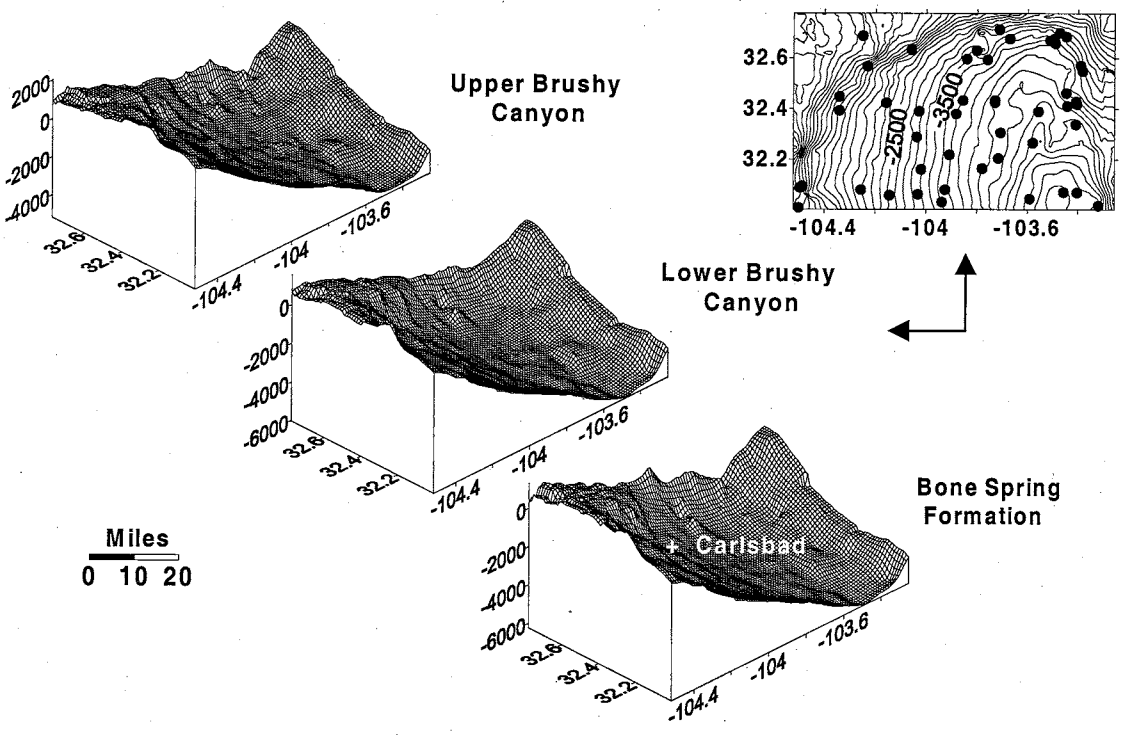

Figure 5—Structure maps for tops of lower Brushy Canyon, upper Brushy Canyon and Bone Spring Formations with lower Brushy Canyon contour map showing geochemical sample locations. Contour interval = 20 feet. X-axes = degrees longitude; Y-axes = degrees latitude; Z-axes = depth in feet.

Thirty-three samples of organic-rich intervals from both the upper and lower Brushy Canyon were sent to Geochem Laboratories, Inc. (Houston, Texas) for petroleum source rock analysis. All of the samples were examined using Rock-Eval pyrolysis, and the Leco Method. Visible contaminants (fibers, mud additives, etc.) were carefully removed by hand. At the lab, samples were washed to remove other contaminants. In addition to Rock-Eval, ten of the thirty-three samples were visually assessed for kerogen type. Some of these organic-rich rock samples were also sent to Caprock Laboratories (Midland, Texas). These samples were made into thin-sections to be used in petrographic studies. Core from the Strata Production Company No. 23 Nash Unit well was described. Supporting evidence for depositional models was obtained from sedimentary structures and the nature of the contacts between organic-rich source units and organic-poor reservoir units.

Methods for Determining Kerogen Type

Rock-Eval Pyrolysis

In Rock-Eval pyrolysis, about 20-25 mg of crushed rock sample is heated in a stream of helium at temperatures starting at around 30 ° C. The temperature in the oven is raised approximately 28 ° C per minute with a maximum temperature in the range of 650 ° C (Geochem Laboratories, Inc., 1980). As the temperature is raised, hydrocarbons evolve from the kerogen. A flame ionization detector (FID) is used to detect the volume (in mg) of hydrocarbons given off.

At a temperature around 300 ° C, only the hydrocarbons that have already been created from the kerogen, but not yet expelled from the source rock are measured. These

hydrocarbons were already present within the source rock. The S_1 peak on a graph plotting time and temperature on the x-axis and FID response on the y-axis (Figure 6) represents this portion of extractable HC. With increasing temperature, an increase in thermal degradation of the kerogen takes place. Breakdown of the kerogen allows further hydrocarbons to be created. These hydrocarbons are measured and are represented by the S_2 peak. This peak represents the remaining hydrocarbon potential of the organic-rich rock.

As the samples are heated to temperatures of up to about 550 ° C, carbon dioxide is given off. Commonly this occurs between 300 and 390 ° C. The S_3 peak on the Rock-Eval curve represents this CO_2. The CO_2 is trapped and used later with a thermal conductivity detector (TCD) to determine more about the organic material, such as the amount of hydrogen and oxygen versus total organic carbon. These values are essential to the determination of the kerogen type using Rock-Eval pyrolysis.

The oxygen index (OI) is a measure of the oxygen in a sample. OI is calculated from the ratio of carbon dioxide to the total organic carbon (mg CO_2 in S_3/g TOC). The hydrogen index (HI) is a measurement of the hydrogen in a sample and is the ratio of potential hydrocarbons to the total organic carbon (mg HC in S_2/ g TOC). A hydrogen index value of less than 150 typically indicates a gas-prone source rock. A value of greater than 300 will result in oil, while a value between 150 and 300 will commonly represent a mixture of oil and gas (Table 1). The oxygen index values are used in combination with the hydrogen index values to determine whether the organic matter is oil prone or gas prone, and mature or immature.

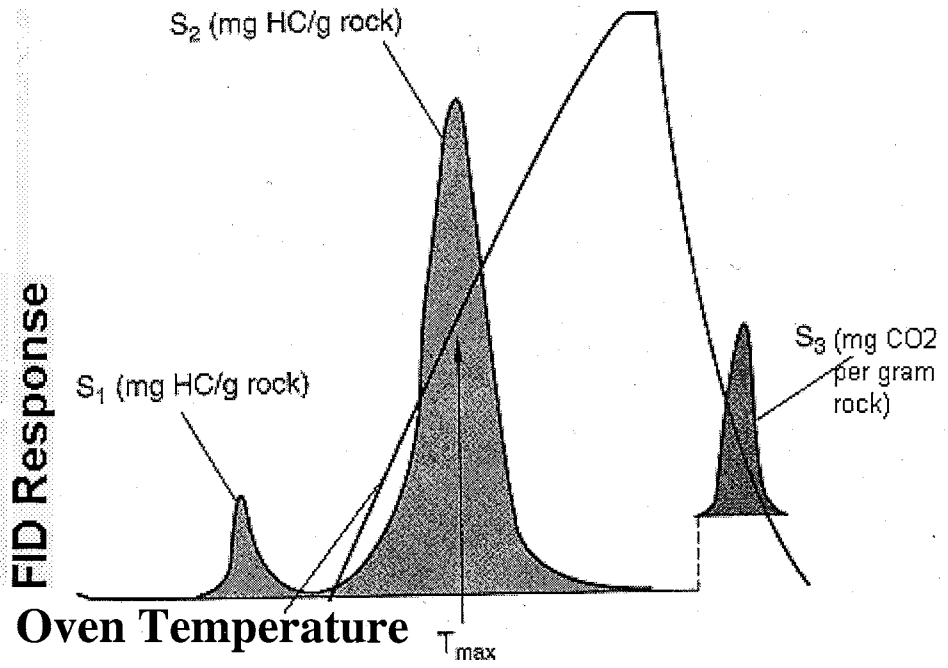

Figure 6—Sample Rock-Eval pyrolysis curve (modified from Peters, 1986). Time and temperature increasing from left to right on x-axis, FID response on y-axis. S_1=Free hydrocarbons (mg HC/g rock). S_2=Hydrocarbons formed by thermal breakdown of kerogen (mg HC/g rock); the source potential. S_3=Amount of carbon dioxide formed by the thermal breakdown of kerogen (mg CO_2/g rock); the amount of oxygen-rich kerogen within the source rock.

Table 1—Oxygen and hydrogen indices and their significance (modified from Merrill, 1991).

	Units	Equation	Values	Significance
Hydrogen Index (HI)	mg HC/g TOC	$\frac{S_2 * 100) \text{ mg/g}}{\%\text{ TOC}}$	<150	Gas
			150-300	Mixed
			>300	Oil
Oxygen Index (OI)	mg CO_2/ g TOC	$\frac{(S_3 * 100) \text{ mg/g}}{\%\text{TOC}}$	<40 mg/g	Low HI= derived organic matter, and / or mature
				High HI= good to excellent source potential
			>40 mg/g	Low HI= gas-prone organic matter; generally immature
				High HI= good oil source; generally immature

When OI and HI are plotted against one another, a rough idea of the type of kerogen is given. Such a plot allows one to evaluate the ratio of oxygen and hydrogen in a rock sample. Varying levels of these compounds exist within different types of kerogen. Therefore, kerogen type can often be determined from the OI/HI plot. Some shortcomings of this method for determining TOC are ambiguity about the exact kerogen type. This is common when there is more than one type of kerogen present in a source rock. Contamination of the sample by mud additives, lubricants or other types of products involved with drilling and production can alter the values of the oxygen index and the hydrogen index, also causing problems with determining kerogen type (Geochem Laboratories, Inc., 1980). Samples for this study were washed in order to remove these possible contaminants during preparation.

Another factor to consider is oxidation of the sample during storage. This could result in much higher oxygen content for the source rock than that which it had in the subsurface. Visual assessments were made in order to test results from the OI/HI plots, and in order to eliminate any confusion as to the kerogen type or types present in the source rock.

Visual Kerogen Assessment

Ten samples from the lower Brushy Canyon were visually assessed for kerogen type. Visual kerogen assessment is a method that determines the exact type of kerogen in a source rock using petrographic techniques. Kerogen is made up of organic matter that has its own unique chemical composition. The organic material has its own unique physical structure as well (Pocock, 1982). Under a high-power microscope, it is possible to view finely disseminated kerogen and differentiate between the types of organic matter

within it based on the organic matter's physical characteristics. Sometimes it is even possible to make positive identifications using only the naked eye. However, it is most convenient to analyze the kerogen types when separated from the rock and mounted on slides for visual examination by transmitted light microscopy (Geochem Laboratories, 1980). To do this, the rock sample is coarse-ground and treated with an excess of hydrochloric acid. This removes any calcium or magnesium present in the form of carbonate. Silicates still remaining are removed using concentrated hydrofluoric acid. The organic material is then separated from the remaining mineral matter by flotation using zinc bromide solution. Once freed up, the organic debris, or kerogen, is rinsed thoroughly and is mounted onto a slide. Oxidation is not permitted during this procedure so that it will not cause any color change to the kerogen (Geochem Laboratories, 1980).

Seven groups of palynological kerogen are positively describable in visual kerogen assessments (Geochem Laboratories, 1980). The seven groups include algal, amorphous-sapropel, herbaceous, woody, coaly-inertinite, pyrobitumen, and unidentifiable organic matter (Table 2). For exploration purposes, only four principal groups are necessary to determine hydrocarbon potential of a source rock. The principle four groups are amorphous-sapropel, herbaceous-membranous, woody-structured, and coaly-inertinitic types.

Methods for Determining TOC Content

Three methods were used in this study for determining TOC content: Rock-Eval pyrolysis, the Leco Method, and a newer approach using geophysical logs. Cuttings were used for sampling. One problem that can occur when using cuttings is mixing of units.

Table 2—Kerogen types and definitions (modified from Geochem Laboratories, Inc., 1980).

Abbreviation	Type organic matter	Definition
Al	Algal	Material that is identifiably algae or of the algal genera.
Am	Amorphous-sapropel	Any material that has an amorphous or non-structured appearance. This can be either lipid-rich degraded algal remains or bacterially degraded herbaceous and spore remains.
H	Herbaceous	All membranous plant materials. This includes cuticle, spore, pollen, or any soft plant portion that is annually regenerated, like leaves and grass.
W	Woody	The lignified portion of plant remains that have a pronounced rib-like structure.
C or I	Coaly-Inertinite	Black, opaque particle debris that is angular in appearance. This material is not coal, but was termed as such due to its black coloration. This material has an inert quality; it does not generate hydrocarbons.
P	Pyrobitumen	Residual, tar-like material, such as that left behind after geothermal degradation of reservoired oil into methane gas and carbonaceous residue. This material is commonly associated with carbonates.
U	Unidentified	Any non-identifiable matter, either because of extreme degradation or due to its extremely fine size.

This can occur from cavings. Cuttings from a labeled ten-foot interval may contain cavings from an interval further up the hole. If the cavings came from a unit very far up the hole, it would likely cause a drastic change in the lithology of the cuttings. No significant changes were noticed in the cuttings when samples were picked. Therefore, it is relatively safe to assume that cavings were not problematic in cuttings samples used in this study.

Rock-Eval Pyrolysis

Using Rock-Eval pyrolysis, TOC can be estimated from the normalized carbon content of the S_1 and S_2 peaks (Jarvie, 1991). S_1 and S_2 are normalized by multiplying their peak values by 0.083, which is the average weight percent of carbon in hydrocarbons, and a conversion of milligrams of HC per gram of rock (in ppt) to parts per hundred (pph). The S_1 value represents the extractable carbon of the source rock. The S_2 represents the convertible carbon. The residual carbon can be derived from the S_3 peak.

Leco Method

This procedure for determining TOC involves oxidation of approximately 1 gram of source rock that has been pre-soaked in hydrochloric acid to remove any inorganic carbon, rinsed with water, and then dried. Copper and iron are sometimes added as a flux (Bayliss, 2000). Calibration of the Leco Carbon Analyzer is done using a steel standard of known carbon content, and the instrument is blanked to subtract the effect, if any, of the combustion crucible, filter paper, or catalyst. The sample is then heated in oxygen and the amount of carbon dioxide (as a weight percent) given off is measured by a thermal conductivity detector or an infrared detector (Jarvie, 1991). Hydrolyzation of the

sample in the water rinse, sulfur dioxide content or analyzing the wrong amount of sample can all result in error for the value of calculated TOC if not carefully watched.

Log Estimations for TOC

A new approach to estimating TOC based on log response has been attempted in this study. For an explanation of the methods used, see "Estimating TOC Based on Log Response".

Methods for Determining Thermal Maturity

There are numerous methods for estimating the thermal maturity of a source rock. The methods used in this study involve both Rock-Eval pyrolysis and visual laboratory analyses of kerogen.

Rock-Eval Pyrolysis

In Rock-Eval pyrolysis, thermal maturity can be measured in two ways. One way is to measure the temperature (T_{max}) at which the maximum amount of hydrocarbon is created from the kerogen. This is an analytical temperature measured in the laboratory and is not to be confused with actual temperatures the source rock has been subjected to in the subsurface. This measurement is the temperature (in ° C) at which the maximum value of the S_2 peak is recorded (Figure 6).

T_{max} values between 430 and 460 ° C commonly reflect a mature kerogen that is within the oil window (Table 3). T_{max} values below 430 ° C indicate an immature kerogen, above the oil window (Merrill, 1991 and Geochem Laboratories, Inc., 1980). T_{max} values above 460 ° C indicate thermal breakdown of the oil that has already been generated into gas, or destruction of the kerogen in which the ratio of carbon to oxygen

Table 3—Thermal maturity indicators and their significance for both Rock-Eval pyrolyis and visual laboratory procedures (modified from Merrill, 1991 and Geochem Laboratories, Inc., 1980).

	Units	Equation	Values	Significance
Production Index (PI)	----------	$\frac{S_1}{S_1+S_2}$	<0.1	Immature
			0.1-0.4	Oil
			>0.4	Gas
T_{max}	Degrees Celsius		<430	Immature
			430-460	Oil generation
			>460	Gas generation or destruction
Visual Kerogen Assessment			1.00-1.70	Immature
Thermal Alteration Index (TAI)			1.80-2.10	Moderately Immature
			2.20-2.50	Moderately Mature
			2.60-3.50	Mature
			3.60-4.10	Very Mature
			4.20-4.90	Severely Altered
			5.00	Metamorphosed

and hydrogen is so high that no additional hydrocarbons can be generated (below the oil window). Different levels of maturity, ranging from moderately mature to very mature, are represented within the T_{max} range of 430 to 460 ° C.

Another estimation of the thermal maturity of a source rock and its kerogen may be made from Rock-Eval pyrolysis by using a combination of the S_1 and S_2 values. All hydrocarbons within the source rock sample, both already generated and those with the potential to be generated through additional maturation, are represented by the sum of both the S_1 and the S_2 values.

A ratio of S_1 to the sum of S_1 and S_2 provides an estimate of the ratio of existing hydrocarbon to total generative potential of the kerogen (Merrill, 1991). This number is called the production index (PI). It can be used to estimate the thermal maturity of the source rock (Table 3).

Thermal Alteration Index

Due to the possibility of contamination of the source rock samples from drilling fluids, oxidation of the samples during storage, or inaccuracy of sampling, the thermal alteration index (TAI) was used to support thermal maturity data obtained from Rock-Eval pyrolysis. The thermal alteration index involves visual assessment of the cuticle coloration or color alteration of kerogen using color charts. Yellow and yellow-orange colored kerogen is commonly indicative of immaturity, or lesser maturity of the source rock. Orange, red-orange, and red coloration reflect mature kerogen, while brown to black colors generally indicate overly mature kerogen and source rock (Tissot et al, 1971; Geochem Laboratories, Inc., 1980). The level of kerogen is assigned a number according

to a numerical scale (Table 3), which can be later computed to the standard $\%R_o$ for comparison (Table 4).

While this technique is adequate for getting an approximation of maturity, it has its shortcomings. It can only be performed on source rocks with type I or type II kerogens; the kerogen must be translucent in order for it to permit transmittal of light under a microscope (Geochem Laboratories, Inc., 1980). Another shortcoming is lack of color definition from person to person. Color is subjective, and therefore some ambiguity is involved in this method. It is, therefore, prudent to have the same person analyze all of the samples, rather than several different people. It is also good for that person to do all of the samples in the same sitting so that their subjectivity is the same for all samples.

Vitrinite reflectance is another method of visually estimating thermal maturity of kerogen. Vitrinite reflectance is measured on vitrain (Geochem Laboratories, Inc., 1980), which is a type III kerogen, and was not used in this study because we have type I and type II kerogens (Figures 7 and 8). Type I and type II kerogen are translucent and transmit light under the microscope. Therefore, they would not reflect light as needed in vitrinite reflectance.

Table 4—Thermal Alteration Index values and their significances (modified from Geochem Laboratories, Inc., 1980).

Visual Kerogen Thermal Alteration Index (TAI)	Numerical Scale	Descriptive Maturity Terminology	Correlative Vitrinite Reflectance (% R_o) Value
1	1.00	Immature	
1 to 1+	1.10	Immature	
1 to 1+	1.20	Immature	
1 to 1+	1.30	Immature	0.3
1+	1.40	Immature	
1+ to 2-	1.50	Immature	
1+ to 2-	1.60	Immature	0.4
1+ to 2-	1.70	Immature	
2-	1.80	Moderately Immature	
2- to 2	1.90	Moderately Immature	
2- to 2	2.00	Moderately Immature	0.5
2- to 2	2.10	Moderately Immature	
2	2.20	Moderately Mature	0.6
2 to 2+	2.30	Moderately Mature	0.7
2 to 2+	2.40	Moderately Mature	
2 to 2+	2.50	Moderately Mature	0.8
2+	2.60	Mature	0.9
2+ to 3-	2.70	Mature	
2+ to 3-	2.80	Mature	
2+ to 3-	2.90	Mature	
3-	3.00	Mature	1.0
3- to 3	3.10	Mature	
3- to 3	3.20	Mature	
3- to 3	3.30	Mature	
3	3.40	Mature	1.5
3 to 3+	3.50	Mature	
3 to 3+	3.60	Very Mature	
3 to 3+	3.70	Very Mature	
3+	3.80	Very Mature	2.0
3+ to 4-	3.90	Very Mature	
3+ to 4-	4.00	Very Mature	
3+ to 4-	4.10	Very Mature	
4-	4.20	Severely Altered	2.5
4- to 4	4.30	Severely Altered	
4- to 4	4.40	Severely Altered	3.0
4- to 4	4.50	Severely Altered	
4	4.60	Severely Altered	4.0
4 to 5	4.70	Severely Altered	
4 to 5	4.80	Severely Altered	
4 to 5	4.90	Severely Altered	
5	5.00	Metamorphosed	

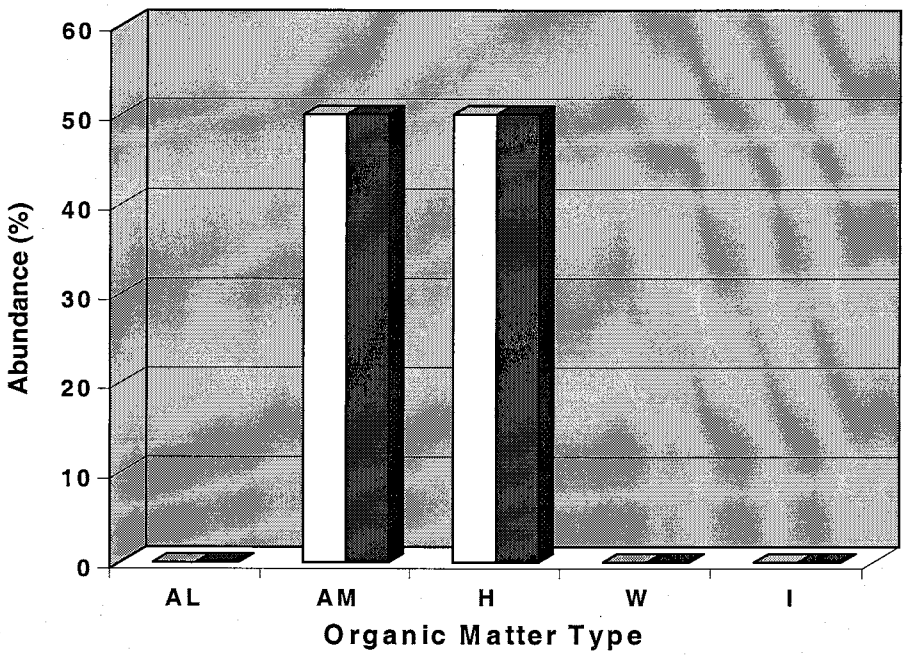

Figure 7—Visual kerogen assessment results for two upper Brushy Canyon samples indicating amorphous-sapropel and herbaceous organic matter. See Table 2 for key.

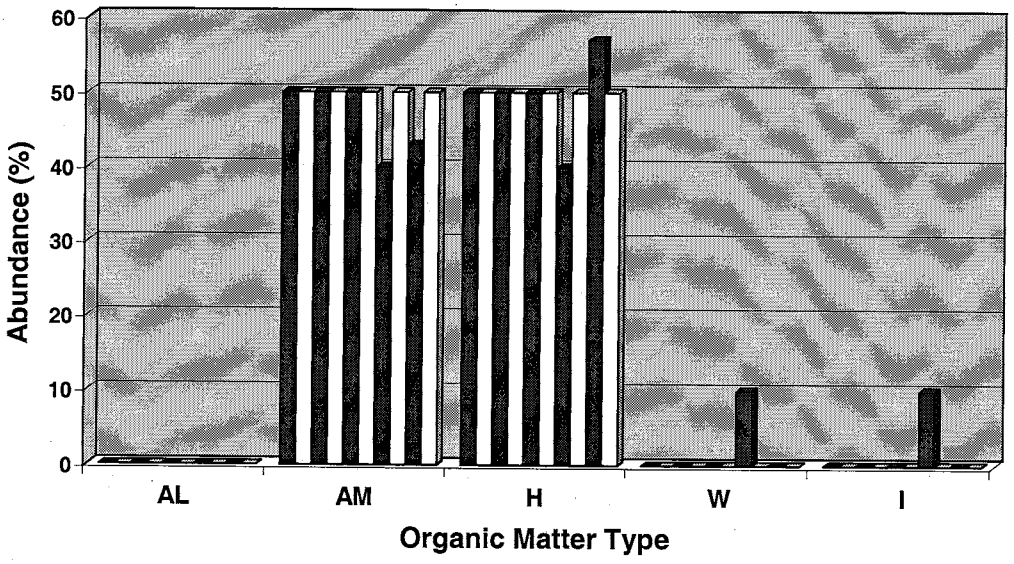

Figure 8—Results for 10 samples from Lower Brushy Canyon indicating dominantly amorphous-sapropel and herbaceous organic matter, with minor woody and inertinitic matter in one sample. See Table 2 for key.

ROCK CHARACTERISTICS

MINERALOGY AND LITHOLOGY

The lower Brushy Canyon Formation is made up of interbedded fine- to very fine-grained subarkosic sandstone and siltstone (Figures 7-16). Minor thin beds of limestone and dolostone are present locally. Mineral content of the organic-rich units is dominantly quartz and feldspar (both potassium feldspar and plagioclase feldspar; Figure 10). Other minerals within the organic-rich units include mica (muscovite), calcite, dolomite, and pyrite. Grain size ranges from silt particles to fine sand. Grains are typically well sorted and subrounded to subangular. Matrix includes kerogen and calcite cement. Shell replacement of organisms within sediment is common. Organisms include foraminiferans, sponges (Figure 11), gastropods (Figure 12), echinoderms, trilobites (Figure 13), and algae. Ooids are also present (Figure 14).

SEDIMENTARY STRUCTURES

For this study, sedimentary structures were observed in a core of the Brushy Canyon Formation from the Strata Production No. 23 Nash Unit well (Figures 15 and 16). The core is from depths of 6650 to 6854 feet, with portions of both the lower Brushy Canyon and the uppermost portion of the Bone Spring Formation present. Stratigraphic units of siltstone and sandstone are interbedded with one another (Figure 15). Minor

Figure 9—Photomicrograph of reservoir rock sample taken from sidewall core. Polars are uncrossed. Note angularity of grains, abundance of quartz (Q) and feldspar (F), and presence of calcite cement (stained red). Frame width is 0.650 mm.

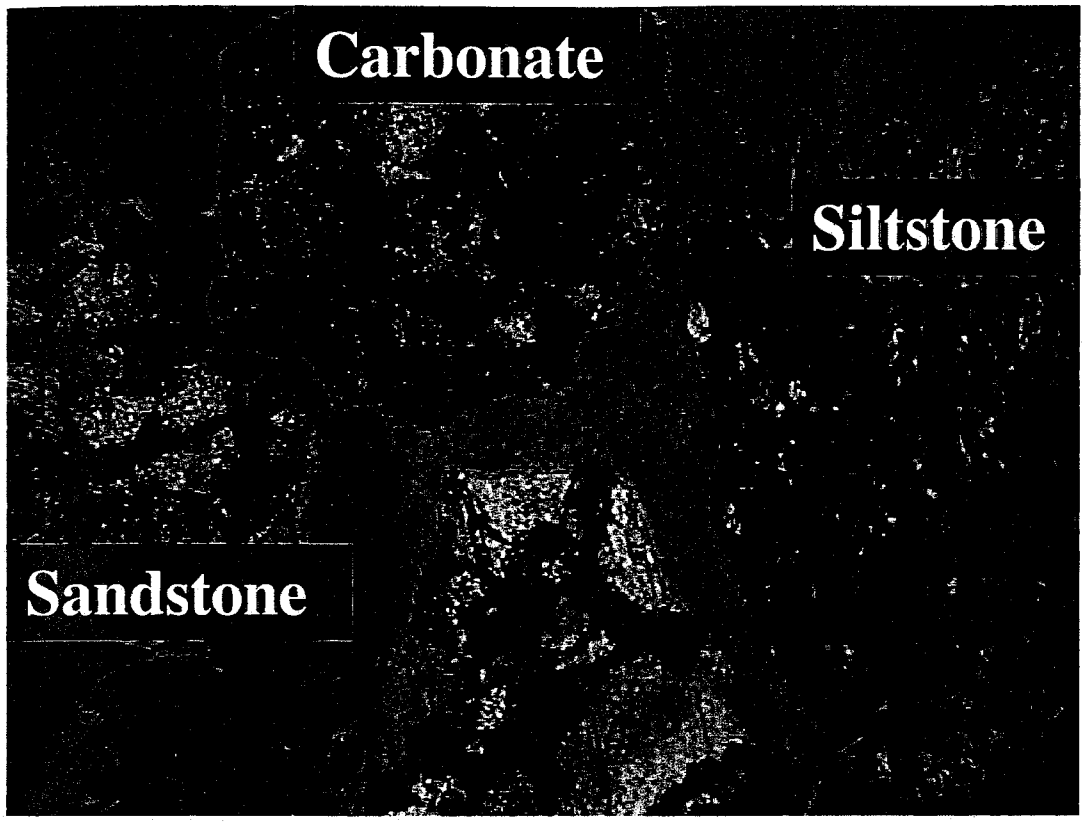

Figure 10—Photomicrograph of cuttings sample from Myco Industries Big Eddy Unit #110 well (9-22S-28E) displaying various organic-rich rock types of lower Brushy Canyon: sandstone, siltstone, and carbonate. Frame width = 1mm.

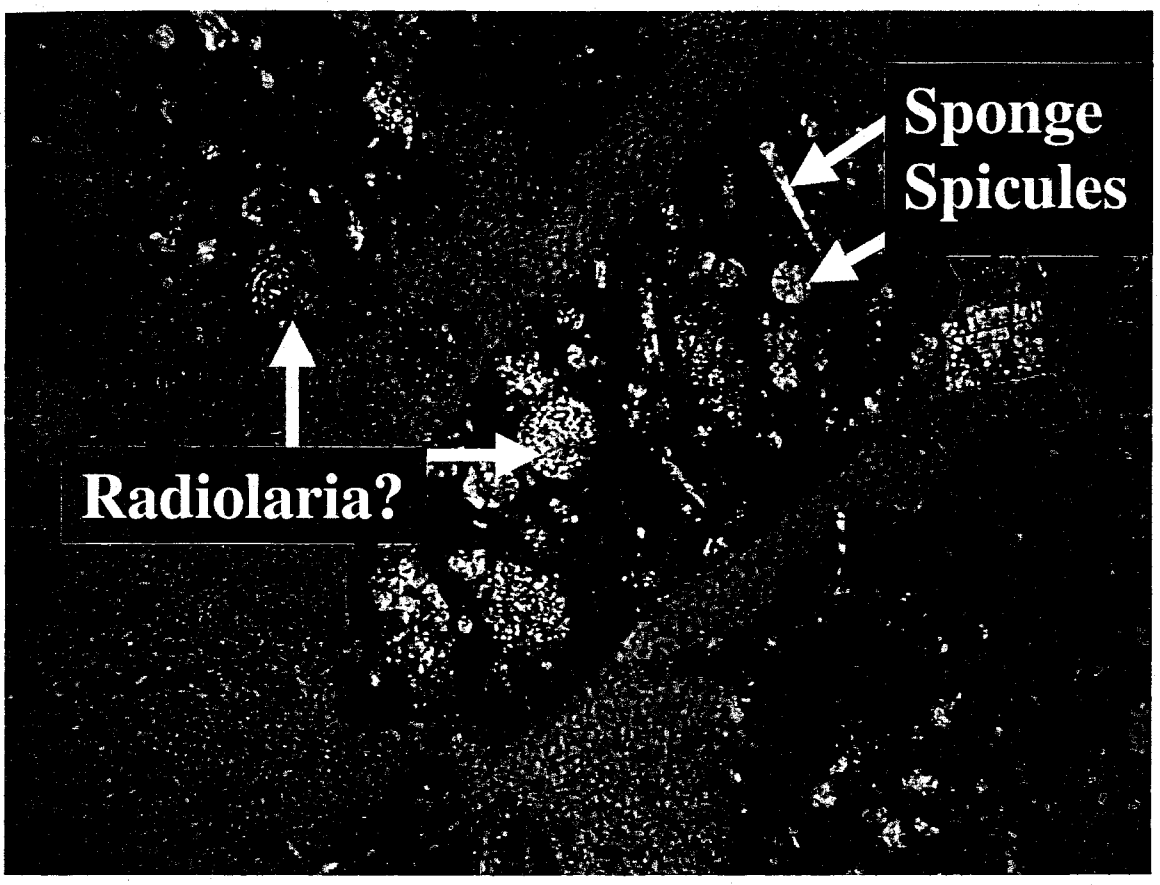

Figure 11—Cuttings sample from Myco Industries Big Eddy Unit #110 well (9-22S-28E). Frame width = 1mm.

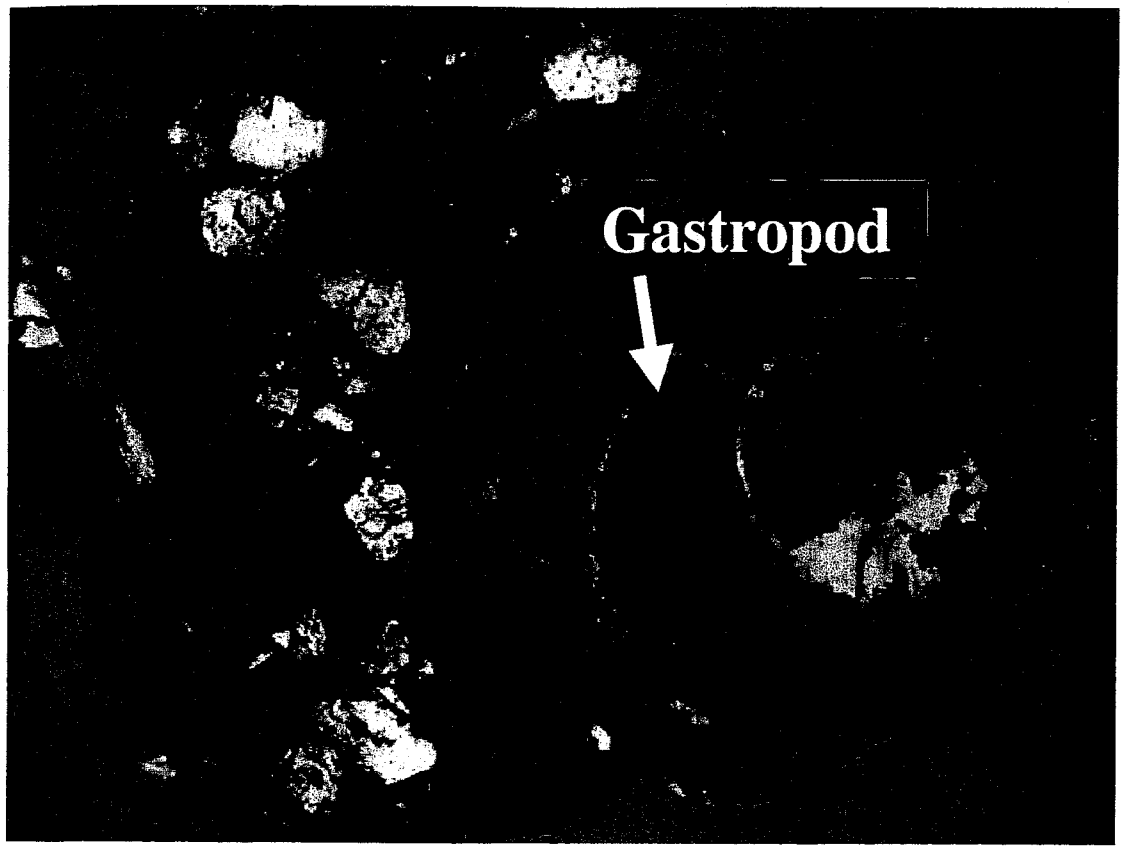

Figure 12—Cuttings sample from Pan American Poker Lake Unit #36 well (28-24S-31E). Stained red for calcite. Frame width = 2mm.

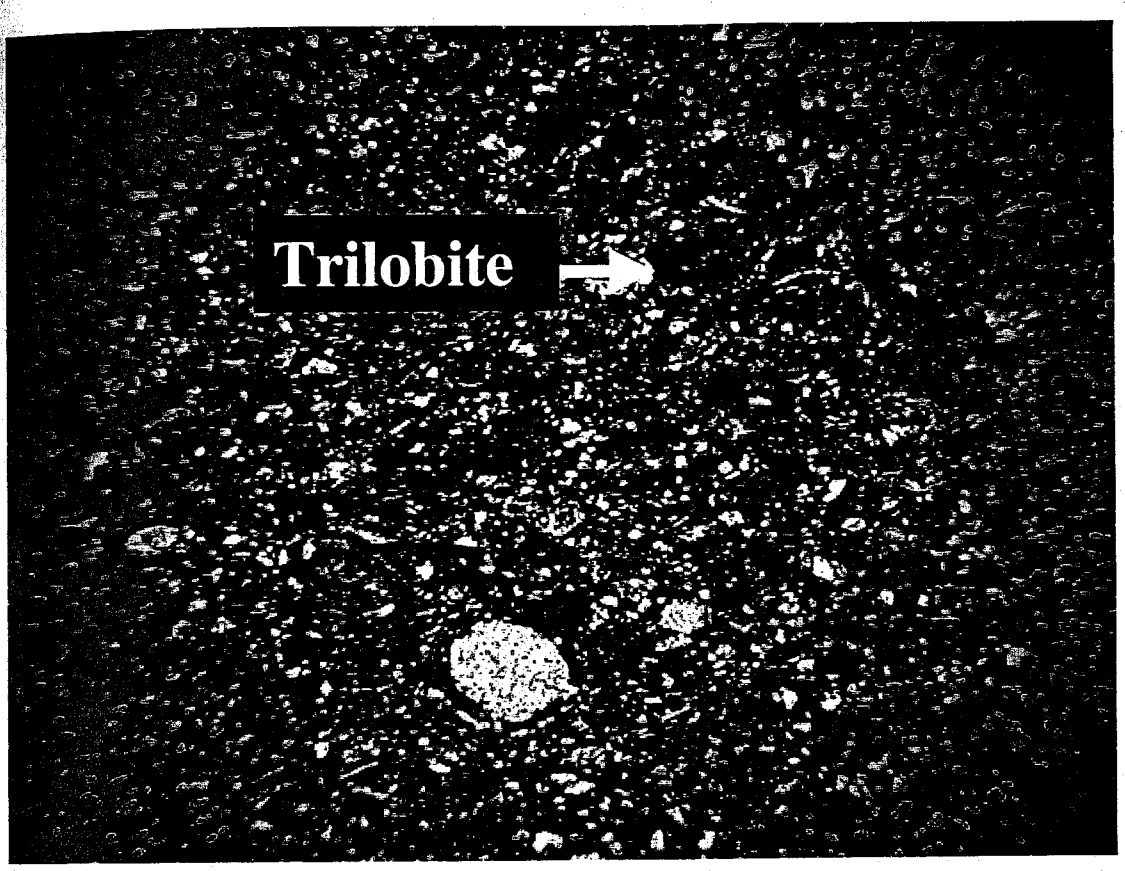

Figure 13—Photomicrograph of kerogen-rich (brown) siltstone from No. 23 Nash Draw Unit core. White grains are combination of quartz and feldspar. Red stain for calcite. Frame width = 4.2 mm.

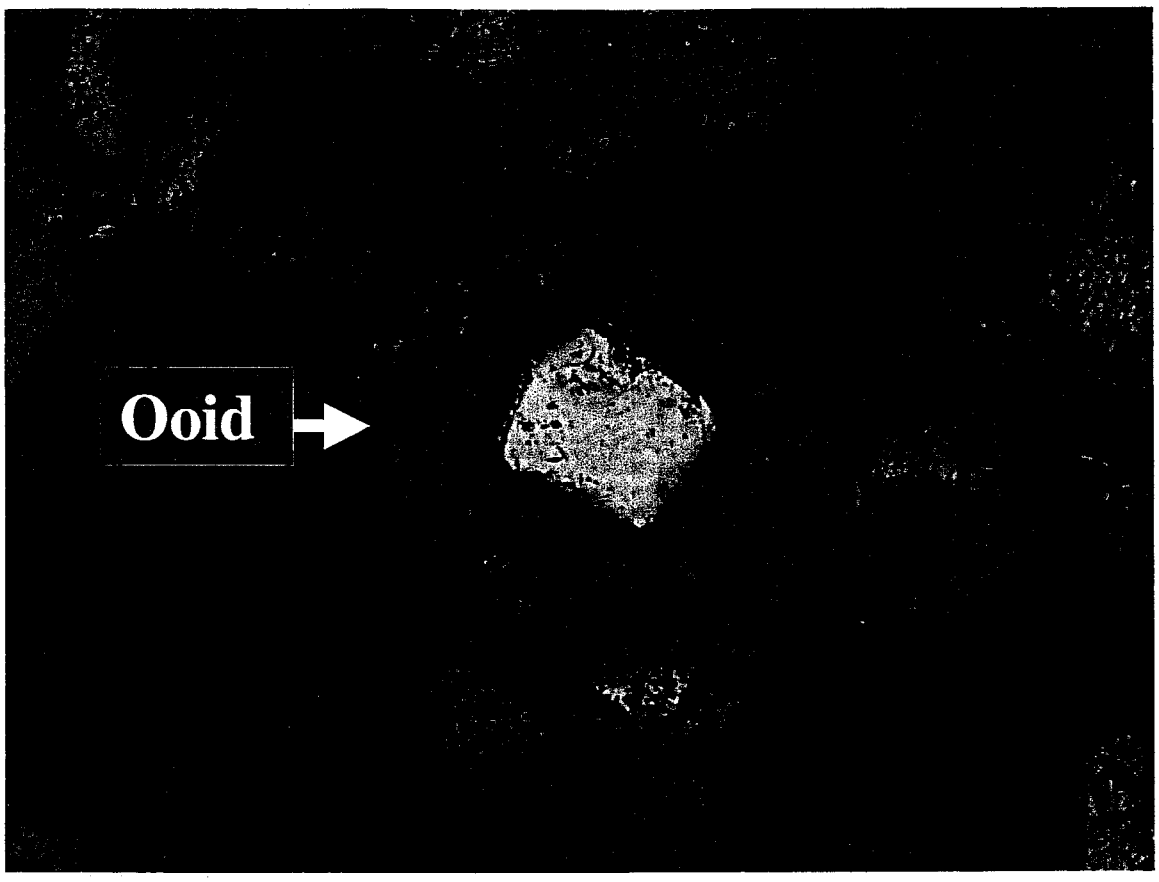

Figure 14—Photomicrograph of cuttings sample from Strata Production Paisano Federal #2 well (15-11S-21E). Frame width = 1mm.

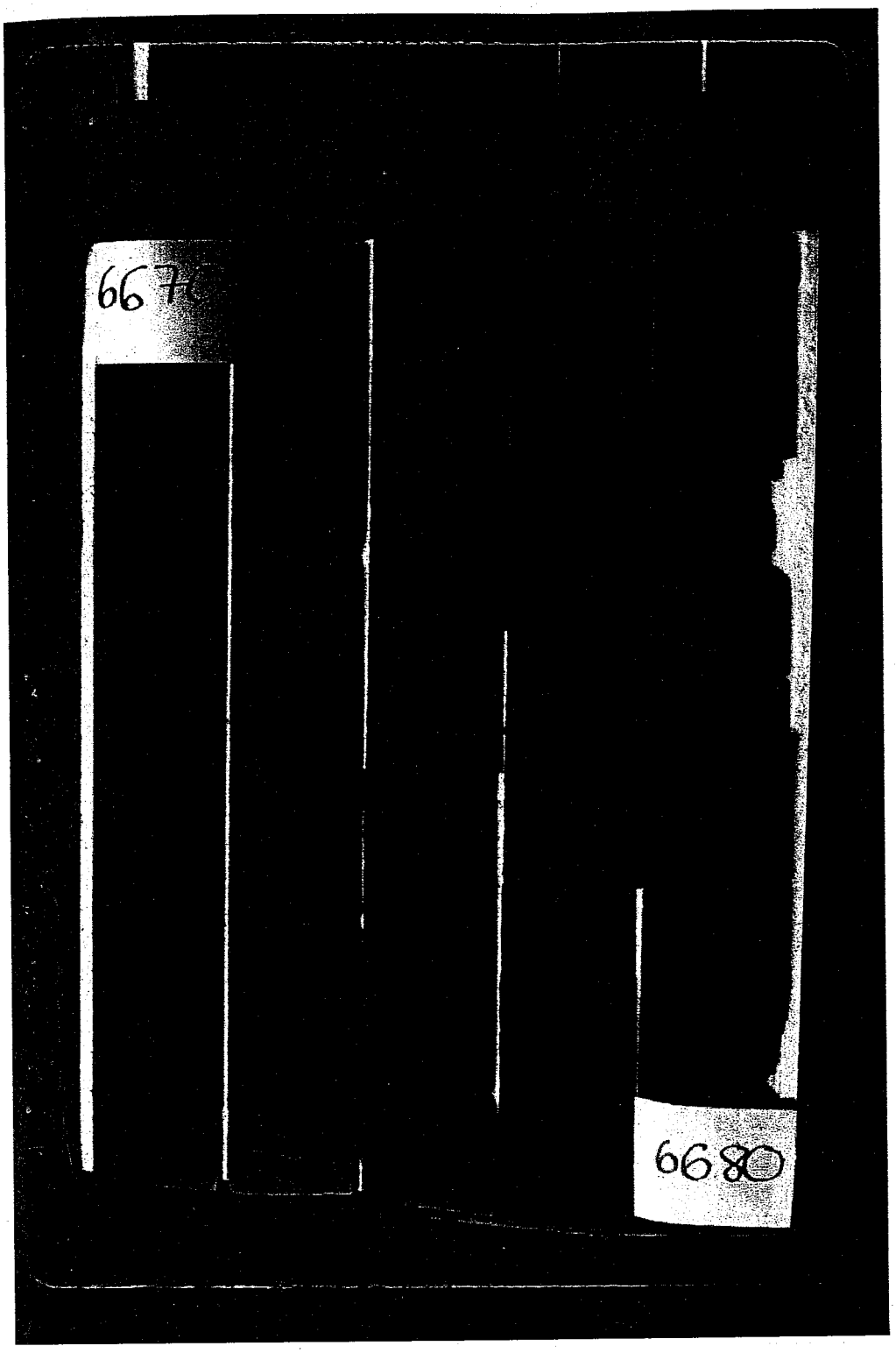

Figure 15—Photo displaying interbedded reservoir sands (lighter colored units) and organic-rich siltstone source rock (dark-colored units) in core taken from Strata Production Company No. 23 Nash Unit well (13-23s-29e). Core is two feet long from top of box to bottom of box (ten total feet of core in box).

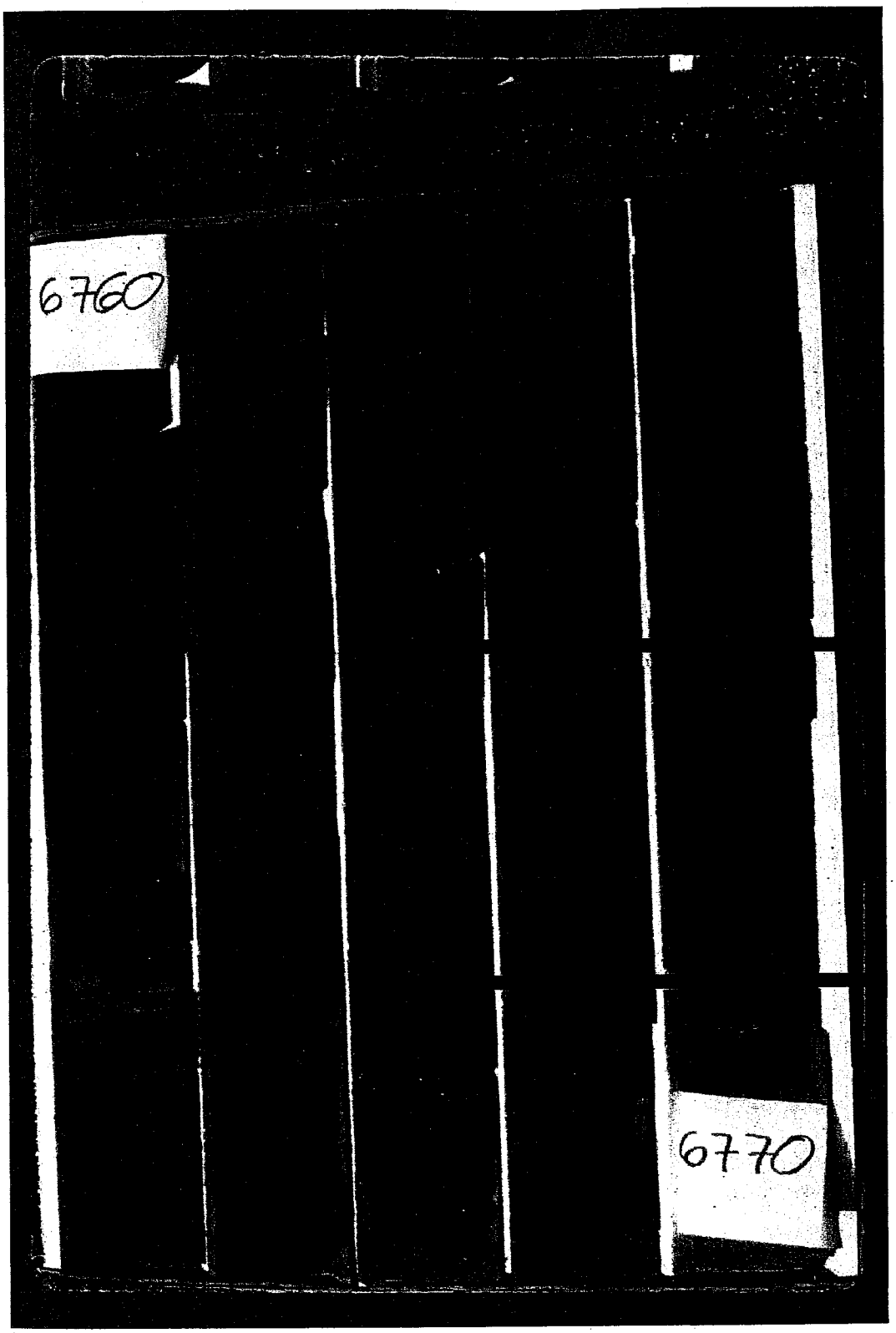

Figure 16—Organic-rich siltstone with interbedded sandstone. Slump feature (red arrow), graded bedding, and rip-up clasts (blue arrow). Note horizontal laminations of organic-rich siltstone. Core is two feet long from top of box to bottom of box (ten total feet of core in box).

units of carbonate-rich siltstones are present as well. Common within the core of the lower Brushy Canyon Formation are finely laminated, horizontal, thin and planar to wavy, or ripple cross-laminated sandstones and siltstones (Figures 15 and 16). Some sands are structureless and fine. Bioturbated sections are present. Many of the contacts between silt-rich units (source) and sand-rich (reservoir) units are sharp and irregular, showing evidence of soft sediment deformation. Other contacts are somewhat gradational, with rip-up clasts sub-parallel to the bedding (Figure 16). The rip-up clasts are very fine sand-sized to gravel-sized. Slump features (Figure 16) and soft-sediment deformation are also present in the core.

DEPOSITIONAL HISTORY OF THE BRUSHY CANYON FORMATION

Currently there are several ideas on the exact method of deposition and origin of the Brushy Canyon sandstones. King (1948), and Newell and others (1953) interpreted the Brushy Canyon rocks as having been marine deposits laid down in shoal waters. Current depositional ideas involve deep-water submarine fans, turbidity currents (Jacka et al., 1967, 1968; Jacka, 1979; Thomerson and Catalano, 1997) and saline density currents (Harms and Williamson, 1988).

Jacka et al. (1967) believe that the Brushy Canyon Formation was deposited by deep sea fans with channel, levee, overbank, and fringe deposits. The channels consist of thick, clean, well-sorted sands. According to their study these sands contain current ripple cross-bedding. The overbank and fringe deposits consist of micro-flame structures, small cut and fill structures, varve-like laminae of sand, silt, and shale, and small climbing ripples or ripple-drift cross-bedding. Overbank deposits are described as flanking the channels, while the fringe deposits form at the distal reaches of the channels

in finely laminated sheets. Both the overbank and fringe deposits contain pelagic-planktonic faunal assemblages (Jacka et al., 1967). Another important aspect of their study is the association of glacially controlled eustatic sea level change. The glacial sea level changes are evidenced by interbedding of the sandstone and siltstone. Times of low sea level allowed for an abundance of clastic sediments to cross the shelf lagoons and platforms and into the submarine canyon heads with the assistance of longshore and tidal currents. From here, the sediments were brought into the basin by a channel-levee-overbank system (Jacka et al., 1967). Growth of the reef on the outer platform was greatly reduced at this time. Fringe deposits were buried with progradation of the fan, eroding the submarine canyon and proximal portion of the fan (Jacka et al, 1967). When the glaciers began to melt, sea level rose. Receding of the fans occurred. The shelf lagoons were allowed to expand, along with carbonate production and reef growth. Fine-grained, laminated, thinly bedded fringe deposits began covering the more proximal fan sediments previously deposited. Similar sediment economics are recorded in the Gulf of Mexico for Pleistocene glacial cycles (Jacka et al., 1967).

Harms and Williamson (1988) believe the Brushy Canyon sediments were deposited within deep, density-stratified water. Shallow, evaporite-clastic shelves introduced saline-rich water to the deeper basin. The saline water spilled over the carbonate banks and reefs surrounding the basin and made its way down the steep margin slope into the greater depths. Channels were identified by Harms and Williamson in both core and outcrops. Straight or slightly sinuous morphology is reportedly exhibited by the channels at high angles to the basin margin. These linear, non-branching channels extend over 70 kilometers into the basin. Very fine-grained sandstone is confined to these

channels, cutting into beds of siltstone. The siltstone beds are laterally extensive and consist of thin layers of silt and organic matter (Harms and Williamson, 1988). The silt and organic matter made its way to the greater reaches of the basin by suspension and, subsequently, settled out of the water column to the basin floor. Harms and Williamson do not believe turbidity currents could have been responsible for these sandstone and siltstone deposits due to the lack of naturally graded sedimentary units and regular vertical sequences of beds. Little areal change in the size or nature of the stratigraphic types or bed thicknesses exists that would indicate a change from proximal to distal fan facies as would occur in such a gravity-induced sediment flow.

Thomerson and Catalano (1997) believe the Brushy Canyon sediments have been deposited by submarine fan and channel complexes that include massive channel and overbank/levee facies with crevasse splays. They agree with authors such as St. Germain (1966), Jack et al (1968, 1972), and Jacka (1979) in their hypotheses for Brushy Canyon Formation deposition. Silt is clean, sands are well sorted and very fine-grained. In support of the work of Fischer and Sarnthein (1987), Thomerson and Catalano believe the siltstones originated as fallout from dust-laden wind that blew over the basin waters. The dunes are believed to have made their way across the platform and onto the shelf where they provided the pre-sorted sand to the channel complexes.

Thomerson and Catalano believe sediments of the Brushy Canyon Formation represent a prograding submarine fan/channel complex, with the basal Brushy Canyon representing the distal-fan facies, and the upper Brushy Canyon representing the intermediate to proximal fan facies. The basal Brushy Canyon contains fringe sands, or very fine-grained sandstone, and siltstone with horizontal microlaminations of organic

material units. These are typical of a distal-fan facies. The upper Brushy Canyon contains sandstones like those of a massive channel, overbank, levee and interchannel facies. Sands are described as quartz-rich, moderately-to-well sorted, and matrix poor. These represent the intermediate and proximal portions of the submarine fan.

Montgomery et al. (1999) support the concept of a gravity-flow mechanism for depositing the Brushy Canyon sediments. They identify turbidity currents and density currents as the most agreed upon transport agents in recent studies, by authors such as Silver and Todd (1969), Berg (1979), Rosser and Sarg (1988), Baser and Bouma (1996), Sonnenfield (96), Harms and Williamson (1988), and Harms and Brady (1996). These currents could be either in deep-water conditions or they could exist during significant sea level fluctuations. Moderate to good sorting of sand grains in their findings give support to the views of Fischer and Sarnthein (1987) in which the sands were supplied by eolian processes. For this scenario, eolian dunes migrated along the platform during low stands of sea level and made their way to the shelf break where the heavy build-up of sands contributed to slumping and turbidity currents. From here the sands were transported deeper into the basin by some form of gravity-flow mechanism. Montgomery et al. (1999) described the Brushy Canyon Formation as containing mostly massive sandstone units, with some local cross-bedding. They also noted microlamination of very fine-grained sandstones and siltstones. The siltstones are described as very organic-rich with some bioturbation. Carbonate beds (limestone or dolomite) are present near the shelf margins, and some calcareous shales are present. Lack of sedimentary structures more indicative of an exact method of deposition and detrital clay, however, made it difficult for Montgomery et al. (1999) to favor upon one particular depositional model.

Regardless, gravity-flow mechanisms require channels. Such channels have already been mapped and identified by authors such as Basham (1996, cited in Montgomery et al., 1999). These channels changed in location, scale, length, and in sedimentary character between the Early and Late Guadalupian time, according to Montgomery et al. (1999). Therefore, they believe, no single model can account for all of the data.

Very fine-grained well-sorted sands and interbedded siltstone, structureless and massive sandstones, horizontally laminated siltstone and sandstone (Figures 15 and 16), flame structures, and slump features (Figure 16) are found in the Nash Draw Unit #23 core of the lower Brushy Canyon unit. These features coincide with what Montgomery et al. (1999), Fisher and Sarnthein (1987), and Jacka et al. (1967) have described in their studies. Submarine fan and channel complexes deposited by saline density or turbidity currents are best suited as depositional models and processes for Brushy Canyon sediments based on these features. The lack of sedimentary structures that could positively indicate one mode over another makes it difficult to favor any one particular mode. As Montgomery et al. (1999) have concluded, no single model can account for everything seen.

TYPES OF KEROGEN

KEROGEN TYPE

Kerogen is defined as the organic matter in rocks that is insoluble in non-oxidizing mineral acids, aqueous alkaline and organic solvents (Brooks et al., 1987). It is generally composed of three main elements: carbon, hydrogen and oxygen. Kerogen can be categorized into four different types based upon elemental composition and origin of the kerogen. These types are liptinite (type I), exinite (type II), vitrinite (type III), and inertinite (type IV).

The types of kerogen in a source rock and the thermal maturity of these kerogens determine the proportion of hydrogen and oxygen in the kerogen. Kerogen type is also important in determining the type of hydrocarbons that will be generated from the source rock with thermal maturity, or whether it will generate hydrocarbons at all. Type I kerogen is composed of bacterially degraded algal material, and the associated lipid-rich components derived from the decomposition of this algal matter (Brooks et al., 1987). The ratio of hydrogen to carbon in type I kerogen is very high, while the oxygen content is low. Hydrocarbons expelled from source rocks with hydrogen contents of greater than seven percent are commonly oil (LaPlante, 1974).

Type II kerogens come from plant debris such as spores and pollen that are the membranous and resistant portions of the plant. Phytoplankton, zooplankton, and bacterial microorganisms deposited in anoxic environments may also create this exinite-

rich material. The hydrogen content in type II kerogen is lower than that of the type I kerogen, but is still significant. The oxygen content of type II kerogen is slightly higher than type I kerogen. Type II kerogen results in source rock that will generate oil and condensate at average maturity, but at high levels of maturity, wet gas is possible (Brooks et al., 1987).

Lignin-rich matter, such as woody parts of higher, terrestrial plants composes vitrinite, or type III kerogen. The hydrogen to carbon ratio in this kerogen is low, but the oxygen content is high (Brooks et al., 1987). Coals and coal-rich shales are commonly formed from vitrinite. Production from type III kerogen is predominantly gas at higher levels of maturity, although oil and condensate may sometimes be produced too.

The last type of kerogen is known as inertinite, or type IV. This type of kerogen is formed from oxidized or highly carbonized lignin (Brooks et al., 1987). It is characterized by low hydrogen content. It will not generate hydrocarbons.

RESULTS OF TYPE KEROGEN ASSESSMENT

The hydrogen index values for all 33 samples range from 47 to 299 g HC/g organic carbon (Figure 17), whereas the oxygen index values range from 9 to 129 mg CO_2/g organic carbon (Figure 18). These values indicate good source potential (Table 1). Plotting the OI versus HI on a graph, a mixture of kerogen types is apparent (Figure 19).

The source rock, based on the visual kerogen analyses for all 10 samples, contains dominantly amorphous-sapropel and herbaceous organic matter (one sample contained a small percentage of vitrinite and inertinite; Figure 8). These types of organic matter

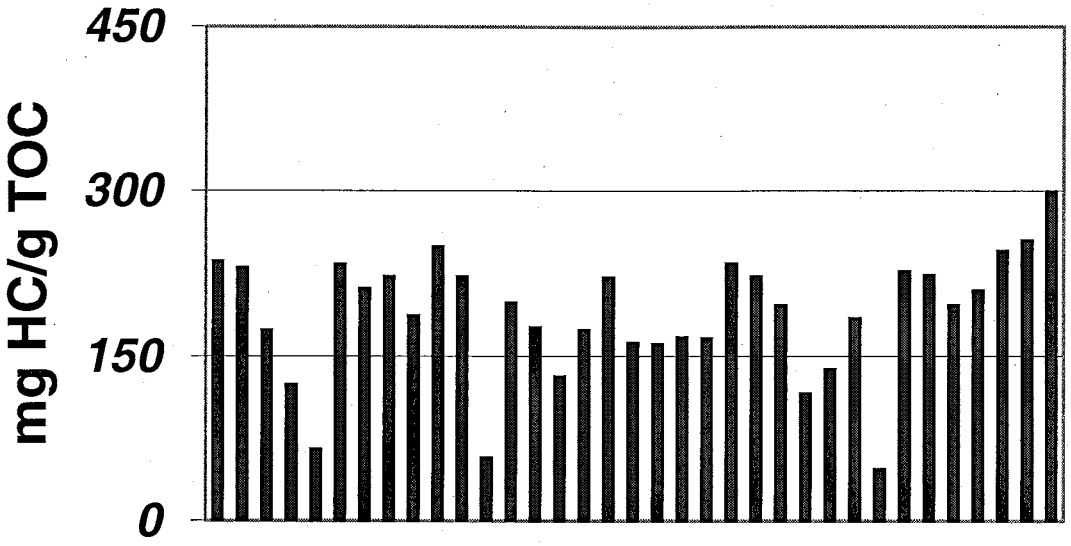

Figure 17—Hydrogen Index values for 33 samples from the lower Brushy Canyon Formation.

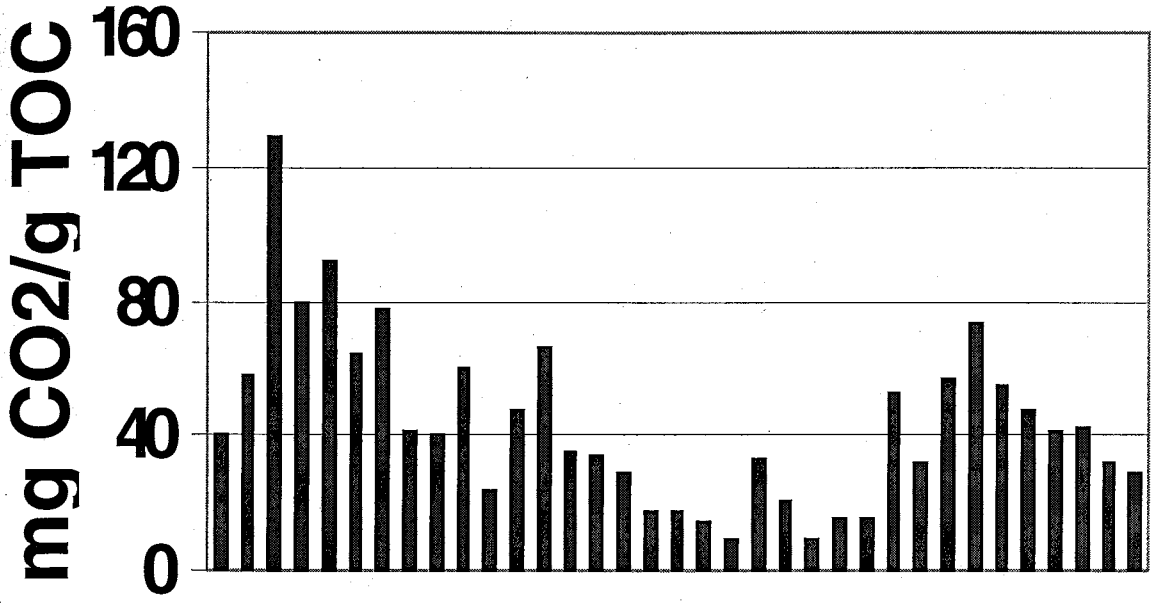

Figure 18—Oxygen Index values for 33 samples from the lower Brushy Canyon Formation.

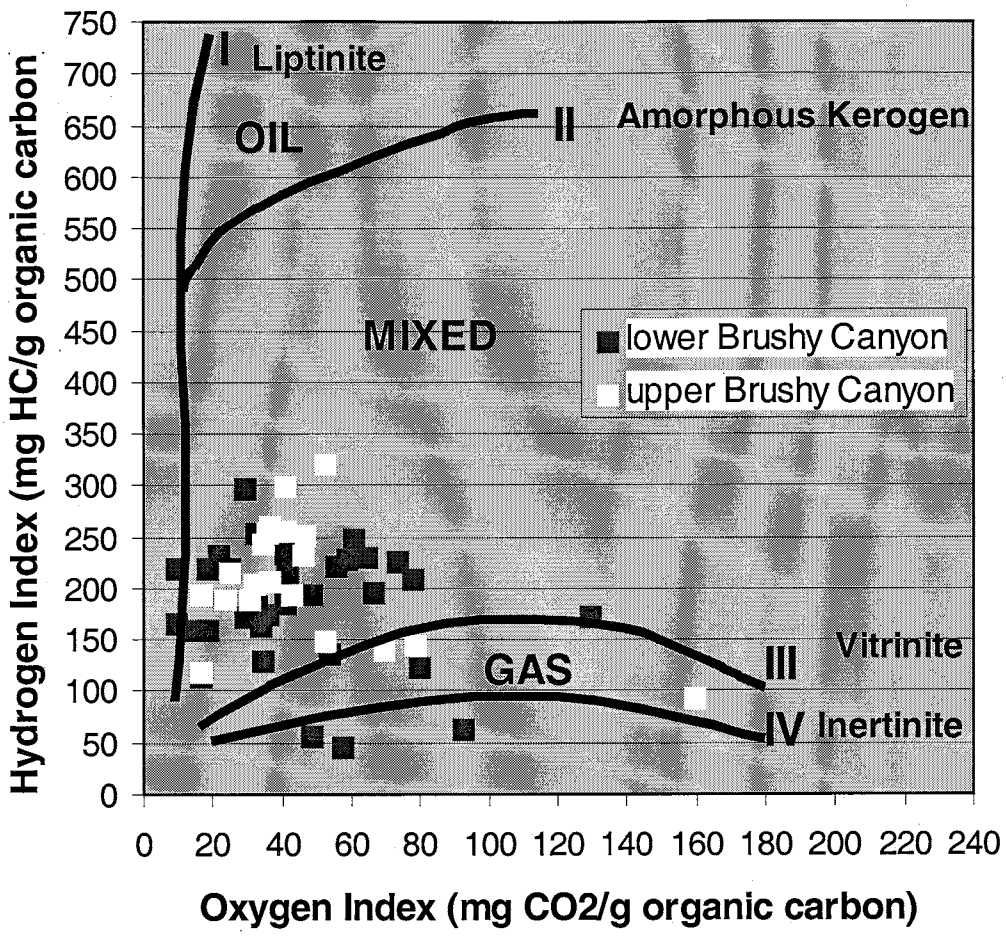

Figure 19—Pseudo Van-Krevelen diagram indicating mixed kerogen type for both upper and lower Brushy Canyon samples.

(amorphous-sapropel and degraded herbaceous) fall in the category of type I and type II kerogen. Most samples have approximately 50% of each type. A map plotting distribution of the kerogen types shows the sample with the woody and inertinitic material closest to the northwest shelf, while the samples with dominantly herbaceous and amorphous-sapropelic organic matter are located at greater depths (Figure 20).

INTERPRETATIONS ON DISTRIBUTION OF KEROGEN TYPE

As was expected, the woody and inertinitic organic material were present in the cuttings sample taken from the well closest to the northwest shelf. These types of organic matter are terrestrial in origin, and therefore are not expected to be in great abundance within the deeper portions of the Delaware Basin. Presence of kerogen types I and II within the source rocks indicates an abundance of algal life and vegetation somewhere proximal to, or within, the basin. Areas that were rich in these forms of life must have been very rich in oxygen and light. The northwest shelf could have served as the origin for these organisms. How did the organisms make their way from light, oxygen-rich areas into deeper portions of the basin where they were deposited and preserved? Strong wind (hurricane), and saline density or turbidity currents could carry the organisms these great distances. Heavier sediments would be first to settle out of the air or water column. As the currents become less turbulent, the finer sediments begin to settle out, and the last particles to be deposited are silt-sized. The fine particle size of the organic matter and silt allows for the two materials to settle out of the water column together.

Why do some samples plot along the type III line on the OI/HI diagram (Figure 19)? Degradation of the kerogen is one possibility. Reworking of sediments can cause

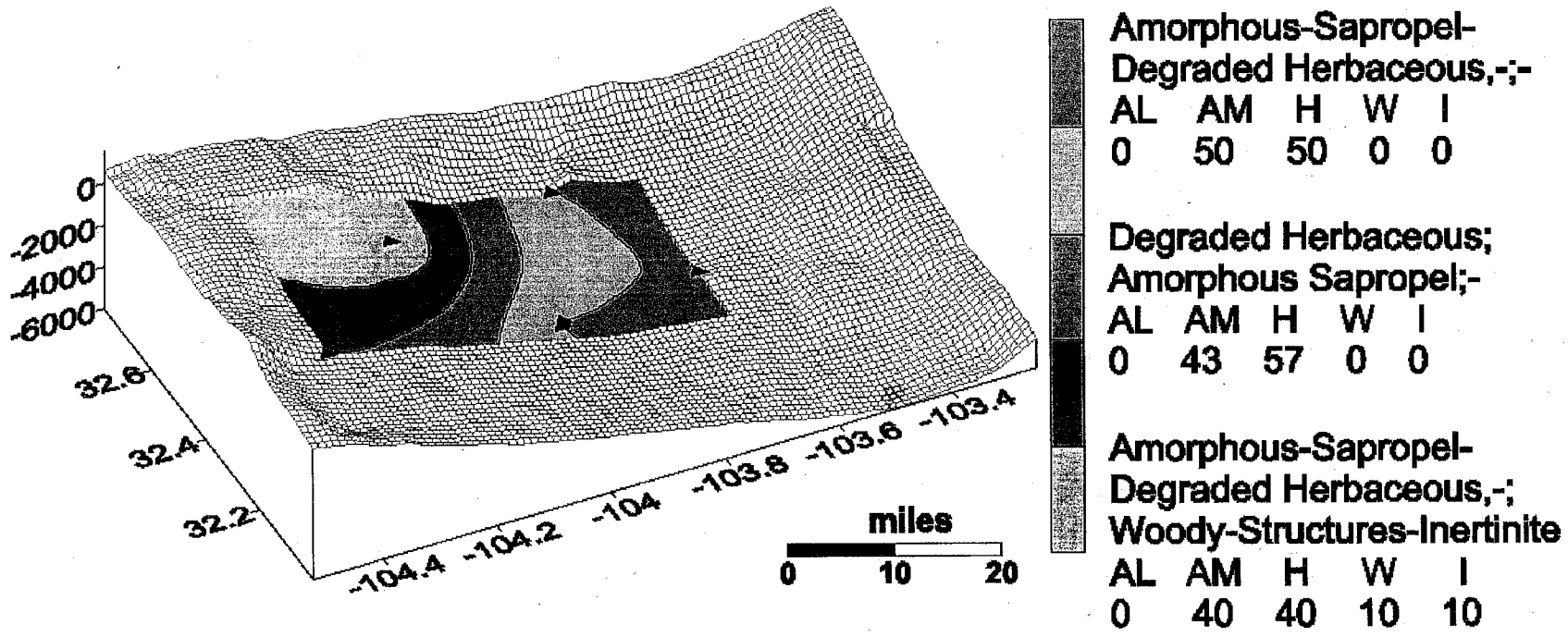

Figure 20—Contour map superimposed on lower Brushy Canyon structure showing change in type kerogen within study area for lower Brushy Canyon source rocks. X-axis = degrees longitude; Y-axis = degrees latitude; Z-axis = depth in feet. AL = algal; AM = amorphous; H = herbaceous; W = woody; I = inertinite. Numbers represent percentage of sample in category. Sample locations marked by black triangles.

oxidation of kerogen. Based on visual kerogen assessments, the organic matter is not type III kerogen. The only possible explanation, therefore, is a chemical change in the organic matter that would make samples plot in more highly oxidized regions of the diagram. Reworking of sediments could have allowed for oxidization of kerogen within it. Bioturbation is the most likely cause for sediment reworking at these depths. Evidence of bioturbation exists within the core. Channels that cut into the siltstone (as suggested by Jacka et al, 1967) could have also allowed for the organic-rich material to become mobile once again. The sediments would return to the water column and then be re-deposited.

Partial oxidation may have also occurred while sediments were settling out of the water column. Exposure to oxygen-rich waters leaves organic carbon vulnerable to such a change. Another possibility is oxidation of the samples during storage. A few samples showed evidence of oxidation in their rusty coloration. This is probably due to alteration of pyrite or other iron-rich crystals in the sediment.

QUANTITY ORGANIC CARBON

TOTAL ORGANIC CARBON

In this chapter, several aspects of total organic carbon (TOC) will be discussed. The first section deals with the importance of total organic carbon in evaluating generating potential of a source rock. Results of geochemical tests are given next, followed by a discussion of results in the "interpretations" section. These first three sections all deal with conventional methods (see Methods and Procedures) for determining TOC. The latter sections deal with a new method tested in this study that involves use of geophysical logs (particularly gamma ray and bulk density logs) for determining TOC in the lower Brushy Canyon Formation.

Background and Importance of TOC in Evaluation of Source Rock

Hydrocarbons are made up of approximately 75 to 95 percent carbon by molecular weight (Jarvie, 1991). Both organic and inorganic carbon may be present in petroleum source rocks. Organic carbon is derived from biogenic matter. Inorganic carbon is an oxidized form of carbon, commonly mixed with calcium or magnesium, and is found in carbonate rocks (Jarvie, 1991). Values of inorganic carbon are not of importance for this portion of the study; only carbon that is organic is crucial. Total organic carbon (TOC) is a measurement of all organic carbon that is extractable, convertible, and residual within the kerogen of a source rock.

Extractable carbon is the organic carbon that is already of an oil and gas composition. It is derived from the thermal breakdown of kerogen. In source rocks, extractable carbon makes up a very small portion (usually less than 25%) of TOC. Convertible carbon is carbon with potential for transformation into oil and gas, but it has not yet been converted by thermal maturation. Finally, residual carbon is the component of the kerogen that has a chemical structure and composition in which there is no potential for generating oil or gas (Jarvie, 1991). All together, these types of carbon represent the organic content of a sedimentary rock and are useful in determining the petroleum potential of that rock.

It is important for the level of total organic carbon in a source rock to be sufficiently large for it to generate significant quantities of hydrocarbons. The lithology of the source rock affects the values for TOC that are necessary for the generation of petroleum from that rock. For example, a carbonate source rock will require slightly smaller values to be considered of good generating potential than a shale (Table 5). Values considered adequate for generation are generally over 1.0 weight percent (Jarvie, 1991). Values between 0.5 and 1.0 are marginal, while values less than 0.5 are inadequate.

Higher levels of TOC usually indicate greater generative potential. However, several factors can alter this trend. Type of kerogen is one factor important in determining usefulness of the TOC value towards generative potential. Each of the three types of kerogen is composed of different percentages of extractable, convertible and residual carbon (Jarvie, 1991). If kerogen is dominantly type I, the proportion of

Table 5—Values of TOC and their correlative generative potential (modified from Jarvie, 1991).

Generative Potential	TOC in shales (wt. %)	TOC in carbonates (wt. %)
Poor	0.0—0.5	0.0—0.2
Fair	0.5—1.0	0.2—0.5
Good	1.0—2.0	0.5—1.0
Very Good	2.0—5.0	1.0—2.0
Excellent	>5.0	>2.0

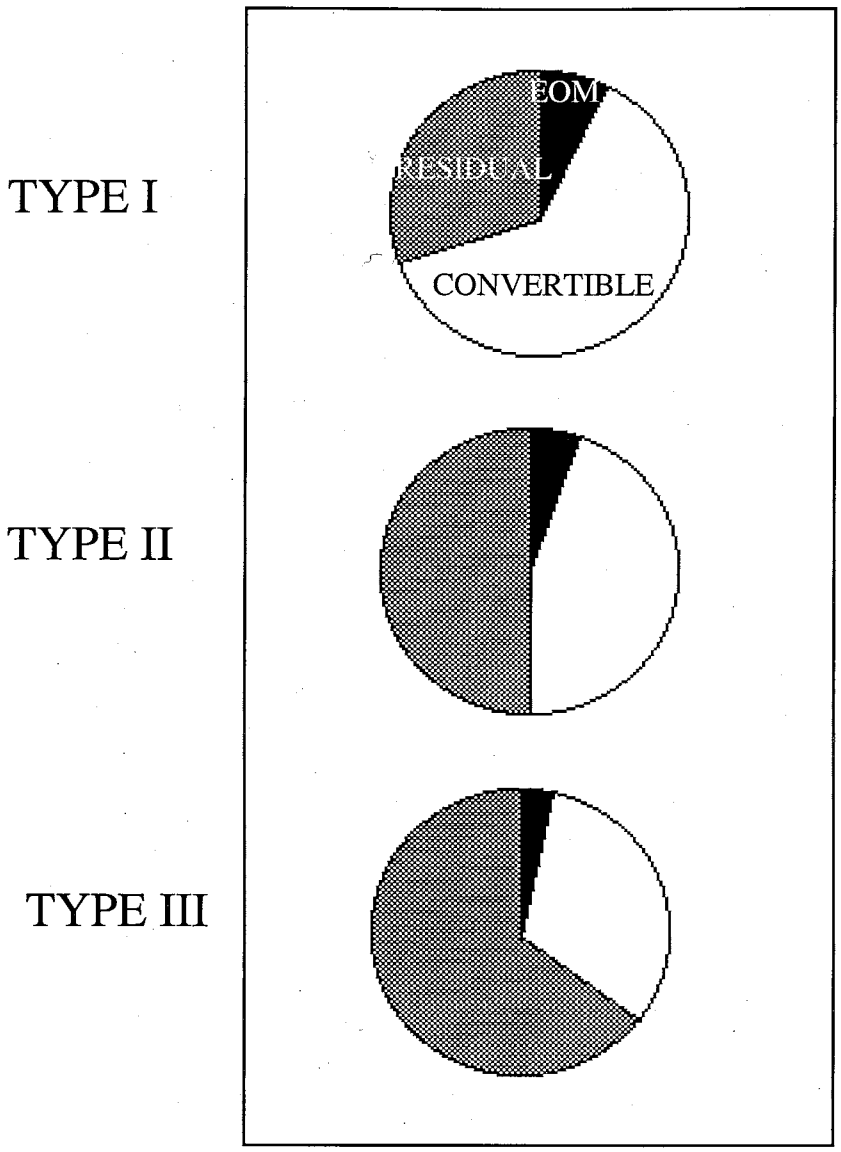

Figure 21—Type kerogen and the respective distribution of organic carbon (modified from Jarvie, 1991). Black = extractable organic matter (EOM) carbon; White = convertible carbon; Gray = residual carbon.

convertible carbon tends to be greater in comparison to extractable and residual carbon (Figure 21). This type of kerogen is likely to produce significantly more oil than a kerogen of type III. A type III kerogen is composed mostly of residual carbon, and would therefore generates less oil. A type II kerogen is almost half convertible carbon and half residual carbon and would probably create a quantity of oil between that of type I and III kerogens.

The following factor needs to be considered when estimating generative potential of a source rock from TOC values. Increased thermal maturity of kerogen results in increased extractable organic carbon, and decreased convertible carbon (Jarvie, 1991). In time, extracted carbon will keep increasing, and so will residual carbon. Also, oil-prone convertible carbon breaks down more completely under lower thermal stress than gas-prone convertible carbon (Jarvie, 1991). High thermal stress may affect the volume of oil created from the kerogen by creating greater amounts of residual carbon than extractable carbon, at the expense of convertible carbon. The TOC value resulting will likely represent almost entirely residual carbon.

RESULTS OF TOC ANALYSES

Total organic carbon levels of lower Brushy Canyon source rocks range from 0.56 to 2.41 weight percent (Figure 22 and Table 6). All TOC measurements were made on cuttings samples with exception to two, which are from core. Upper Brushy Canyon samples range from 0.54 to 1.92 weight percent (Table 7). All upper Brushy Canyon samples were taken from cuttings. Leco method values of TOC support values from Rock-Eval pyrolysis for both upper and lower Brushy Canyon samples (Tables 6 and 7).

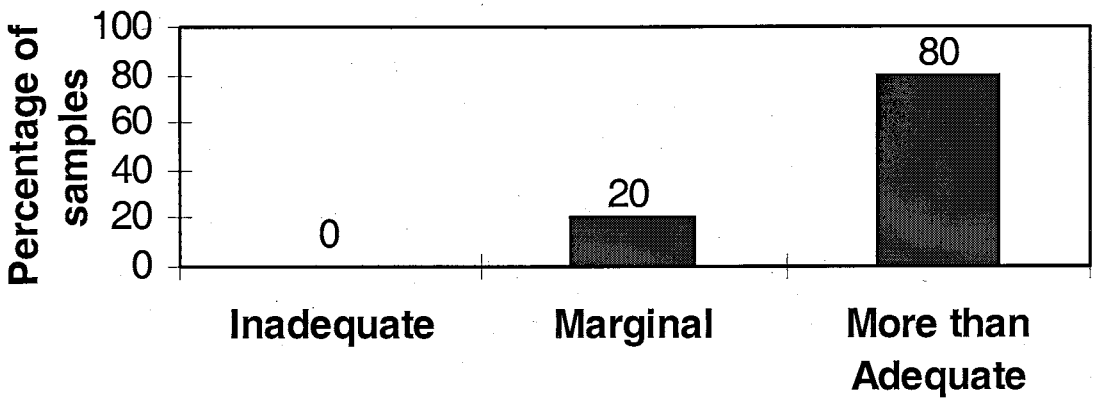

Figure 22—Total organic carbon content (in weight percent) for 32 samples from the lower Brushy Canyon Formation. TOC values are from Rock-Eval pyrolysis.

Table 6—Comparison chart for TOC values (in weight percent) derived from Rock-Eval pyrolysis, versus those derived from the Leco Method for samples from the lower Brushy Canyon. All samples taken from cuttings except for one (marked with *) which is from core.

Operator	Well Lease Name	Sec/T/R	Sample Depth (ft)	Leco TOC	Rock-Eval TOC
Strata Production	19 NASH UNIT	12-23s-29e	6620-6680	1.76	1.76
			6750-6780	0.98	1.07
Strata Production	PAISANO FED NO 2	15-22s-32e	8640-8650	1.43	1.43
Siete Oil & Gas	NUGGET STATE NO 1	36-19s-31e	7060-7070	1.32	1.32
			7140-7160	0.98	1.01
Strata Production	7 LEE FEDERAL	25-20s-28e	5220-5230	1.49	1.49
			5270-5275	0.98	1.32
Collins & Ware	NO 1 MULEY FED	26-26s-25e	4540-4550	0.98	1.6
			4640-4650	1.21	1.21
Cities Service	17 BIG EDDY UNIT	2-21s-29e	6670-6680	1.26	1.26
Myco Industries	110 BIG EDDY UNIT	9-22s-28e	5780-5790	1.93	1.93
Read & Stevens	2 NORTH LEA FED	10-20s-34e	8210-8220	1.52	1.52
Continental	BELL LAKE NO 6	6-23s-34e	8380-8390	0.98	0.98
Pogo Production Co.	NO 1 STATE 58 WELL	15-24s-27e	5610-5620	1.10	1.10
Superior Oil Co.	1 MEANDER FED	14-25s-25e	4710-4740	1.02	1.02
Gulf Oil Corp.	PECOS IRRIGATION ST COM NO 1	20-25s-28e	5840-5860	1.40	1.40
Pan American	NO 36 POKER LAKE UNIT	28-24s-31e	7960-7980	1.38	1.38
			8040-8060	1.11	1.11
Ike Lovelady Inc.	ROSS DRAW FED COM NO 1	33-26s-30e	6960-6980	1.55	1.55
			7160-7170	1.51	1.51
Strata Production	GANSO STATE NO 2	32-20s-33e	8030-8055	1.23	1.23
Strata Production	1 PAPAGAYO FED	27-23s-34e	8410-8420	1.63	1.63
			8560-8570	1.53	1.53
Strata Production	NO 5 LECHUZA PROD	15-22s-32e	8370-8400	1.22	1.22
Morris T. Antwell	1 MESA GRANDE	11-22s-26e	4750-4760	1.17	1.17
Gulf Oil Corp.	ESTILL 'AD' NO 2	20-24s-26e	4800-4830	1.33	1.33
			5120-5140	0.60	0.60
Pogo Production Co.	NO 2 CAL-MON	35-23s-31e	8010-8030	0.79	0.79
			8140-8150	0.92	0.92
H.N.G. Oil Co.	NO 1 VALDEZ 5 COM	5-24s-28e	5750-5800	1.14	1.14
			5970-6100	1.00	1.00
Skelly Oil	NO 1 CEDAR CANYON	9-24s-29e	6390-6400	0.86	0.86
			6640-6650	1.77	1.77
Strata Production	NASH UNIT NO 23	13-23s-29e	6814	*2.41	*2.41

INDICATES VARIATION IN TOC VALUES

Table 7—Leco versus Rock-Eval TOC values (in weight percent) for samples from the upper Brushy Canyon. All samples taken from cuttings.

Operator	Well Lease Name	Sec/T/R	Sample Depth (ft)	Leco TOC	Rock-Eval TOC
Strata Production	PAISANO FED NO 2	15-22s-32e	8220-8230	0.54	0.54
Collins & Ware	NO 1 MULEY FED	26-23s-25e	4090-4100	1.50	1.50
Pogo Production Co.	NO 1 STATE 58 WELL	15-24s-27e	5170-5180	1.92	1.92
Superior Oil Co.	1 MEANDER FED	14-25s-25e	4470-4500	0.94	0.94
Gulf Oil Corp.	PECOS IRRIGATION ST COM NO 1	20-25s-28e	5670-5680	1.13	1.13
Pan American	NO 36 POKER LAKE UNIT	28-24s-31e	7600-7610	1.71	1.71
Strata Production	GANSO STATE NO 2	32-20s-33e	7800-7810	0.95	0.95
Strata Production	1 PAPAGAYO FED	27-23s-34e	7940-7950	0.84	0.84
Phillips Pet. Co.	NO 1 STATE K-2538	32-23s-27e	4270-4300	1.13	1.13
Harvey E. Yates	NO 1-Y TAYLOR DEEP '12'	12-18s-31e	5470-5480	1.36	1.36
Morris R. Antwell	1 MESA GRANDE	11-22s-26e	3720-3730	1.43	1.43
Yates Petroleum Corp.	S AVALON 'MA' FED	14-21s-26e	3430-3440	1.57	1.57
Gulf Oil Corp.	ESTILL 'AD' NO 2	20-24s-26e	3760-3830	1.05	1.05
Pogo Production Co.	NO 2 CAL-MON	35-23s-31e	7030-7040	1.16	1.16
H.N.G. Oil Company	NO 1 VALDEZ 5 COM	5-24s-28e	4800-4830	1.68	1.68
			4890-4900	1.38	1.38
			5530-5550	0.95	0.95
Skelly Oil	NO 1 CEDAR CANYON	9-24s-29e	5410-5460	1.14	1.14
			6120-6140	0.58	0.58

Greatest percentages of TOC in the lower unit of the Brushy Canyon Formation are present along a trend that begins along the shelf margin in the northwestern portion of our study area and reaches southwestward into the deeper basinal region (Figures 23 and 24). The product of TOC and net thickness source rock was calculated in order to estimate generative potential of source rocks within the project area. Source rock intervals were determined from zones with a combination of high gamma ray intensity and high resistivity in the logs. All of these zones were added cumulatively to come up with the net thickness of source rock.

Trends of the generative potential are similar to that of TOC (Figure 25). Both contour maps plotted from data from 33 samples show greatest values in a northwest-southeast trending region in the western portion of our study area. The samples for both the upper and lower Brushy Canyon Formation prove to be marginal to more than adequate for generating hydrocarbons, and good to very good overall for generating oil.

INTERPRETATIONS

Trends of TOC reflect that there must be some sort of control on the quantity of organic matter within the study area. Organic productivity, accumulation, and preservation are likely controls responsible for distribution of organic carbon. Terrestrial matter is most often found along continental margins, or in areas of river runoff, whereas marine matter is usually from the euphotic zone, where sunlight can pass through the water (Calvert, 1987). Because the Brushy Canyon Formation contains amorphous sapropel and herbaceous organic matter, this organic matter may have originated from the euphotic zone, or have been transported through channel and fan complexes to deeper portions of the basin.

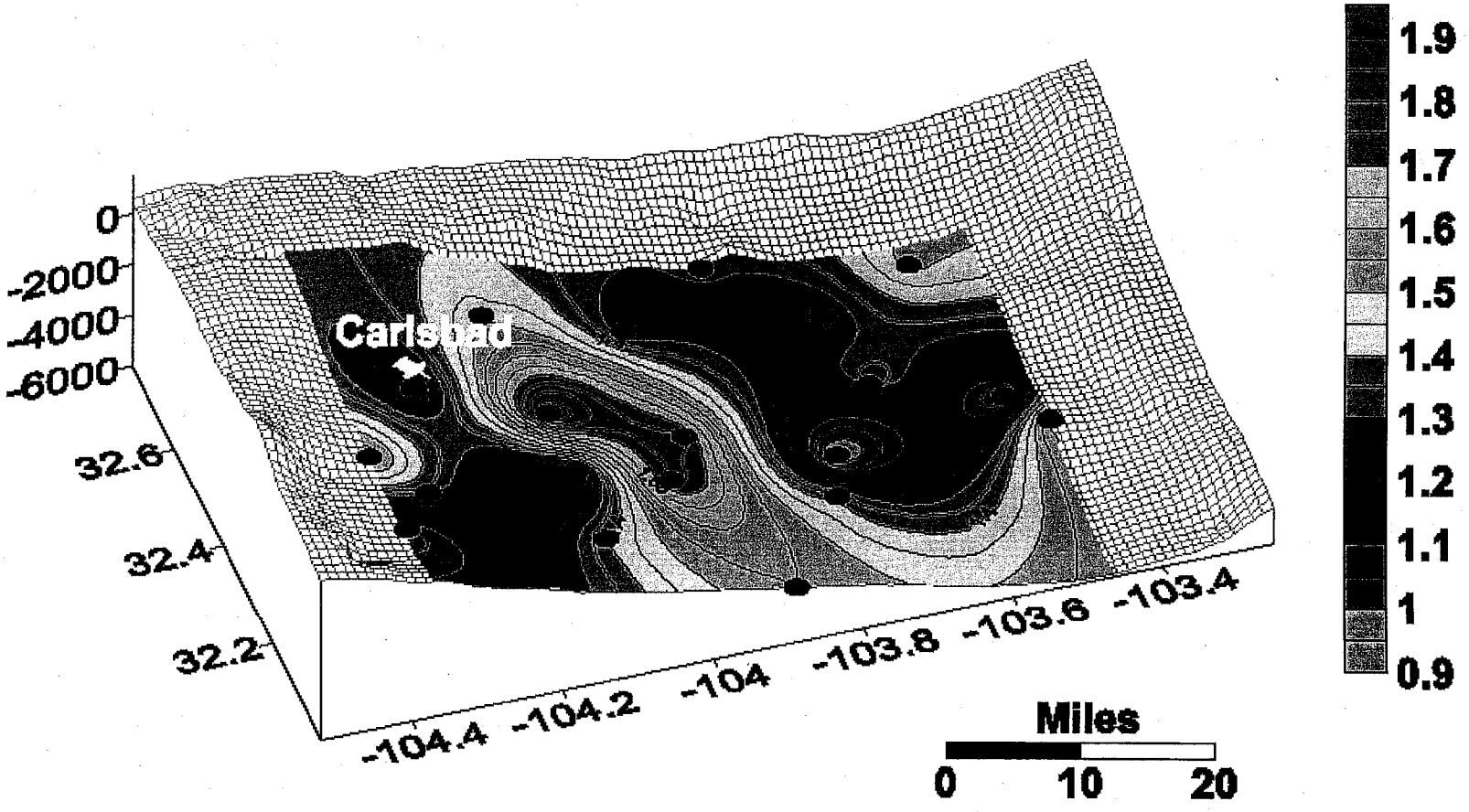

Figure 23—Contour map of total organic carbon (TOC in weight percent) for lower Brushy Canyon organic-rich siltstones superimposed on lower Brushy Canyon structure.

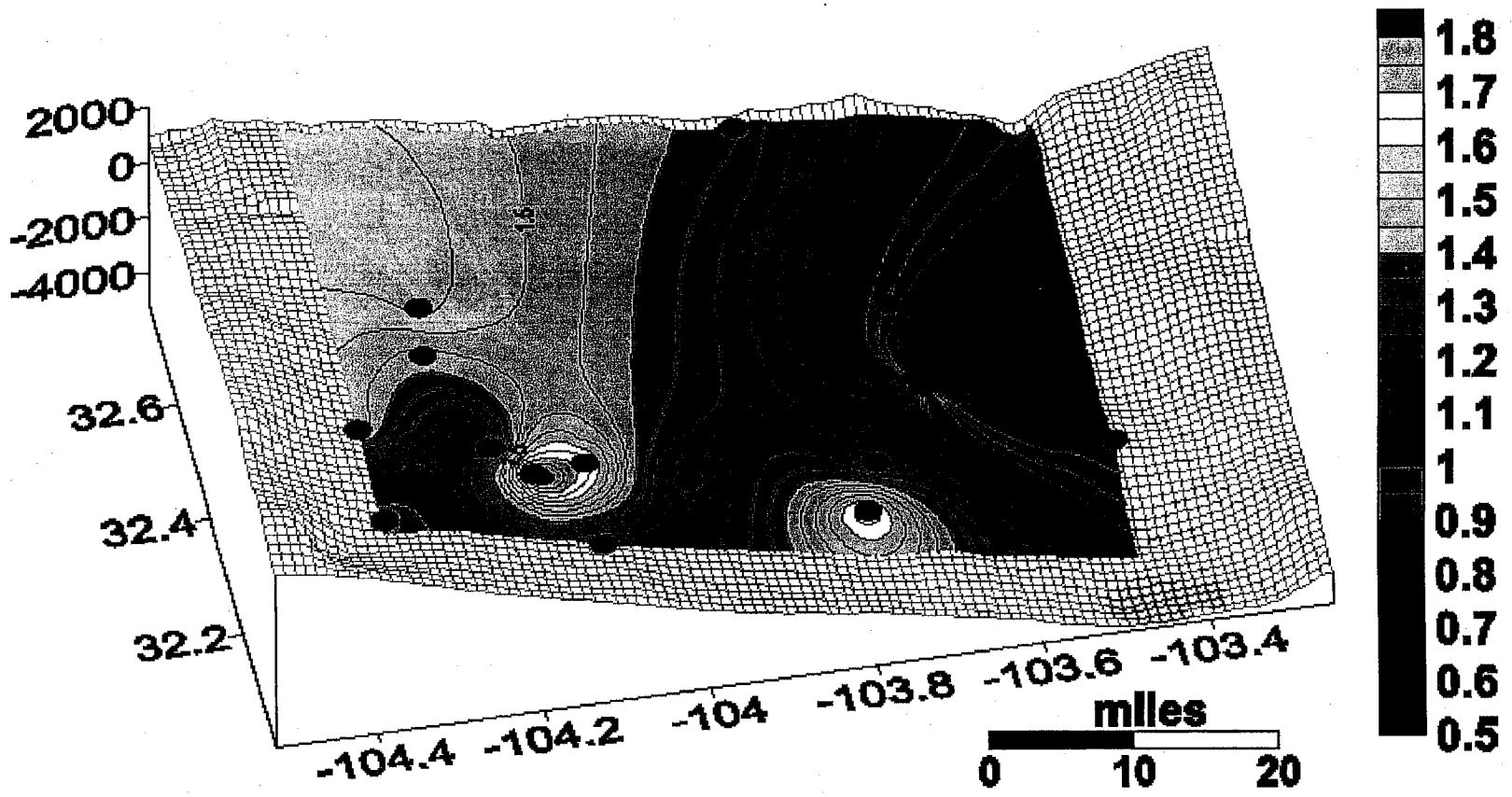

Figure 24—Contour map of TOC (in weight percent) for upper Brushy Canyon superimposed on upper Brushy Canyon structure. X-axis = degrees longitude; Y-axis = degrees latitude; Z-axis = depth in feet.

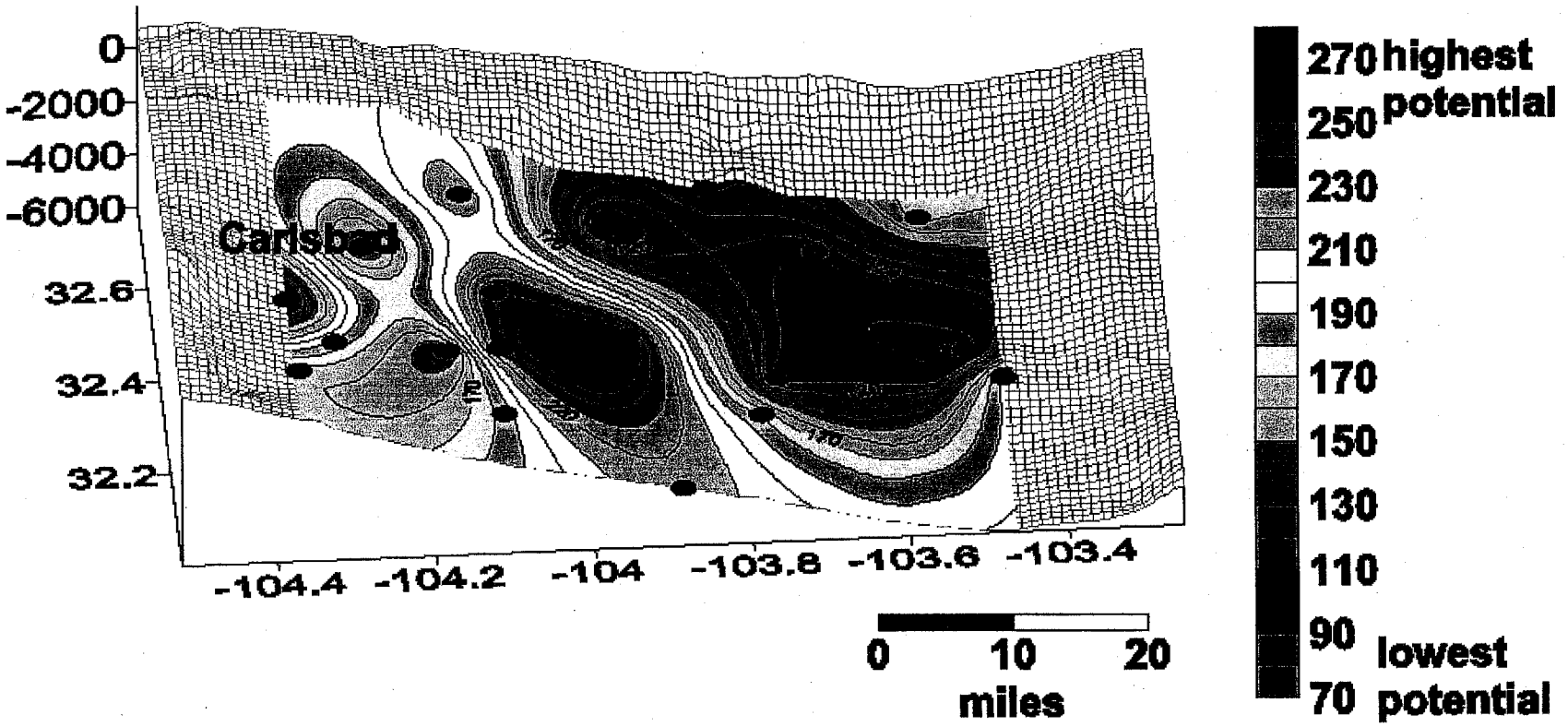

Figure 25—Generative potential for lower Brushy Canyon source rocks superimposed on lower Brushy Canyon structure. Values derived from product of net thickness and TOC for lower Brushy Canyon organic-rich siltstones. X-axis = degrees longitude; Y-axis = degrees latitude; Z-axis = depth in feet.

The high TOC trend from the northwest to the southeast is possibly a result of dilution of TOC in the surrounding areas caused by the influx of clastic sediment. Sediments introduced by submarine channels would rework sediments already deposited. Oxidation of the organic matter could occur. The greater grain size of the sediment in which the organic matter is re-deposited would also leave the matter vulnerable to further oxidation and consumption due to the looser packing of the grains. This mixing would result in an overall decrease of TOC in comparison to neighboring areas with finer-grained sediments. Many channels have been identified and mapped within both the upper and lower Brushy Canyon by authors such as Basham (1996, cited in Montgomery et. al, 1999) and Thomerson and Catalano (1996). Incision of the siltstones by these channels would have introduced coarser sediments. No grain size vs. TOC analysis was performed in this study, therefore it is not certain whether or not these channels were the cause of variation in the TOC levels.

Another possible control on trends of TOC is water depth. There is a decrease in carbon content with increasing water depth due to the decrease of sedimentation rate in deeper water environments (Calvert, 1987). Less organic matter makes its way into the deepest portions of the basin because of the longer transit time involved. The longer the organics are suspended in the water column, the greater the chance for consumption by organisms or degradation by oxygen. Fast sedimentation or anoxic water environments will minimize these affects and allow for a greater concentration of organic matter. Sediment supply for the lower Brushy Canyon appears to have originated from the northwest shelf based on channel-forms previously mapped. If lower Brushy Canyon paleogeography was somewhat similar to the current geography, with the shelf edge to

the northwest, the water depths would have increased from the northwest portion of the study area to the southeast. If so, water depth doesn't seem to play a major role in the variation of TOC levels within the study area. It could have a greater effect in much deeper portions of the basin outside of this study area (Pecos and Reeves Counties, Texas).

Zones of higher TOC levels could also be explained by the presence of upwelling. Upwelling zones may include anoxic zones, oxic zones, or both. Upwelling occurs when water moves vertically within the sea, with bottom water rising to the surface (Demaison and Moore, 1980). The upwelling could be due to wind stress and the Coriolis force, as well as temperature, density, or salinity differences within the water column. If the sediments were indeed deposited by density currents, zones of upwelling would be a great explanation for Brushy Canyon TOC patterns, because areas of upwelling are common sites of high organic productivity and preservation (Calvert, 1987). Evidence of an area of upwelling would be the presence of phosphate and nitrate compounds. Further analyses would need to be performed to determine whether these compounds are present.

Higher productivity is not sufficient by itself as an explanation for regions of greater organic content. Accumulation and preservation are also important factors. Less than one percent of organic matter that is produced accumulates for inclusion in sediments (Dow, 1977). The organic matter may be transported by turbidity currents or saline density currents, destroyed by grazing organisms, or chemically reduced while in the water column before it reaches the bottom sediment. The grain size, texture, and lithology of the sediment also make a difference in the concentration of organic matter. Finer-grained sediments such as silt and clay are more likely to accumulate greater

amounts of organic matter due to the similar hydrodynamics they share with the organic material (Tyson, 1987). Closer packing of the sedimentary particles also decreases the chance of oxidation of the organic matter by pore waters. An anoxic water environment is best for preservation of organic matter because in not only reduces degradation by oxygen, but it also decreases the chance of consumption by organisms. Very few organisms can survive in environments with extremely low levels of oxygen.

Greater TOC levels are indicative of regions with higher percentages of fine-grained material, fast sedimentation rates of these fine-grained sediments, and adequate preservation factors. Regions of lower TOC indicate possible oxidation, degradation, or consumption of organic matter, or perhaps simply lower organic productivity. Although our TOC values are indicative of adequate generative potential, it is necessary to also consider kerogen types and maturity levels of the organic matter. Organic matter in the lower Brushy Canyon is dominantly type I and II kerogen. These types of kerogen are indicative of carbon levels in which a higher ratio of extractable and convertible carbon to residual carbon exists (Figure 21). The TOC should therefore be a good estimate of generative potential for oil. Maturity, however, is another aspect of the source rock to consider in determining generative potential for oil. In regions of extensive thermal maturity, we can expect to see higher percentages of residual carbon than in regions of lower thermal maturity. Higher maturity will reflect lower remaining generative potential, even if TOC content is high.

The majority of samples evaluated using Rock-Eval pyrolysis and other procedures were taken from cuttings over intervals often in excess of tens of feet. Samples taken from the core resulted in much greater TOC than many of the cuttings

samples values (2.41 wt % for core sample vs. 0.56 to 1.91 wt % in cuttings samples). It is likely that higher values of TOC are actually present throughout organic-rich siltstones of the lower Brushy Canyon. However, averaging of high and low TOC values from different depths resulted in slightly lower TOC values in cuttings samples. Because these values are still considered moderate to more than adequate for generation of hydrocarbons, it is possible to predict much greater generative potential than our data indicates.

ESTIMATING TOC BASED ON LOG RESPONSE

Efforts to calculate TOC based on log response proved to be successful in other basins (Schmoker, 1981; Meyer and Nederlof, 1984). These studies involve models and equations that incorporate total organic content, and resistivity, neutron porosity, density, and gamma ray logs. In studying the relationship between gamma ray intensity (radioactivity), bulk density, neutron porosity, and resistivity to total organic content, it was determined that gamma ray logs and bulk density logs were most useful in estimating TOC for this study of the Brushy Canyon Formation.

In the Delaware Basin, there is a proportional relationship between the gamma ray response for the source rock of the lower Brushy Canyon and the TOC content (Figures 26 and 27). Natural radioactivity of a rock is caused by three factors: potassium content, thorium content, or uranium content. Factors that may control the association between gamma ray intensity and organic matter content according to Schmoker (1981) are: the uranium content of the seawater at the time of deposition, the type of organic matter deposited, the water chemistry near the water-sediment interface, or the rate of sediment

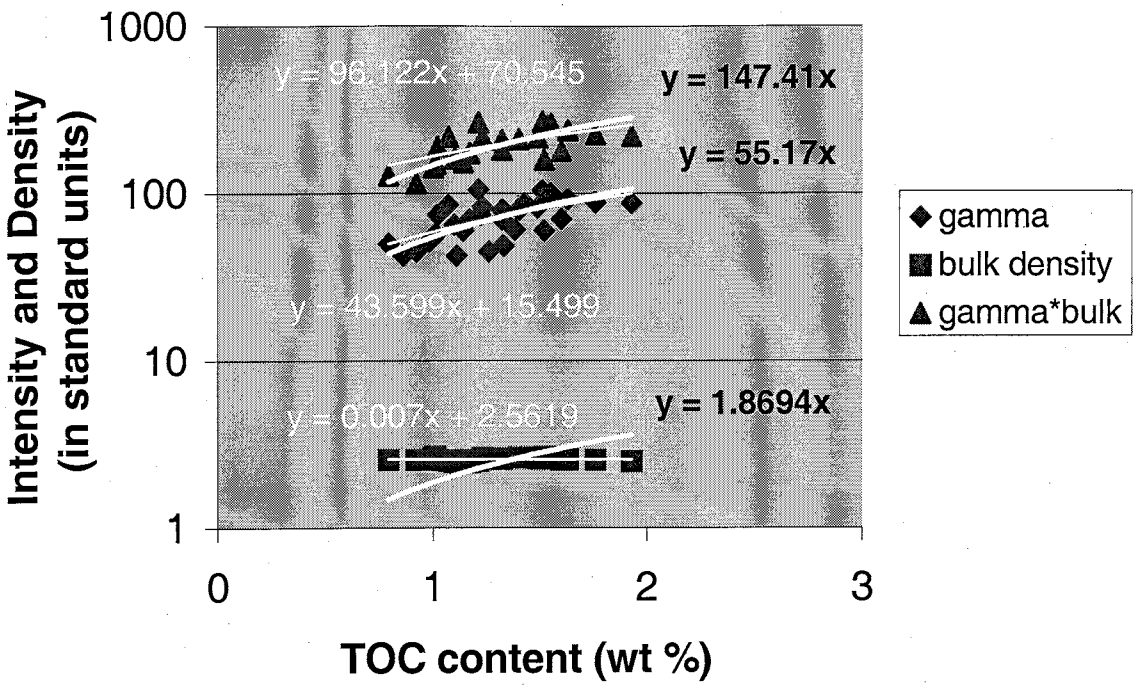

Figure 26—Comparison chart: gamma ray intensity, bulk density, and gamma-bulk combination vs. TOC content showing linear relationships. Thin white line indicates equation of best-fit line through data points. Thick white line is equation of line fitting data points with a 0-0 intercept.

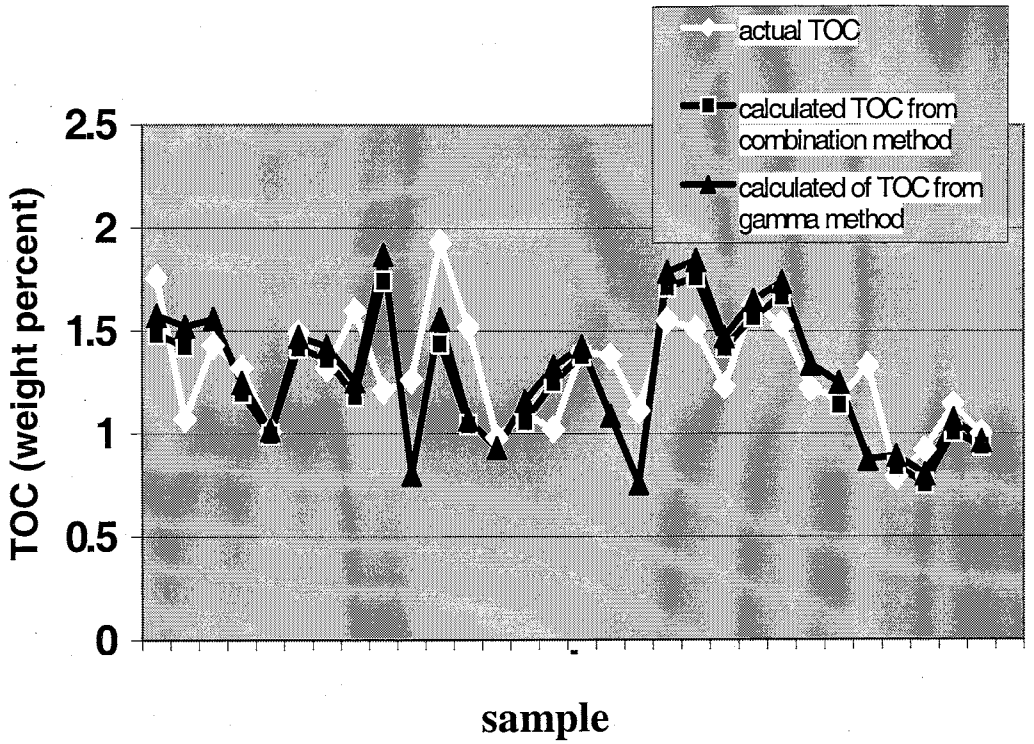

Figure 27—Actual versus calculated TOC for samples in random order. Actual TOC values in white. Calculated values in black.

deposition. Any correlation between gamma ray intensity and total organic content must suggest a relative constant character of these controlling factors in both time and location.

Gamma Ray Log Method

The proportional relationship between radioactivity of the source rock and levels of total organic content indicate the possibility of a straightforward approach to calculating TOC from the gamma ray log alone. The slope of the line relating laboratory determined TOC values for over 32 well cuttings samples to gamma ray intensity averaged over the same sampling interval is approximately 55.17 (Figure 26). In order to calculate TOC based on gamma ray log intensity, high and low gamma ray values for each sampling interval were first averaged. This value acts as a representative of the unit sampled from (unit is section from log showing high gamma ray response over several feet or more). Subsequently, these numbers were divided by 55.17 (the slope of the line relating the averaged gamma ray value to the measured TOC value; Figure 26). This method, which involves only one type of log value to calculate TOC, gives a correlation of 0.3596 (Figure 28). Greatest error is off by approximately 0.69 weight percent, while the smallest error is off by less than –0.01 weight percent (Figure 29 and Table 8).

Combination Log Method

Bulk density values were also used in this study in an attempt to reduce the error in the TOC estimations. In previous studies, it was found that the bulk density was commonly inversely related to the TOC. In this study, however, the TOC and bulk density were related by a slope of 0.007 (Figure 26) indicating that they are less likely to be as useful in estimation of TOC. Regardless, a product of the bulk density and gamma

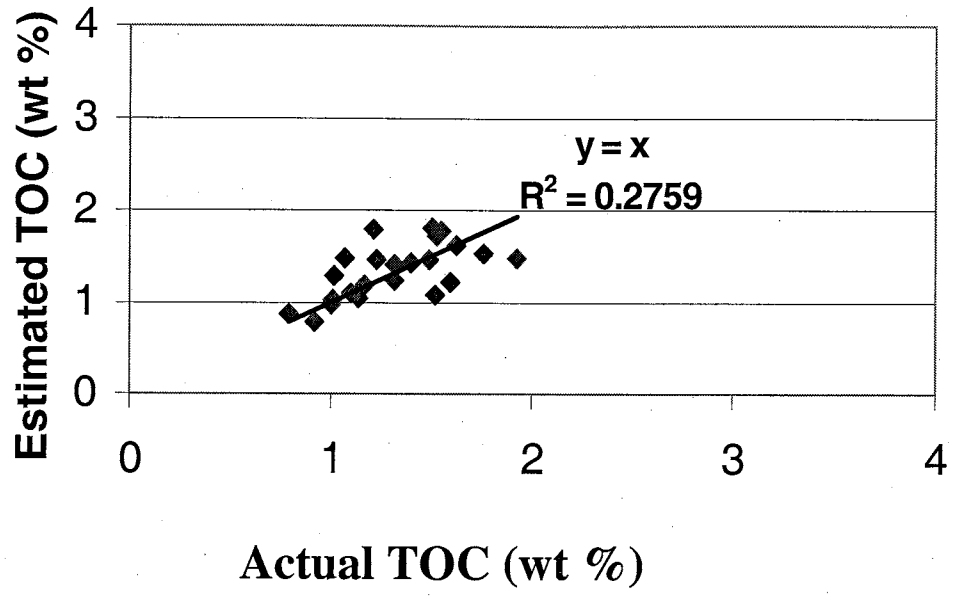

Figure 28—Calculated versus actual TOC using gamma ray method. R^2 = correlation coefficient.

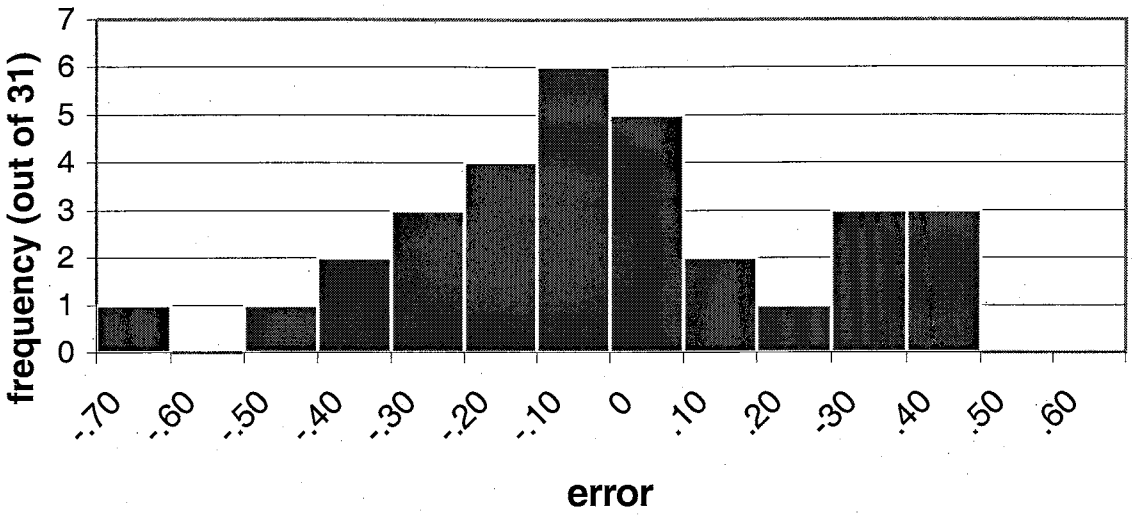

Figure 29—Error histogram. Frequency and error distribution (by weight percent) for TOC calculations using gamma method.

Table 8—List of values for TOC (actual and calculated), and errors (calculated TOC – actual TOC for both gamma method and combination method). Black row contains averages of columns.

Measured TOC content (wt %)	Calculated TOC using Gamma method	Calculated TOC (Gamma) less Measured TOC	Calculated TOC using Combination Method	Calculated TOC (Combination) less Measured TOC
0.79	0.91	0.12	0.86	0.07
0.86	0.77	-0.09		
0.92	0.82	-0.10	0.78	-0.14
0.98	0.93	-0.05		
1	0.98	-0.02	0.97	-0.03
1.01	1.03	0.02	1.02	0.01
1.02	1.35	0.33	1.29	0.27
1.07	1.55	0.48	1.47	0.40
1.1	1.18	0.08	1.09	-0.01
1.11	0.77	-0.34		
1.14	1.09	-0.05	1.04	-0.10
1.17	1.27	0.10	1.18	0.01
1.21	1.90	0.69	1.80	0.59
1.22	1.36	0.14		
1.23	1.50	0.27	1.46	0.23
1.26	0.82	-0.44		
1.32	1.27	-0.05	1.23	-0.09
1.32	1.45	0.13	1.40	0.08
1.33	0.89	-0.44		
1.38	1.11	-0.27		
1.4	1.45	0.05	1.42	0.02
1.43	1.59	0.16		
1.49	1.50	0.01	1.46	-0.03
1.51	1.88	0.37	1.82	0.31
1.52	1.09	-0.43	1.07	-0.45
1.53	1.77	0.24	1.72	0.19
1.55	1.82	0.27	1.77	0.22
1.6	1.28	-0.32	1.22	-0.38
1.63	1.68	0.05	1.62	-0.01
1.76	1.60	-0.16	1.53	-0.23
1.93	1.59	-0.34	1.48	-0.45
1.28	1.30	0.01	1.34	0.02

ray logs was used in an attempt to reduce the error of the gamma ray method in estimating TOC.

High and low bulk density values were averaged for each sampling depth unit and divided by the slope of the line comparing the product of the radioactivity and bulk density to TOC (wt %). The product of the radioactivity and bulk density compared with TOC (Figure 26) had a slope of 147.41. The correlation factor for this method is 0.2759 (Figure 30), with the highest error being off by 0.59 weight percent and the smallest error being off by less than 0.01 weight percent (Figure 31 and Table 8).

TESTING OF EXCLUDED DATA POINTS

Two samples of source rock taken from the Nash Unit No. 23 well core were evaluated in the laboratory in addition to the cutting samples used to determine the accuracy of log estimated values for TOC. The TOC levels for the samples were measured to be 2.41 and 4.49. The latter value is for a sample from the top of the Bone Spring Formation, and is therefore irreproducible using our estimation technique, because the estimation method has been tested only for the lower Brushy Canyon source rocks. The first value, however, should be possible to reproduce since it is from the lower Brushy Canyon.

Another issue to consider is that the log estimation technique was calibrated from well cuttings sampled over sometimes hundreds of feet. The log values over these intervals have been averaged. The core sample, however, is from one specific depth and is not an average. How close can we get to the actual value for TOC based on the log responses at this depth? These are issues to consider in our estimations using core samples versus cutting samples.

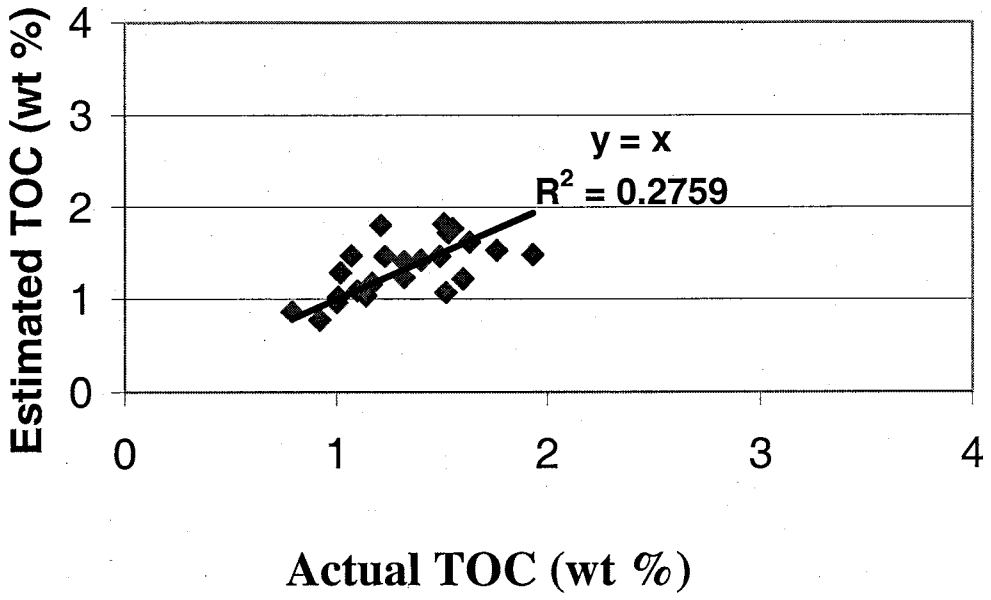

Figure 30—Calculated versus actual TOC using combination method. R^2 = correlation coefficient.

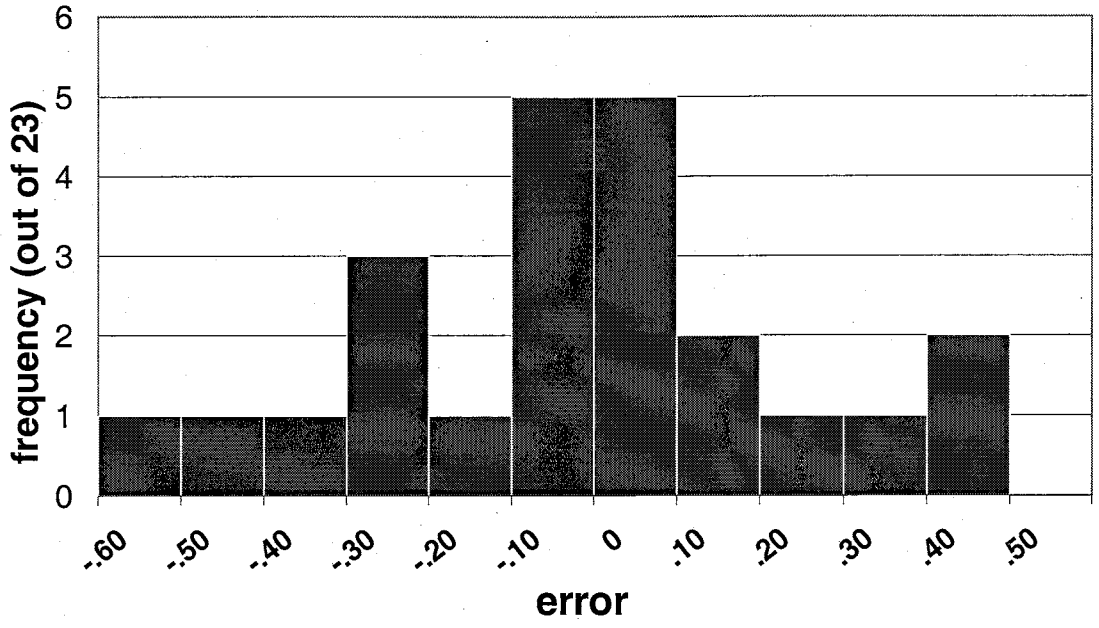

Figure 31—Error histogram. Frequency and error distribution (by weight percent) for TOC calculations using combination method.

For the first core sample, the gamma ray intensity is approximately 87 API units at the depth of 6814 feet. This gives us a predicted value of approximately 1.58 for the TOC at this depth. Laboratory results for TOC indicate a value of 2.41, which is 0.83 weight percent higher than that estimated. This error is on the high end of the scale (Figure 29 and Table 8).

CONCLUSIONS FOR TOTAL ORGANIC CARBON ESTIMATION BASED ON LOG RESPONSE

The gamma ray method is more convenient due to the availability of this log within the Delaware Basin and gives a slightly better correlation than our combination method. The bulk density log is often not as readily available throughout the Delaware Basin, and when used in calculating TOC has not proven helpful.

Some error could be contributed to the samples having been taken from cuttings. Cuttings are usually grouped in intervals of tens of feet. Organic-rich rock from these intervals could therefore have come from anywhere in this interval. The result is an average of all of the values of TOC in that interval. In an attempt to sufficiently represent this in the log readings for gamma ray response, a measurement of the high and low value of gamma ray intensity over a few tens of feet within this sampling depth was averaged.

Cuttings create the possibility for what seems to be endless error in trying to calculate TOC from the log values due to mixing of units and averaging of TOC values. Scientists that have been successful in calculating TOC from logs have commonly used core samples in their work. Using core could eliminate the possibility of many errors that result in using cuttings samples, such as cavings and mixed samples.

There is further work to be done in establishing a more accurate method for calculating TOC based on log response. More consideration might be given to other log data available. In addition, there are perhaps better mathematical equations, with greater complexity, that could be used to allow for smaller error in the estimations. Such equations could take into account aspects of the source rock such as the lithology, which would alter intensities of the log values. Samples should be taken from core when at all possible in order to get the most accurate representative of organic-rich rock from a given depth. This is most important when comparing TOC levels to log values.

KEROGEN MATURATION

THERMAL MATURITY

Thermal maturity is an essential component of oil and gas generation. Time and temperature are the key influences on the thermal maturity of a source rock. At low levels of maturity, kerogen is less capable of creating hydrocarbons. With an increase in maturity, oil is created from kerogen. As the maturity increases further, thermal breakdown of oil already generated results in gas and, ultimately, destruction of kerogen occurs. With destruction of kerogen, the ratio of carbon to oxygen and hydrogen is so high that no additional hydrocarbons can be generated. For a source rock to generate hydrocarbons, it must have reached the oil window. In order for kerogen to create significant quantities of hydrocarbons, the source rock must remain within the oil window for a substantial length of time. Based on production records from the lower Brushy Canyon, the source rock for the lower Brushy Canyon reservoirs has met these requirements.

RESULTS OF THERMAL MATURITY ANALYSES

T_{max} values were recorded for over 30 samples. Resulting temperatures ranged from 439 ° C to 448 ° C (Figure 32). These analyses indicate all of the samples are within the oil window (Table 3). As shown by the contour map of T_{max} over structure,

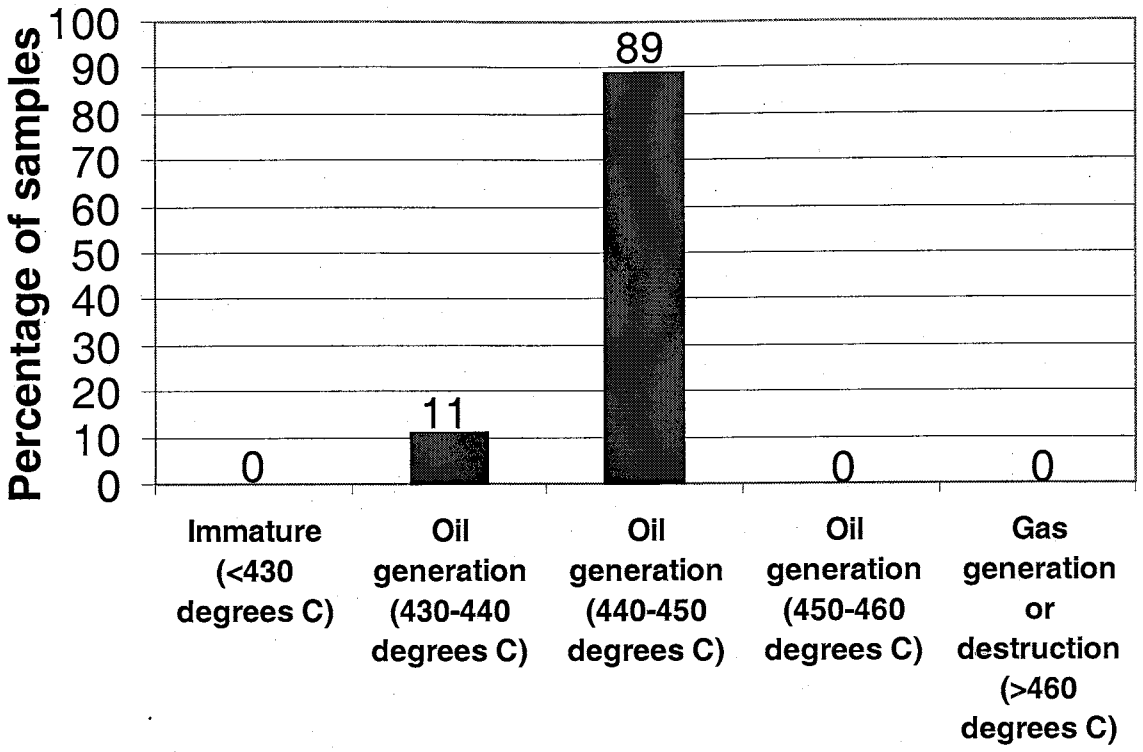

Figure 32— Results for maturity of source rock for 30+ lower Brushy Canyon samples using T_{max}.

(Figure 33), the highest values of T_{max}, and therefore the highest levels of maturity, are present along the western portion of the basin. This area is where the lower Brushy Canyon Formation is at its shallowest depth of burial. The same general relationship between T_{max} and burial depth is apparent for the upper Brushy Canyon Formation (Figure 34).

The production index, calculated for over 30 samples, ranges from 0.1 to 0.42 for the lower Brushy Canyon (Figure 35). The average value was 0.19, with the majority of samples falling between 0.1 and 0.25. These values indicate that these kerogens are mature and within the oil window, which is supportive of the Rock-Eval T_{max} values.

The ten samples from the lower Brushy Canyon that were analyzed using the thermal alteration index have values that are all 2.4, 2.5, 2.6, or 2.8 (Figure 36). These values indicate moderately mature to mature kerogen and support the Rock-Eval thermal maturity results (Table 3).

INTERPRETATION OF THERMAL MATURITY RESULTS

Higher levels of maturity are present where the lower Brushy Canyon is the least deeply buried. Because temperature increases with increasing burial depth, it would be expected that thermal maturity, and therefore values of T_{max}, PI, and TAI, should increase with burial depth. In this study, the Brushy Canyon is least mature where it is the most deeply buried. Perhaps the western portion of the basin was once more deeply buried than the eastern portion prior to tilting to the east, and subsequently there has been erosion in the west. If the western Delaware Basin was not more deeply buried than the east, an additional source of heat or increased heat flow in the west must have been responsible for this maturity pattern.

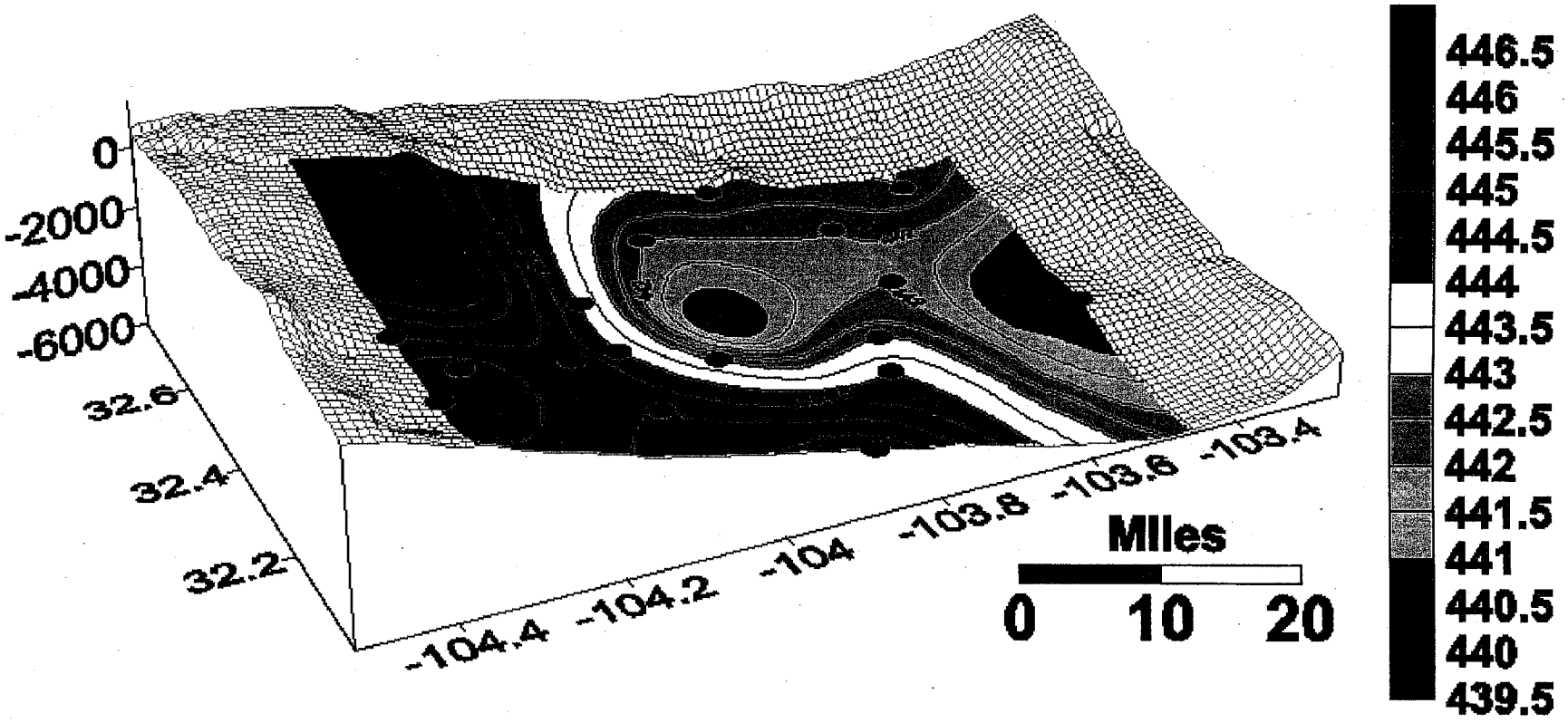

Figure 33—Contour map of T_{max} indicating change in maturity for lower Brushy Canyon source rock across study area superimposed on lower Brushy Canyon structure. Scale is in degrees Celsius. X-axis = degrees longitude; Y-axis = degrees latitude; Z-axis = depth in feet. Black circles mark sample locations.

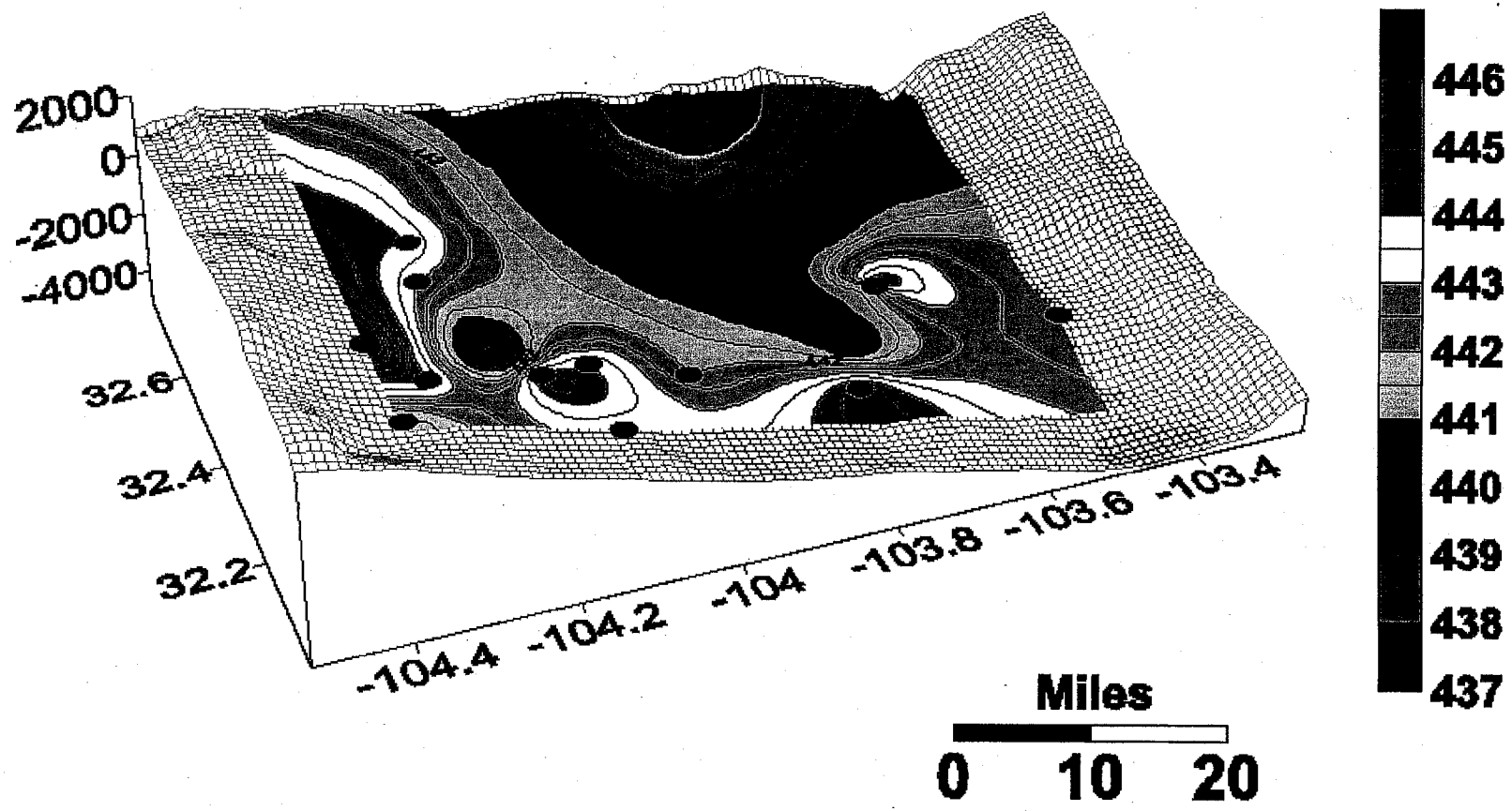

Figure 34—Contour map of T_{max} indicating change in maturity for upper Brushy Canyon source rock across study area superimposed on upper Brushy Canyon structure. Scale is in degrees Celsius. X-axis = degrees longitude; Y-axis = degrees latitude; Z-axis = depth in feet. Black circles mark sample locations.

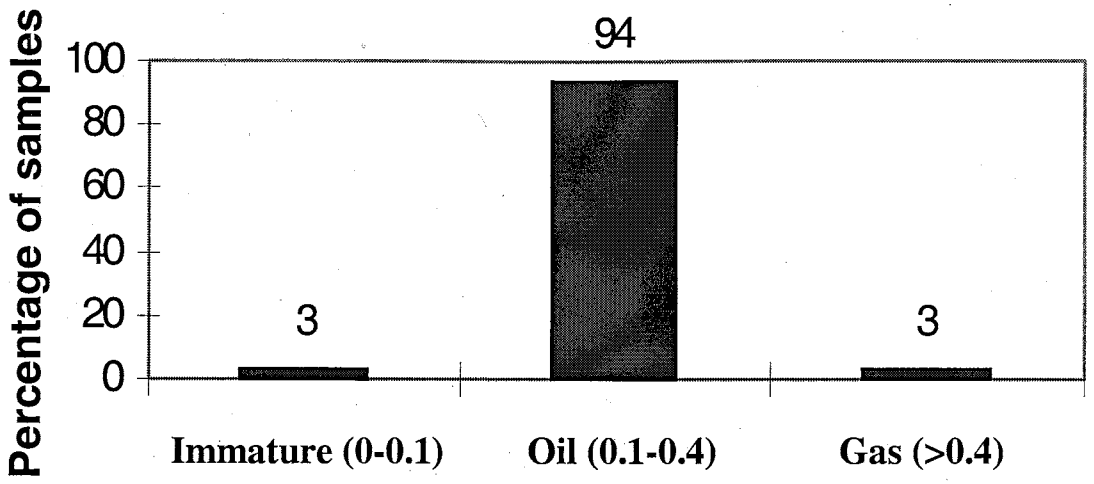

Figure 35—Productivity index results for 30+ lower Brushy Canyon samples.

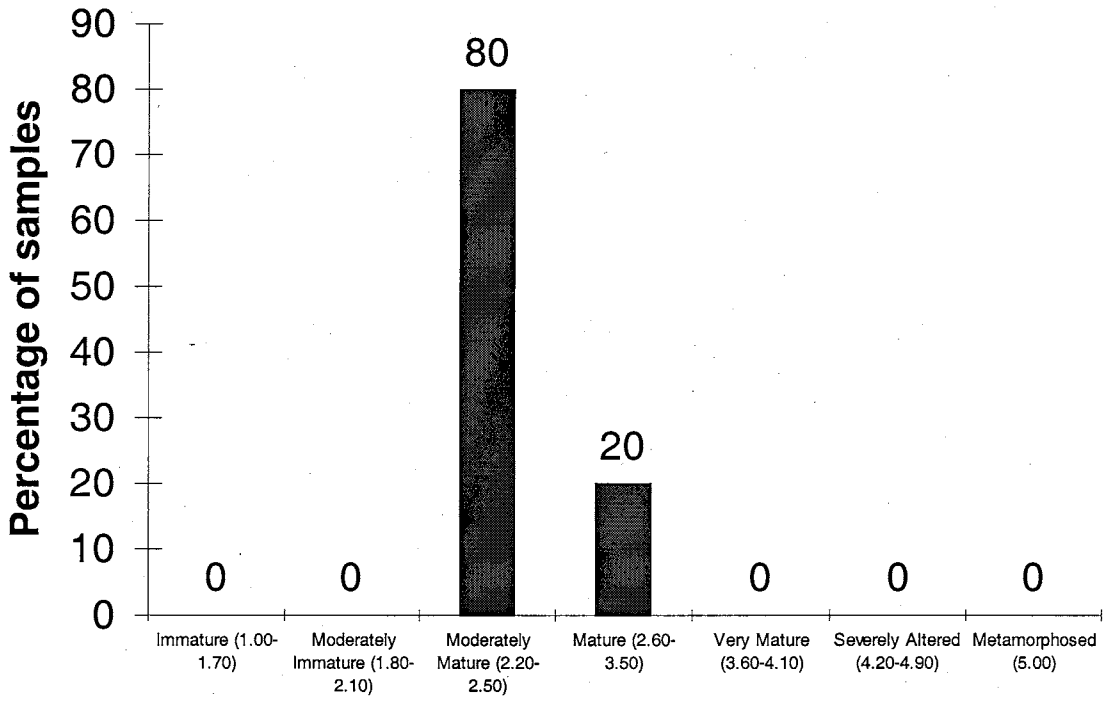

Figure 36—Maturity for 10 lower Brushy Canyon samples based on visual assessment of kerogen (Thermal Alteration Index).

Geological features such as igneous intrusions (dikes and sills; Figure 37) and faults (Figure 38) are present along the western portion of the Delaware Basin (Barker and Pawlewicz, 1987; Hills, 1970). The igneous intrusions indicate magma bodies at depth. Hydrothermal fluid movement, or heat generated from movement along the borders of the basin from faulting, folding, or from deeply buried igneous intrusions may be possible factors involved in greater levels of maturity in this western portion of the study area.

Several phases of structural tilting have been recorded for the Delaware Basin. A fault zone along the eastern portion has assisted in tilting the basin to the east starting early in the basin's history, with possible recurrent movement as late as the Late Cretaceous during events of the Laramide Orogeny (Hills, 1984). This geological activity could have triggered the folding and faulting mentioned above, causing additional heat and greater kerogen maturity in the far, western portion of the Delaware Basin by creating faults and fractures in the west. Another aspect to consider is the thickness variation of crust across the southeastern portion of the state due to the Rio Grande rift. This rifting had created a great amount of high heat flow along the rift area, as well as in the basin and range provinces during the Late Cenozoic (Olsen, 1992). Its effect on heat conductivity along the western portion of our study area is unknown, but something to consider.

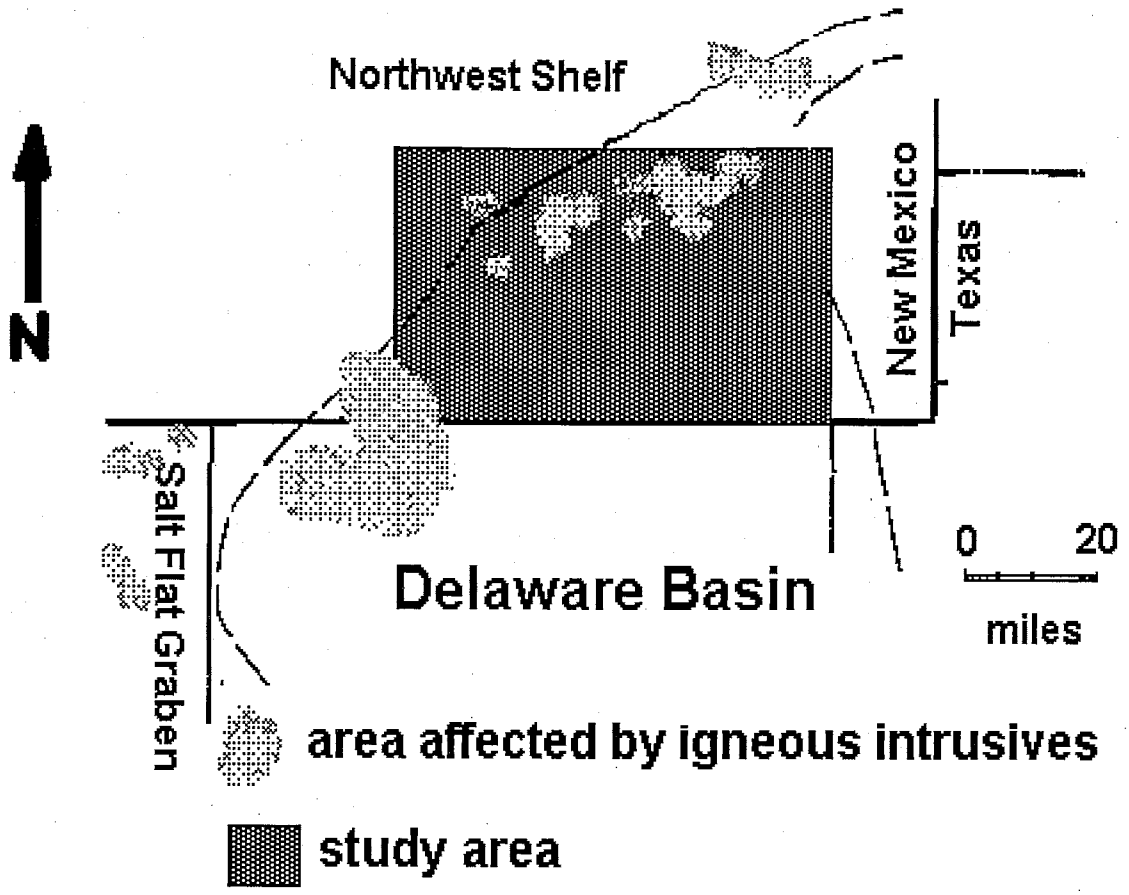

Figure 37—Igneous intrusions indicating magma bodies at depth within study area (modified from Barker and Pawlewicz, 1984).

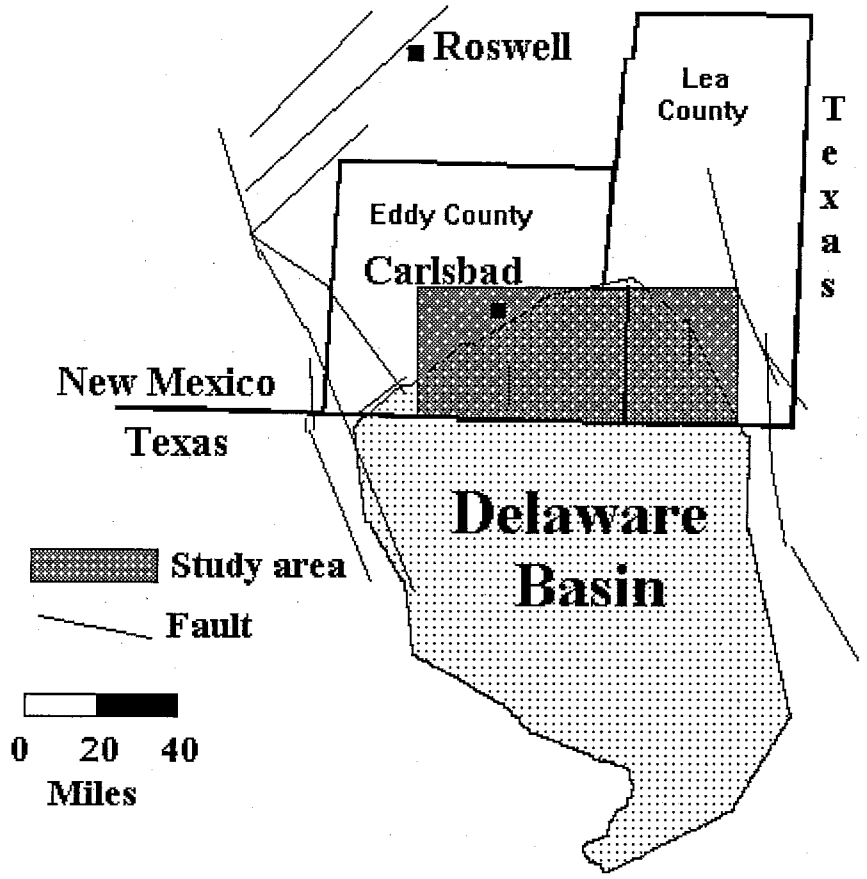

Figure 38—Faulting around western Delaware Basin and study area (modified from Hills, 1984).

RELATIONSHIP BETWEEN PRODUCTION AND SOURCE ROCK VARIABILITY

Production trends show that the greatest amount of oil has been produced from the central and eastern portion of the study area, as well as from an area southeast of Carlsbad (Figure 39). Outlying areas of lesser production surround these productive areas. Maps of total organic carbon show greatest weight percent trending southeasterly into the basin from the northwestern portion of the study area (Figure 24). Greatest TOC shows *some* correlation to the greatest production areas, with the higher TOC containing source rock downdip from the oil pools along the west (Figure 40). However, it does not offer an explanation for why there is greater production to the east over lower TOC trends. A similar trend is apparent with maps of the product of TOC and net thickness (generative potential). The oil pools tend to be updip of source rocks with the greater generative potential to the west (Figure 41), but does not correlate well to the east.

Why are we seeing greater production in regions of lower TOC and low production in regions of high TOC? Also, the greatest maturity is along the western and southern parts of the study area (Figure 33). If the greatest maturity is along the western region of the study area, how can it be explained that the greatest oil production is in the area of less mature source rocks (easterly; Figure 42)? The percentage source rock map offers a better explanation for the larger oil pools to the east (Figure 43). The best

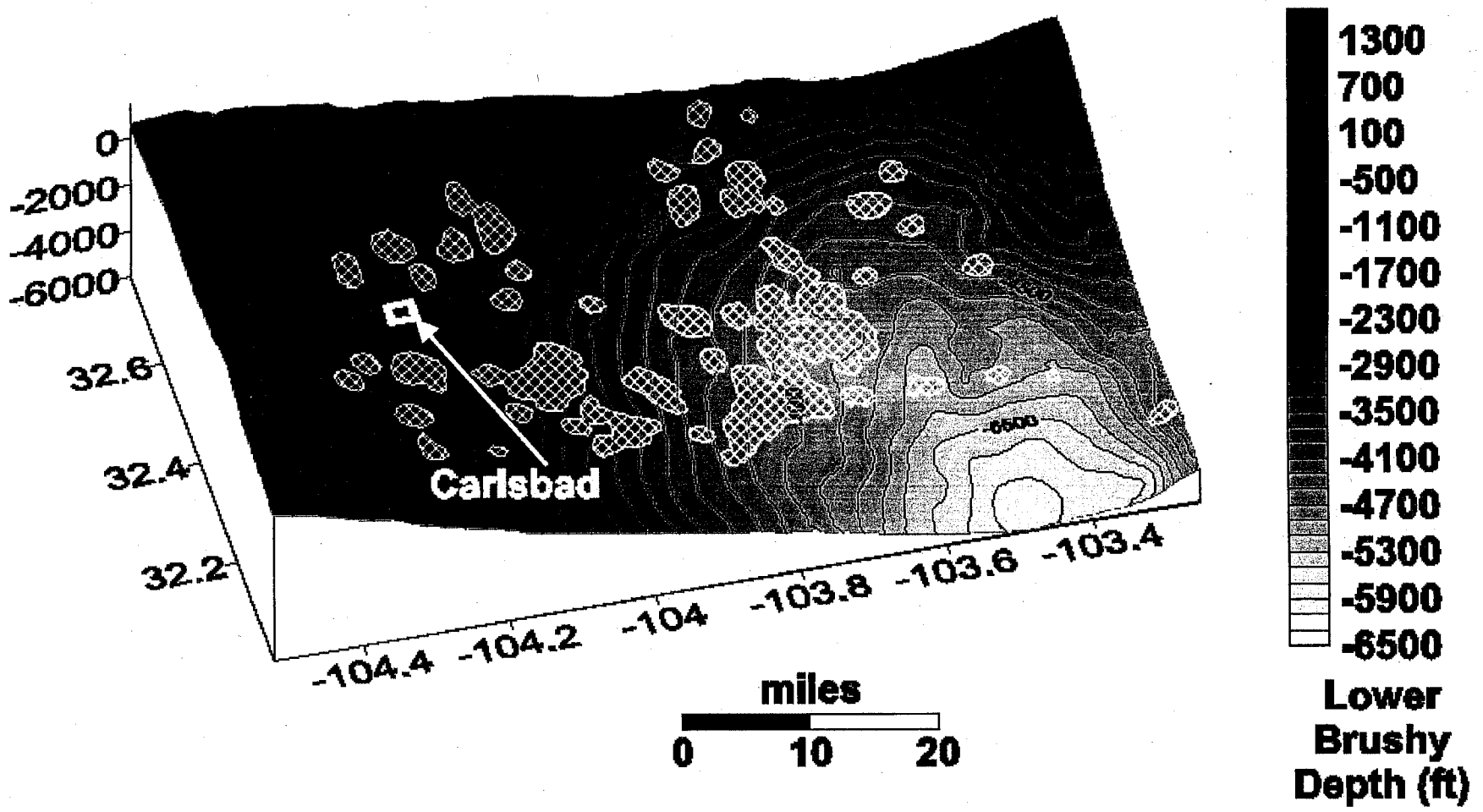

Figure 39—Production map for lower Brushy Canyon superimposed on lower Brushy Canyon structure. X-axis = degrees longitude; Y-axis = degrees latitude; Z-axis = depth in feet. Zones of production are represented by yellow hatch marks.

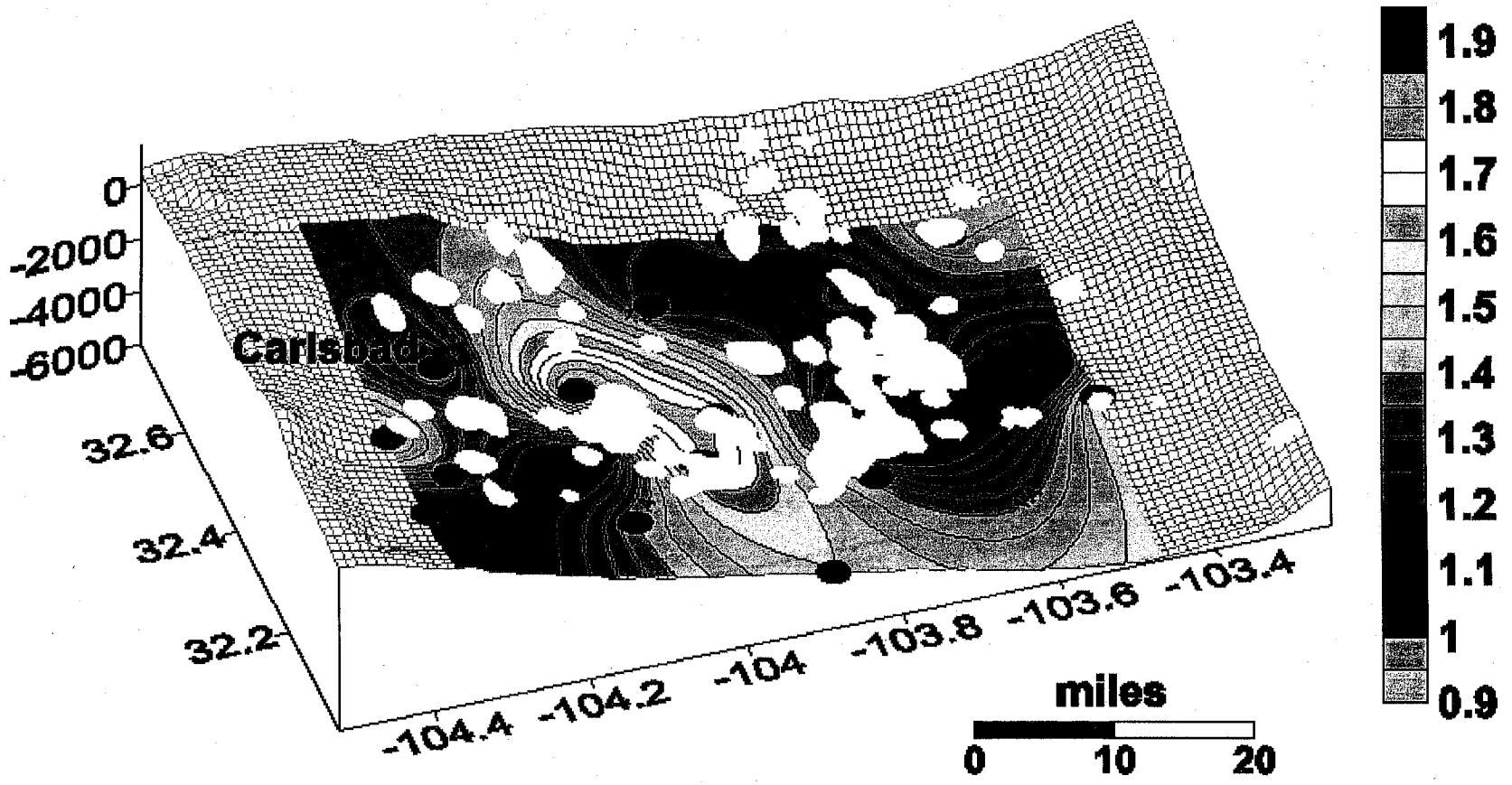

Figure 40—Production (in white) over TOC for lower Brushy Canyon superimposed on lower Brushy Canyon structure. X-axis = degrees longitude; Y-axis = degrees latitude; Z-axis = depth in feet.

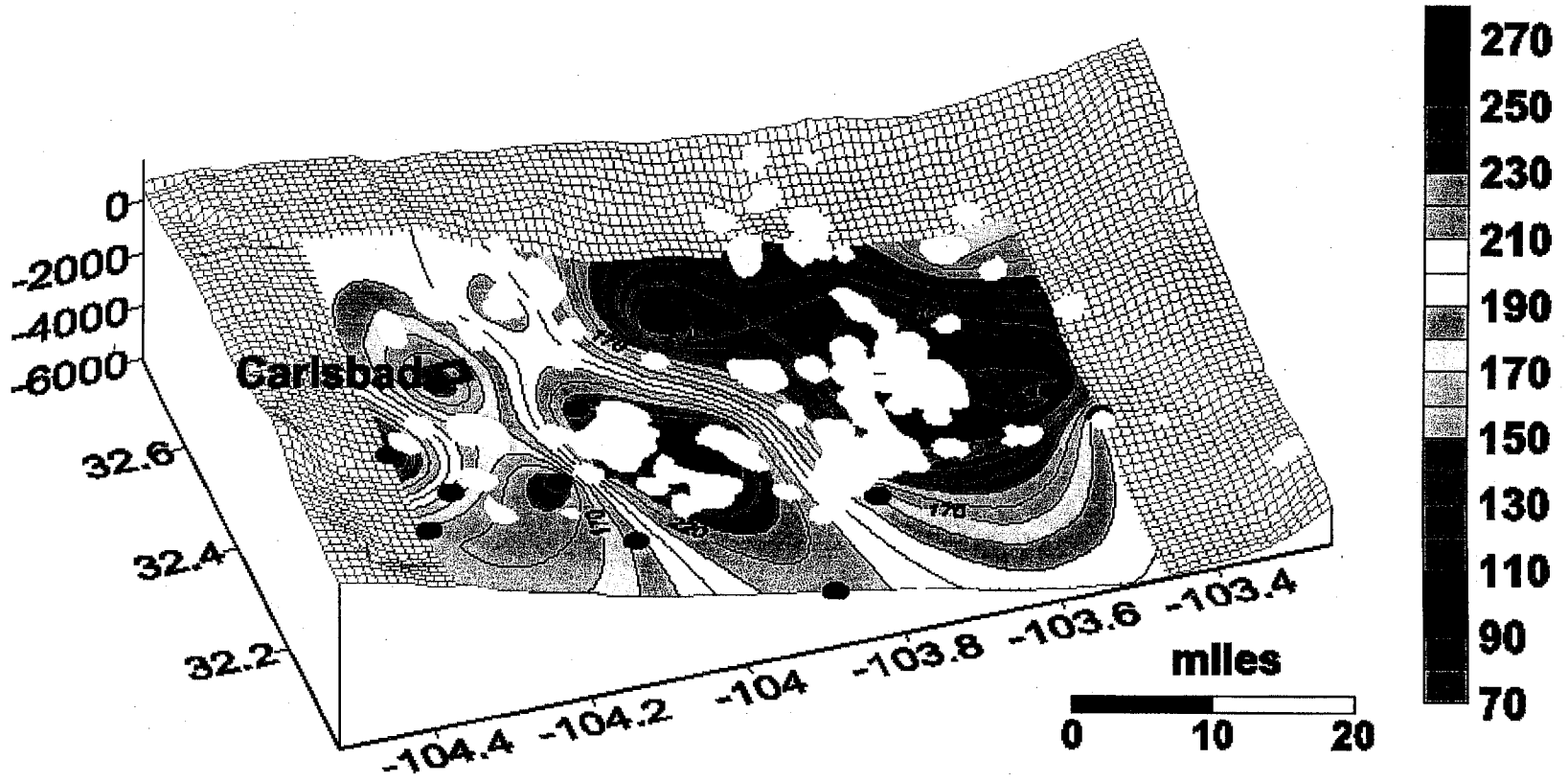

Figure 41—Production (in white) over generative potential for lower Brushy Canyon superimposed on lower Brushy Canyon structure. X-axis = degrees longitude; Y-axis = degrees latitude; Z-axis = depth in feet. Generative potential is the product of the TOC (in weight percent) and the net thickness of the source rock (in feet).

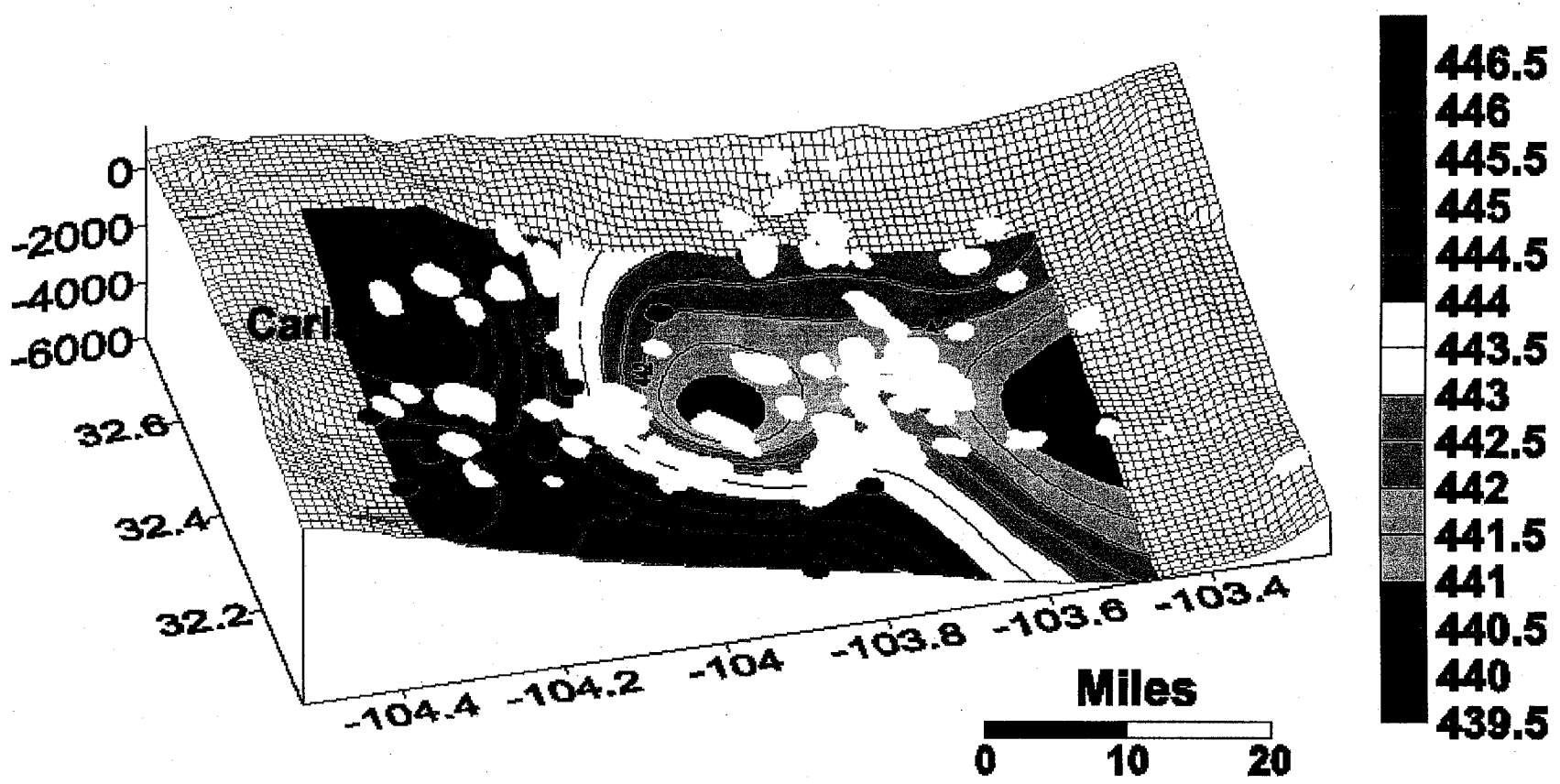

Figure 42—Production (in white) over T_{max} for lower Brushy Canyon superimposed on lower Brushy Canyon structure. Scale is in degrees Celsius. X-axis = degrees longitude; Y-axis = degrees latitude; Z-axis = depth in feet.

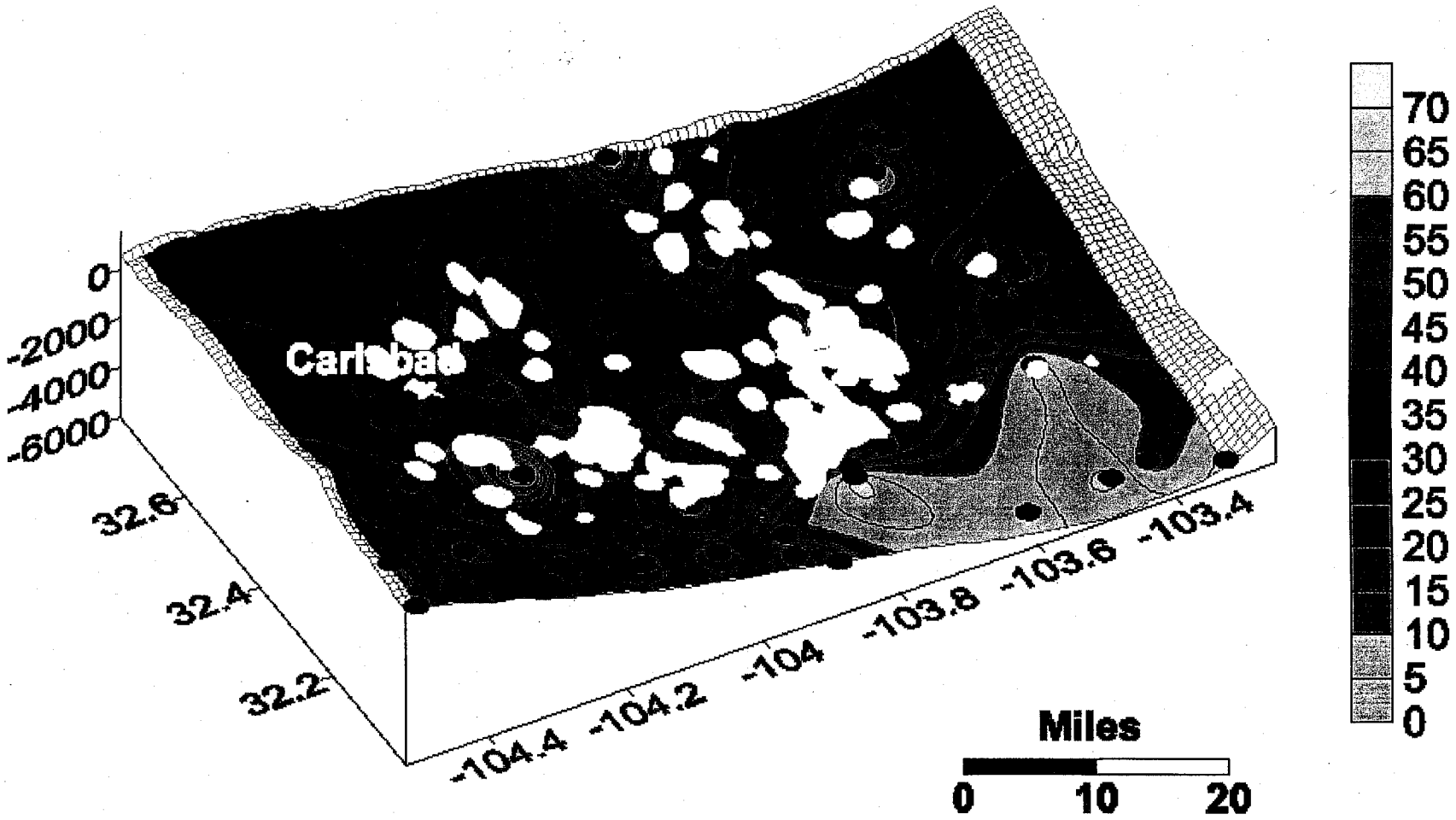

Figure 43—Production over percentage source rock superimposed on lower Brushy Canyon structure. X-axis = degrees longitude; Y-axis = -axis = depth in feet. Color scale bar represents net thickness organic-rich (source) rock in feet.

correlation, however is between the map of the net thickness of source rock and production. Greatest thicknesses of source rock are quite proportional and correlate well to lower Brushy Canyon oil production (Figure 44). The greatest thickness of source rock tends to be downdip of the oil pools. Another region of high net thickness lies in the southeastern study area. There does not seem to be an oil pool directly associated with it. This may be due to a lack of reservoirs, or the oil generated from this source rock may have migrated away through faults that have been reactivated in this area.

Another correlation can be made between the nature of the lower Brushy Canyon kerogen type and the API gravity of the oil in the lower Brushy Canyon. Trends of the kerogen within our study area indicate dominantly amorphous-sapropel and herbaceous organic matter throughout our project area, with a composition of nearly half-amorphous and half-herbaceous material in both the eastern- and southernmost regions (Figure 20). Approaching the northwestern portion of the area, the composition of organic matter becomes slightly more herbaceous. Even further north and west organic matter becomes slightly woody and inertinitic in addition to the dominant amorphous and herbaceous composition.

In regions with portions of woody material and inertinite in the organic matter, the oil gravity is commonly between 25 and 35 API degrees. Further into the basin, where the organic matter is a composition of only amorphous and herbaceous material, the oil gravity increases to 35 to 40 API degrees. The maximum oil gravity reaches values between 40 and 50 API degrees where the organic matter is half-herbaceous and half amorphous-sapropel. It is not unlikely that thermal maturity also plays a major role in the

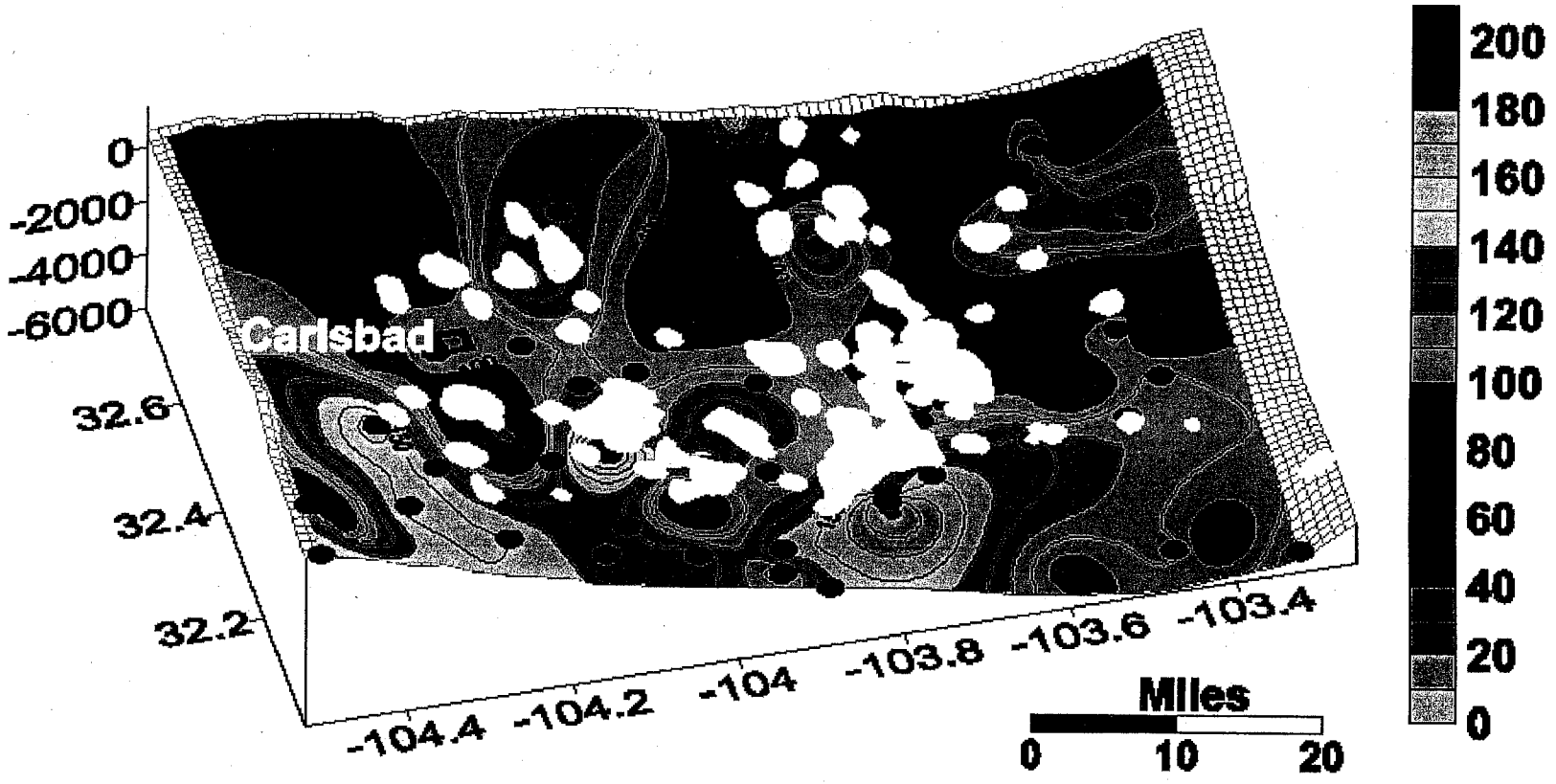

Figure 44—Production (in white) over net thickness source rock (in feet) for lower Brushy Canyon superimposed on lower Brushy Canyon structure. X-axis = degrees longitude; Y-axis = degrees latitude; Z-axis = depth in feet.

nature of the oils within lower Brushy Canyon reservoirs. The northwestern portion of our study area is also the most thermally mature area, according to our T_{max} data. Lower API gravity oils are more stable under greater thermal conditions. Therefore, thermal maturity may also be contributing to the pattern of oil gravity present.

CONCLUSIONS

The Brushy Canyon petroleum system is very complex. In order to understand it in its entirety, a wide range of geological aspects must be considered. The Brushy Canyon Formation is composed of a combination of sandstone, siltstone, and silty carbonate. Interbedded siltstones and very fine-grained to fine-grained sub-arkosic sandstones make up the majority of the lower Brushy Canyon. The organic-rich siltstones, silty lime-mud units, and very fine-grained sandstones contain sufficient quantities of kerogen (based on TOC values in weight percent) to produce oil and gas. Kerogen in these units is mostly types I and II, and is composed of amorphous-sapropel and herbaceous organic matter.

Thermal maturity of these organic-rich units is well within the oil window with T_{max} temperatures ranging from 439 ° C to 448 ° C. Thermal alteration index values range from 2.4 to 2.8, while productivity index values are around 0.1 to 0.42 (0.19 average), both indicating maturity.

Definite trends exist within the geochemical data. The greatest percentage of source rock lies within the deepest portion of the lower Brushy Canyon in the study area, with some TOC-rich elongate forms extending onto the northern and western shelfal regions. Thickness of the source rock tends to also follow these elongate forms as well as in the present-day deepest portion of the lower Brushy Canyon. Explanations for these

patterns include the finer grain size of the sediments in these areas, as well as increase in organic productivity and preservation of the organic matter in these areas.

Kerogen type varies slightly throughout the study area. More terrestrial type organic matter, such as woody and inertinitic material, tends to be preserved in areas surrounding the shelf. Algal or marine biotas, as well as lightweight plant material such as spores and pollen, tend to be more commonly preserved further into the basin.

Patterns in total organic content may be explained by a combination of factors including variation of organic productivity, effects of sediment influx rates, and changing water conditions that effect organic preservation.

Thermal maturity of source rocks in the lower Brushy Canyon increases in the western and shallowest portions of our study area. This portion of the study area may have once been more deeply buried than the eastern portion of the basin before easterly tilting in the Tertiary. Subsequently, the overlying sediments have been eroded away. Other possible contributors to increased maturity in the western portion are effects of rifting to the west of the basin. Increased heat flow from the rifting process, or tectonically induced deep-seated faults, the related hydrothermal fluids, and igneous activity could also have played some part in the temperature history.

As in any petroleum system, production for the lower Brushy Canyon is controlled by reservoir availability; porosity and permeability limitations; presence or lack of structural and stratigraphic trapping mechanisms; and, to some degree, the presence of source rock. The greatest correlation between production and source rock characteristics is with variation in source rock net thickness. The type kerogen, amount of total organic carbon, and the maturity of the source rock are also very important, but

do not offer a correlation that is as straightforward based on the overlay maps. The interbedded nature of the reservoir and source rock of the lower Brushy Canyon allows the source rock to both generate the hydrocarbons and serve as a seal for these fluids in the sandstone reservoirs.

REFERENCES

Barker, C. E. and Pawlewicz, M. J., 1987, The Effects of Igneous Intrusions and Higher Heat Flow on the Thermal Maturity of Leonardian and Younger Rocks, Western Delaware Basin, Texas, *in* Cromwell, D. and Mazzullo, L., eds., 1987, The Leonardian Facies in W. Texas and S. E. New Mexico and Guidebook of the Glass Mountains, West Texas—1987 Permian Basin Section: Society of Economic Petrologists and Mineralogists, pp. 69-81.

Bayliss, G., [Personal Communication, Geochem Laboratories, Houston, Texas]. Fall 2000.

Bozanich, R. G., 1979, The Bell Canyon and Cherry Canyon Formations, Eastern Delaware Basin, Texas: Lithology, Environments and Mechanisms of Deposition, *in* Sullivan, N. M., ed., Guadalupian Delaware Mountain Group of West Texas and Southeast New Mexico, Symposium and Field Conference Guidebook: Society of Economic Paleontologists and Mineralogists (Permian basin Section), Pub. 79-18, pp. 121-141.

Brooks J., Cornford, C., and Archer, R., 1987, The role of hydrocarbon source rocks in petroleum exploration; *in* Brooks, J., and Fleet, A. J., Marine petroleum source rocks: Geological Society of London, Special publication no. 26, pp. 17-46.

Calvert, S. E., 1987, Oceanographic controls on the accumulation of organic matter in marine sediments; *in* Brooks, J., and Fleet, A. J., Marine petroleum source rocks: Geological Society of London, Special publication no. 26, pp. 137-152.

Demaison, G. J., and Moore, G. T., 1980, Anoxic environments and oil source bed genesis: American Association of Petroleum Geologists, Bulletin, v. 64, pp. 1179-1209.

Dow, W. G., 1978, Petroleum source beds on continental slopes and rises: American Association of Petroleum Geologists, Bulletin, v. 62, pp. 1584-1606.

Fischer, A. G., and Sarnheim, M., 1987 Airborne Silts and Dune-derived Sands in the Permian of the Delaware Basin: Journal of Sedimentary Petrology, v. 58, pp. 637-643.

Geochem Laboratories, Inc., 1980, Source Rock Evaluation Reference Manual.

Harms, J. C., 1979, Brushy Canyon Formation, Texas: a deep-water density current deposit, *in* Sullivan, N. M., ed., Guadalupian Delaware Mountain Group of West Texas

and Southeast New Mexico, Symposium and Field Conference Guidebook, Permian Basin Section Society of Economic Paleontologists and Mineralogists, Pub. 79-18, pp. 205-226

Harms, J. C., and Williamson, C. R., 1998, Deep-water Density Current Deposits of Delaware Mountain Group (Permian), Delaware Basin, Texas and New Mexico: American Association of Petroleum Geologists Bulletin, v. 72, pp. 299-317.

Hayes, P. T., 1964, Geology of the Guadalupe Mountains, New Mexico: U. S. Geological Survey Professional Paper 446, 69 p.

Hayes, M. O., 1967, Hurricanes as Geologic Agents: Case Studies of Hurricanes Carla, 1961, and Cindy, 1963, 1963: University of Texas Bureau of Economic Geology Report of Investigation 61, 56 p.

Hays, P. D. and Tieh, T. T., 1992, Organic Geochemistry and Diagenesis of the Delaware Mountain group West Texas and Southeast New Mexico, *in* Cromwell, D. W., Moussa, M. T., and Mazzullo, L. J., eds., 1992, Transactions—Southwest Section American Association of Petroleum Geologists Convention, Publication SW2-92-90, pp. 155-175.

Hills, J.M., 1970, Late Paleozoic Structural Directions in Southern Permian Basin, west Texas and Southeastern New Mexico: American Association of Petroleum Geologists, Bulletin, v. 54, no. 10, pp. 1809-1827.

Hills, J.M., 1984, Sedimentation, Tectonism, and Hydrocarbon Generation in Delaware Basin, West Texas and Southeastern New Mexico: American Association of Petroleum Geologists Bulletin, v. 68, no. 3, pp. 250-267.

Jacka, A. D., 1979, Deposition and Entrapment of Hydrocarbons in Bell Canyon and Cherry Canyon Deep-Sean Fans of the Delaware Basin, *in* Sullivan, N. M., ed., Guadalupian Delaware Mountain Group of West Texas and Southeast New Mexico, Symposium and Field Conference Guidebook: Society of Economic Paleontologists and Mineralogists (Permian basin Section), Pub. 79-18, pp. 104-120.

Jacka, A. D., Beck, R. H., St. Germain, L. C., and Harrison, S. C., 1968, Permian deep-sea fans of the Delaware Mountain Group (Guadalupian), Delaware basin, *in* Guadalupian Facies, Apache Mountains area, west Texas: Society of Economic Paleontologists and Mineralogists (Permian Basin Section), Pub. 68-11, pp. 49-90.

Jacka, A. D., Thomas, C. M., Beck, R. H., Williams, K. W., and Harrison, S.C., 1967, Guadalupian Depositional Cycles of the Delaware Basin and Northwest Shelf, *in* Cyclic Sedimentation in the Permian Basin-Symposium, Midland, Texas: West Texas Geological Society, Pub. 69-56, pp. 151-195.

Jarvie, D. M., 1991, Total Organic Carbon (TOC) Analysis, *in* Merrill, R. K., ed., 1991, Treatise of Petroleum Geology and Handbook of Petroleum Geology—Source rock and Migration Processes and Evaluation of Techniques, pp., 113-118.

LaPlante, R. E., 1974, Hydrocarbon generation in Gulf Coast Tertiary sediments: American Association of Petroleum Geologists, Bulletin, v. 58, pp. 1281-1289.

Magoon, L. B., and Dow, W. G., 1994, The Petroleum System, *in* Magoon, L. B., and Dow, W. G., eds., The Petroleum System-from source to trap: American Association of Petroleum Geologists, Memoir 60, pp. 3-24.

Merrill, R. K., ed., 1991, Treatise of Petroleum Geology and Handbook of Petroleum Geology—Source rock and Migration Processes and Evaluation of Techniques, p. xvii.

Montgomery, S. L., Worrall, J., Hamilton, D., 1999, Delaware Mountain Group, West Texas and Southeastern New Mexico, A Case of Refound Opportunity: Part 1—Brushy Canyon: American Association of Petroleum Geologists, Bulletin, v. 83, no. 12, pp. 1901-1926.

Olsen, K. H., 1992, Continental Rifting, in Encyclopedia of Earth System Science, V. 1, pp. 627-641.

Payne, M. W., 1976, Basinal Sandstone Facies, Delaware Basin, West Texas and Southeast New Mexico: American Association of Petroleum Geologists, Bulletin, v.60, pp. 517-527.

Payne, M. W., 1979, Submarine-Fan Channel Depositional Processes in the Permian Bell Canyon Formation, West Texas and Southeast New Mexico, *in* Sullivan, N. M., ed., Guadalupian Delaware Mountain Group of West Texas and Southeast New Mexico, Symposium and Field Conference Guidebook: Society of Economic Paleontologists and Mineralogists (Permian basin Section), Pub. 79-18, pp. 96-103.

Peters, K. E., 1986, Guidelines for Evaluating Petroleum Source Rock Using Programmed Pyrolysis: American Association of Petroleum Geologists, Bulletin, v. 70, pp. 318-329.

Peters, K. E., and Cassa, M. R., 1994, Applied Source Rock Geochemistry, *in* Magoon, L. B., and Dow, W. G., eds., The Petroleum System—from Source to Trap: American Association of Petroleum Geologists, Memoir 60, pp. 93-120.

Pocock, S. A. J., 1982, Identification and Recording of Particulate Sedimentary Organic Matter, *in* How to Assess Maturation and Paleotemperatures, Society of Economic Paleontologists and Mineralogists, Short Course Number 7, pp.13-132.

Schmoker, J. W., 1981, Determination of Organic-Matter Content of Appalachian Devonian Shales from Gamma-Ray Logs: American Association of Petroleum Geologists, Bulletin, v. 65, no. 7, pp. 1285-1298.

Thomerson, M. D., and Catalano, L. E., 1997, Depositional Regimes and Reservoir Characteristics of the Brushy Canyon Sandstones, East Livingston Ridge Delaware Field Lea County, New Mexico, West Texas Geological Society, Volume 36, no. 7, pp. 5-13.
Tissot, B., Califet-Debyser, Y., Deroo, G., and Oudin, J. L., 1971, Origin and Evolution of Hydrocarbons in Early Toarcian Shales, Paris Basin, France: American Association of Petroleum Geologists, Bulletin, v. 55, pp. 2177-2193.

Tyson, R. V., 1987, The Genesis and Palynofacies Characteristics of Marine Petroleum Source Rocks; *in* Brooks, J., and Fleet, A. J., eds., Marine Petroleum Source Rocks: Geological Society of London, Special Publication no. 26, pp. 47-67.

APPENDIX

Core Description-
Nash Unit #23
Strata Production
13-23s-29e, 1650 FNL, 990 FWL
30-015-28272
6650 to 6854 feet
Producing Intervals: (Brushy Canyon) 6654-6703, 6755-6801 *all colors describing wet core

6650-6661.3

Siltstone interbedded with sandstone.
80% siltstone, 20% sandstone.

Siltstone:

Light olive gray (5Y 6/1) and olive gray (5Y 4/1).
Thinly laminated, planar to very slightly wavy laminations.
5-10% burrowed and bioturbated.
Beds <0.1 ft. – 3 ft. thick.

Sharp planar contacts between sandstone and siltstone.

Sandstone:

Light olive gray (5Y 6/1).
Very fine-grained.
Internally structureless and cross-laminated, mostly structureless.
Beds 0.3 ft.- 0.7 ft. thick.

6661.3-6713

Sandstone interbedded with siltstone.
>95% sandstone, <5% siltstone.

Sandstone:

Light olive gray (5Y 6/1), spots of olive gray (HC staining?).
Very fine-grained, well-sorted.
Internally structureless and cross-laminated.
0.5-6.6 feet thick.
Darker sandstone tends to be calcareously cemented.

Upper contact sandstone sharp.
Basal contact sharp or graded.

Siltstone:

Light olive gray (5Y 6/1) and olive gray (5Y 4/1).
Thinly laminated.

Contacts sharp to gradational, upper contacts siltstone wavy and irregular (undulatory).
Basal contacts gradational to irregular, interfingering?

6713-6729.8

Siltstone:

Light olive gray (5Y 6/1) and olive gray (5Y 4/1).
Thinly laminated, some laminations very faint.
90% fine planar to wavy laminated, 10% faint laminations.
Minor ripple cross-laminations.
Wavy laminations with truncated bedding surface (scour surface).
Non-calcareous.

Sharp contacts.

6729.8-6735.4 *Thin-section at depth 6733.

Sandstone:

Light olive gray (5Y 6/1) and olive gray (5Y 4/1).
Very fine to fine-grained.
Very thin, minor laminations, and faint laminations.
Minor burrowing, top 0.1ft.
Cross-laminated.

6735.4-6739.5

Sandstone and siltstone

Sandstone:

Light olive gray (5Y 6/1) and olive gray (5Y 4/1).
Very fine to fine-grained.
Structureless with faint laminations and bioturbation.
Gravel-sized shale clasts.
~50% bioturbation.

Upper contact gradational.
Basal contact sharp and planar or irregular (slight interfingering).

Siltstone:

Light olive gray (5Y 6/1) and olive gray (5Y 4/1).
Thin planar laminations.

Upper contact sharp and planar or sharp and irregular (interfingering).
Basal contact bioturbated with gravel-sized rip up clasts-sub-parallel to bedding.

*This interval represents two turbidity cycles.

6739.5-6742.8

Sandstone:

Light olive gray (5Y 6/1) and olive gray (5Y 4/1).
Very fine to fine-grained sand.
Darker sands very calcareous, lighter are less calcareous or non-calcareous.

Upper contact contains thin zone of cross-lamination.
Basal contact sharp.

6742.8-6763.4

Siltstone interbedded with sandstone.
95% siltstone, 5% sandstone.

Siltstone:

Light olive gray (5Y 6/1) and olive gray (5Y 4/1).
Thinly laminated and planar, some interval scour surfaces with truncation of laminations, some wavy laminations.
Deformation of planar laminations around calcareous concretions.
Shaly lamination interval.
Bioturbation, intensive in parts.
Flame structures, soft sediment deformation-basal contacts.

Sandstone:

Light olive gray (5Y 6/1).
Very fine-grained.
Mostly structureless.
Upper contact gradational or sharp with slight cross-lamination.
Basal contact sharp and planar.

6763.4-6766.8

Sandstone:
Light olive gray (5Y 6/1).
Very fine-grained.
Non-laminated/structureless to faint wavy parallel laminations.
Wavy to irregular argillaceous streaks in laminae.
Large branching burrows up to 1 or 2 cm diameter.
Lower 1/3 –1/2 ft contains up to 5% calcareous angular fossil fragments dispersed through the matrix.

6766.8-6780

Sandstone interbedded with siltstone.

Sandstone:
Yellowish gray (5Y 8/1) to light olive gray (5Y 6/1) and olive gray (5Y 4/1).
Very fine to fine-grained.
Structureless to finely laminated.
HC staining?
Upper contact gradational with cross-laminations into siltstone laminae or sharp and planar.
Basal contact sharp and irregular to graded irregular-soft sediment deformation.

Siltstone:
Light olive gray (5Y 6/1) and olive gray (5Y 4/1).
Well-defined planar laminations…alternation of tan/black (silt, OM, sand).
Faint cross-laminations to planar, some wavy laminations (near basal contacts).
Flame structures and soft-sediment deformation at tops.
Minor bioturbation near lower contact.
Top 0.2 feet fine cross-laminations .
Upper contact sharp and irregular-soft sediment deformation.

6779.4-6783.1 (continuation of interval above)

Same as above but with some shale and wavy units with cross-lamination mid siltstone unit.

6780.0-6785.5 sealed
6787.2-6787.7 sealed

6784.1-6786.1

Sandstone:
Light olive gray (5Y 6/1) and olive gray (5Y 4/1).
Dominantly fine-grained, very fine-grained.
Structureless.
HC staining?

6786.1-6788.85

Siltstone interbedded with sandstone.
80% siltstone, 20% sandstone.

Siltstone:
Light olive gray (5Y 6/1).
Mostly planar thin laminations, some wavy.

Upper contacts sharp and irregular.
Basal contacts sharp and irregular (soft sediment deformation) or graded and slightly wavy.

Sandstone:
Light olive gray (5Y 6/1).
Dominantly fine-grained, very fine-grained.
Faint wavy laminations and cross-laminations between silty areas.
0.5-<1 ft. thick.

6788.85-6792.05

Sandstone:
Light olive gray (5Y 6/1) and olive gray (5Y 4/1).
Very fine-grained.
Structureless, w/ some thin, faint cross-laminations at top.
Darker structureless sandstone very calcareous.
Upper contact grades into faint laminations in sandstone with fossils, sharp irregular contact, into wavy laminations of siltstone.

6792.05-6797.0

Siltstone interbedded with sandstone.
80% siltstone, 20% sandstone.

Siltstone:
Light olive gray (5Y 6/1) and olive gray (5Y 4/1).
Thin, planar laminations.
Slump features at base, soft sediment deformation.
Upper contact sharp and irregular.
Basal contact gradational and irregular, wavy and bioturbated, soft sed. Deformation.

Sandstone:
Light olive gray (5Y 6/1) and olive gray (5Y 4/1).
Very fine-grained.
Structureless to faint wavy laminations.
Upper contact graded, and in some cases bioturbated.
Basal contact sharp and irregular, soft sediment deformation.

6797.0-6803.5

Sandstone interbedded with siltstone.
95% sandstone, 5% siltstone.

Sandstone:
Light olive gray (5Y 6/1) and olive gray (5Y 4/1).
Fine-grained and very fine-grained.
Structureless.
Fines upward to very fine, then becomes fine again toward top.
Very base is fine to medium (1/8 –1/2 mm sand and fossil fragments) grades into siltstone ~0.3ft.
Calcareous cement.
Upper contact sharp, planar to wavy and irregular.
Basal contact gradational and planar laminated.

Siltstone:
Light olive gray (5Y 6/1) and olive gray (5Y 4/1).
Planar laminated, faint at top, distinguished at base.
Upper contacts gradational into sandstone.
Basal contacts sharp and wavy or irregular, slight cross-lamination.

6803.5-6810.0

Siltstone, minor sandstone.

Siltstone:

Light olive gray (5Y 6/1) and olive gray (5Y 4/1).
Planar laminated, some slightly wavy, irregular (mixed with sand).

Sandstone:

Light olive gray (5Y 6/1).
Very fine-grained.
Very fossil-rich at base.
Thin micro-laminations, cross-laminations, wavy laminations.

Upper contact sharp and irregular.
Basal contact sharp and irregular (soft sediment deformation).

6810.0-6812.5

Sandstone interbedded with siltstone.
80% sandstone, 20% siltstone.

Sandstone:

Light olive gray (5Y 6/1).
Mostly fine-grained, some medium grained sand, slightly coarsens upward.
Structureless to extremely faint laminations.
Top 0.1 ft. of interval fossil-rich fragments ~0.5-15 mm length.

Upper contact gradational or sharp planar.
Basal contact sharp and irregular (soft sediment deformation) or gradational thin-planar laminations with some minor cross-lamination, wavy lamination (siltstone).

Siltstone:

Light olive gray (5Y 6/1) and olive gray (5Y 4/1).
Planar laminated.

Upper contact-soft sediment deformation.
Basal contact sharp, planar.

6815.5-6816 sealed

6812.5-6820.5

*Thin-section and geochem at depth 6814.
*Thin-section at depth 6815.4.

Siltstone interbedded with sandstone, some carbonate turbidite (limey siltstone?).
95% siltstone, 5% sandstone.

Siltstone:

Olive gray (5Y 4/1).
Thin, planar laminations, some wavy.

Upper contact sharp with wavy sandstone laminations or soft sediment deformation.
Basal contact sharp and planar or wavy and irregular.

Sandstone:

Light olive gray (5Y 6/1) and olive gray (5Y 4/1).
Fine to very fine-grained.
Structureless, some cross-laminations at base.

Carbonate turbidite @ 6815

Olive black.
Clastic, very fine-grained, fines upward into siltstone.
Contains rip up clasts, mudstone.

6820.5-6822.5

Sandstone, minor siltstone, carbonate turbidite.

Sandstone:

Light olive gray (5Y 6/1).
Fine-grained.
Structureless, fining upwards.
Rip up clasts of mud in carbonate.
Gradational.

6822.5-6829.5

Siltstone and minor sandstone.

Siltstone:

Olive gray (5Y 4/1) and olive black.
Fine laminations, planar to slightly wavy, and massive (pure black).
Disseminated pyrite at upper contact with sandier units @~6828 feet.

Sandstone:

Light olive gray (5Y 6/1) to yellowish gray (silicified concretions).
Very fine-grained.
Fossil fragments.
Some bioturbation.

6830.2-6830.6 sealed

6829.8-6832.35

Siltstone and sandstone interbedded.
~50% siltstone, 50% sandstone.

Siltstone:

Light olive gray (5Y 6/1) and olive gray (5Y 4/1).
Wavy and irregular laminations, slumping/micro-faulting.

Sandstone:

Light olive gray (5Y 6/1) .
Coarse to fine and very-fine (0.1ft base coarse).
Fining upwards.

Upper contact wavy and irregular.
Basal contact sharp and wavy.

6835.6-6836.0 sealed

6832.35-6839.2

Sandstone interbedded with siltstone, minor mudstone?
95% sandstone, 5% siltstone.

Sandstone:

Light olive gray (5Y 6/1).
Fine, very fine-grained.
Structureless to faint thin laminations, wavy or contorted.

Upper contact sharp and irregular.
Basal contact irregular and soft sediment deformation (flame structures).

6839.2-6854.0 *Thin-section and geochem at depth 6848.1.

Siltstone, minor sandstone.

Siltstone:

Olive black to black.
Planar and slightly wavy laminations to massive.
Very organic rich.
Disseminated pyrite and fossil fragments---~6839.9, 6844.2 ft.

This thesis is accepted on behalf of the
Faculty of the Institute by the following committee:

Advisor

April 25, 2001
Date

I release this document to the New Mexico Institute of Mining and Technology.

Student's Signature

April 25, 2001
Date